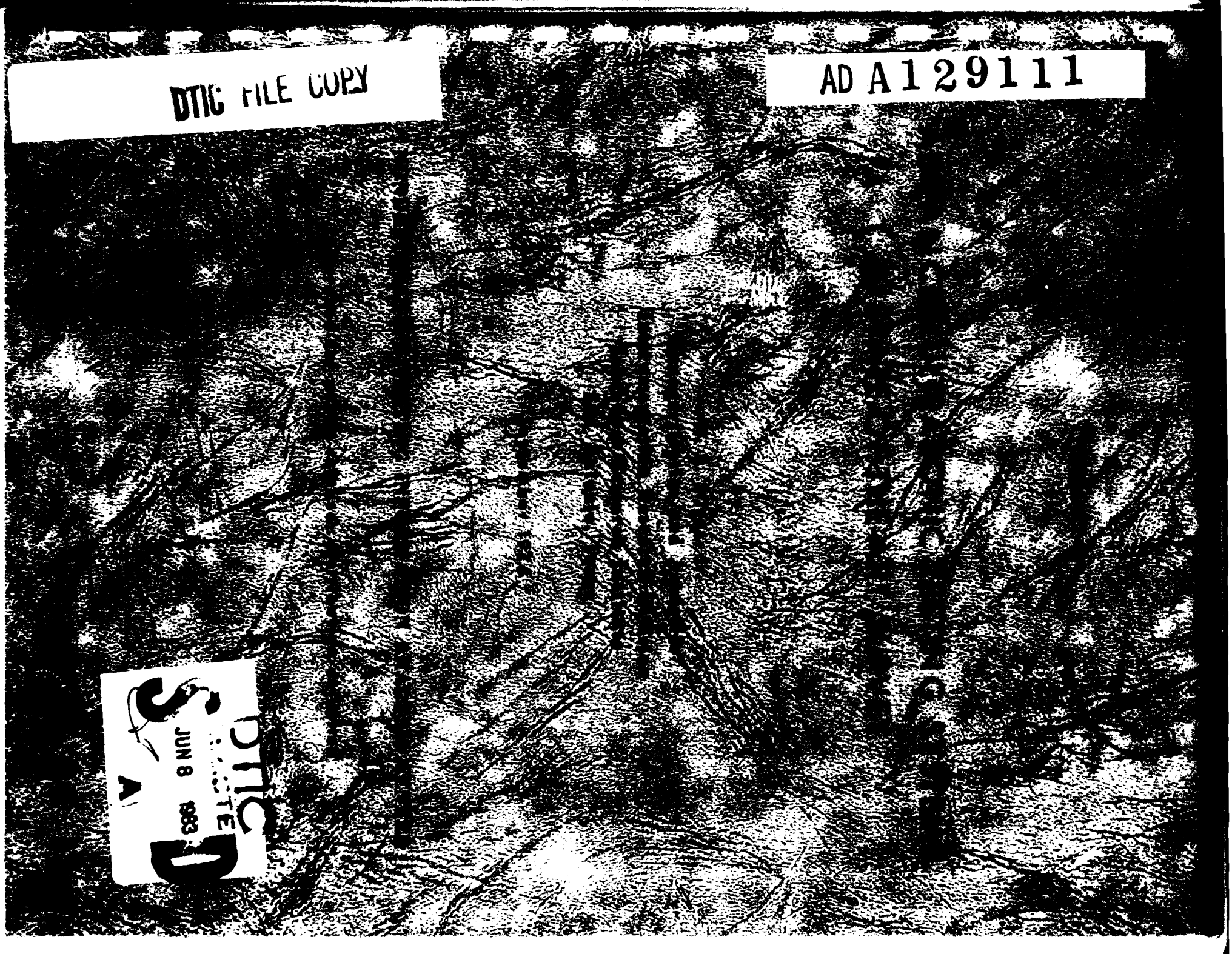

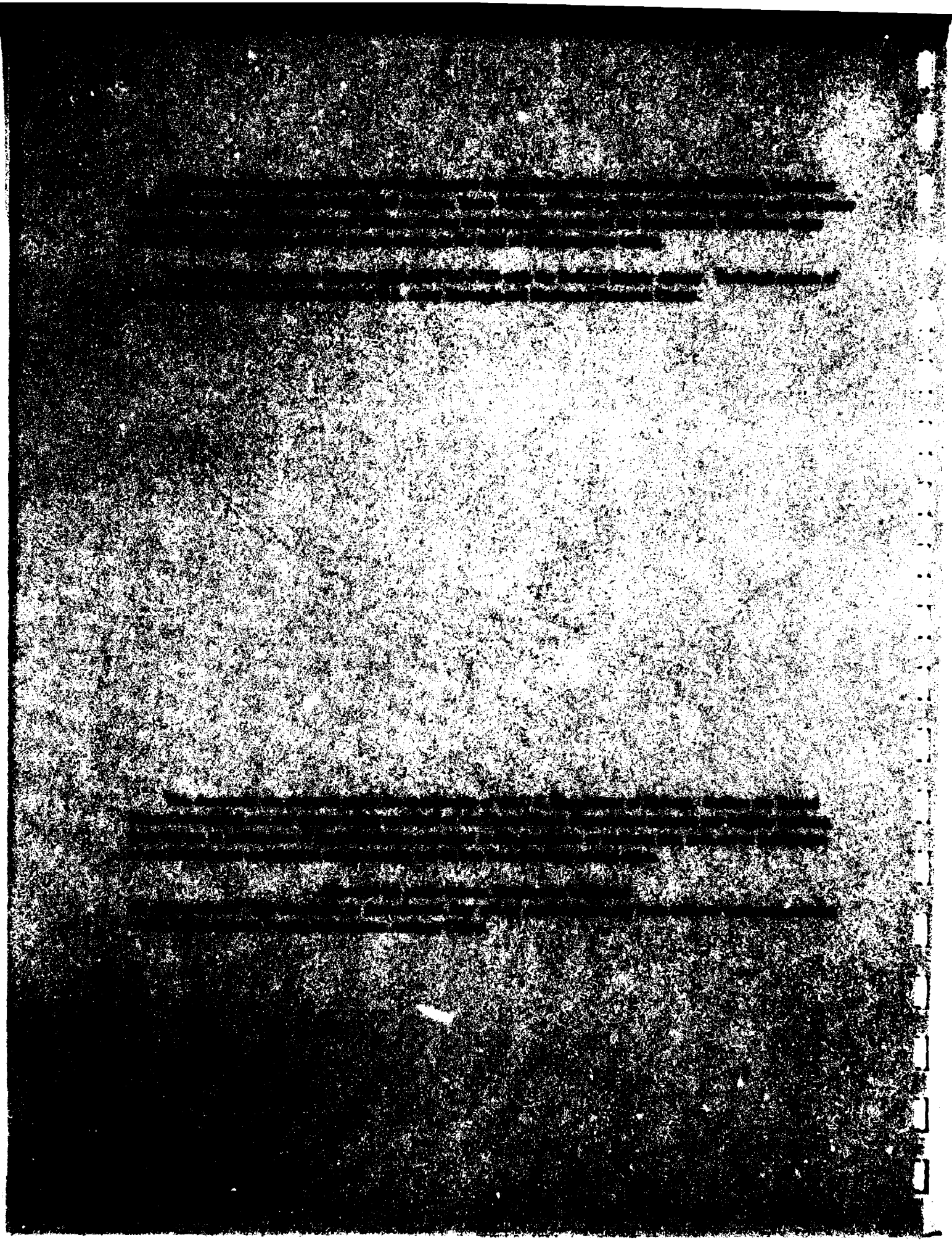

UNCLASSIFIED

SECURITY CLASSIFICATION OF THIS PAGE *(When Data Entered)*

REPORT DOCUMENTATION PAGE		READ INSTRUCTIONS BEFORE COMPLETING FORM
1. REPORT NUMBER	2. GOVT ACCESSION NO. AD-A129 111	3. RECIPIENT'S CATALOG NUMBER
4. TITLE *(and Subtitle)* Advanced Ultrasonic Testing Systems - A State-of-the-Art Survey		5. TYPE OF REPORT & PERIOD COVERED
		6. PERFORMING ORG. REPORT NUMBER NTIAC 77-1
7. AUTHOR(s) H. S. Silvus, Jr.		8. CONTRACT OR GRANT NUMBER(s) DLA900-77-C-3733
9. PERFORMING ORGANIZATION NAME AND ADDRESSES NTIAC, Southwest Research Institute P.O. Drawer 28510 San Antonio, TX 78284		10. PROGRAM ELEMENT, PROJECT, TASK AREA & WORK UNIT NUMBERS
11. CONTROLLING OFFICE NAME AND ADDRESS Defense Logistics Agency Headquarters Cameron Station Alexandria, VA 22314		12. REPORT DATE September 1976
		13. NUMBER OF PAGES 74
14. MONITORING AGENCY NAME & ADDRESS *(if different from Controlling Office)* Army Materials and Mechanics Research Center Watertown, MA 02172		15. SECURITY CLASS. *(of this report)* Unclassified
		15a. DECLASSIFICATION/DOWNGRADING SCHEDULE

16. DISTRIBUTION STATEMENT *(of this Report)*

Approved for public release; distribution unlimited.

17. DISTRIBUTION STATEMENT *(of the abstract entered in Block 20, if different from Report)*

18. SUPPLEMENTARY NOTES

For Sale by NTIAC, Southwest Research Institute, P.O. Drawer 28510, San Antonio, TX 78284 ($23.00)

19. KEY WORDS *(Continue on reverse side if necessary and identify by block number)*

State-of-the-art reviews, ultrasonics, ultrasonic testing, systems, technique, components, information, inspection, equipment, test equipment, plates, welds, billets, forging, pipes, tubes, spectrum analysis, signal processing, delta technique, correlation, filters, convolutions, imaging, materials, physical properties, transducers, scanning, digital systems, NTIAC

20. ABSTRACT *(Continue on reverse side if necessary and identify by block number)*

The purpose of this document is present a concise survey of the state-of-the-art in advanced ultrasonic testing systems, techniques, and system components. Information presented is intended to give a practical overview of the types of ultrasonic nondestructive inspection apparatus presently in use and of relatively new techniques which are being applied to improve the capabilities of such systems. The technical level of the discussion is such that this document will be useful to the reader who has only an introductory

DD FORM 1 JAN 73 1473 EDITION OF 1 NOV 65 IS OBSOLETE

UNCLASSIFIED

SECURITY CLASSIFICATION OF THIS PAGE *(When Data Entered)*

(20) Cont'd.

knowledge of ultrasonic nondestructive evaluation, but who wants to know what can be done and what is being done in this field. The sophisticated reader can use this document to review with minimum expenditure of time and effort approximately 120 relatively recent papers in the field of ultrasonic nondestructive evaluation of materials.

NTIAC-77-1

ADVANCED ULTRASONIC TESTING SYSTEMS
A STATE-OF-THE-ART SURVEY

by

H. S. Silvus, Jr.
Manager, Optics and Acoustics
Instrumentation Research Division
Southwest Research Institute
San Antonio, Texas

September 1976

NONDESTRUCTIVE TESTING INFORMATION ANALYSIS CENTER

Approved for public release; distribution unlimited

TABLE OF CONTENTS

TABLE OF CONTENTS (Cont'd)

LIST OF ILLUSTRATIONS

LIST OF ILLUSTRATIONS (Cont'd)

LIST OF ILLUSTRATIONS (Cont'd)

LIST OF ILLUSTRATIONS

I. INTRODUCTION

A. Purpose

The purpose of this document is to present a concise survey of the state of the art in advanced ultrasonic testing systems, techniques, and system components. Information presented is intended to give a practical overview of the types of ultrasonic nondestructive inspection apparatus presently in use and of relatively new techniques which are being applied to improve the capabilities of such systems. The technical level of the discussion is such that this document will be useful to the reader who has only an introductory knowledge of ultrasonic nondestructive evaluation, but who wants to know what can be done and what is being done in this field. The sophisticated reader can use this document to review with a minimum expenditure of time and effort approximately 120 relatively recent papers in the field of ultrasonic nondestructive evaluation of materials.

B. Scope

Computer retrieval facilities of the Nondestructive Testing Information Analysis Center (NTIAC) were used to search the open literature in ultrasonics and related subjects from 1968 through 1975. Technical journals, conference proceedings, research reports, Department of Defense technical reports, and trade journals were included in the body of literature surveyed. In selecting documents to be cited in this survey, those which dealt with practical systems and presented experimental data were given primary consideration; thus, relatively few purely analytical papers are included. Most of the documents cited in this survey are available in the English language.

This state-of-the-art survey includes discussions on (1) automated ultrasonic inspection systems for a variety of applications, (2) signal processing techniques as applied to ultrasonic inspection, (3) ultrasonic imaging systems, including direct and holographic types, (4) methods of inferring material properties from ultrasonic measurements, (5) special ultrasonic techniques (i.e., the Delta technique and stress enhancement of fatigue crack detection), and (6) ultrasonic inspection system components including transducers, scanning devices, and pulsers. Because of the magnitude of the subject covered by this survey, discussions of individual items are necessarily brief; frequent references are made to the literature from which the reader may obtain detailed information.

C. Organization

The body of this survey document is divided into three major sections:

1. Automated Ultrasonic Inspection Systems

This section discusses relatively elaborate ultrasonic systems which operate automatically and usually unattended in a production line environment for the purpose of inspecting plates, billets, forgings, pipe, tubing, and welded joints.

2. Techniques

This section presents discussions of a variety of signal processing techniques which may be used to improve flaw detection capability or resolution of a system. Additionally, ultrasonic imaging, inference of material properties from ultrasonic measurements, and special techniques are included in this section.

3. System Components

This section describes relatively recent developments in ultrasonic transducers, scanning devices, and pulsers. The document concludes with a bibliography of 126 references to the literature on ultrasonic nondestructive inspection and related subjects.

TABLE I. ABBREVIATIONS FOR UNITS OF MEASUREMENT AND MULTIPLIER PREFIXES USED IN THIS DOCUMENT

Units		Prefixes		
B	= bel	G	= giga-	$= 10^{9}$
Hz	= hertz	M	= mega-	$= 10^{6}$
in	= inch	k	= kilo-	$= 10^{3}$
ft	= foot	d	= deci-	$= 10^{-1}$
lb	= pound	c	= centi-	$= 10^{-2}$
m	= meter	m	= milli-	$= 10^{-3}$
min	= minute	μ	= micro-	$= 10^{-6}$
N	= newton	p	= pico-	$= 10^{-12}$
rev	= revolution			
s	= second			
W	= watt			

D. Units of Measurement

Throughout the text of this survey, *Systeme Internationale* (SI) units are used in accordance with American National Standard ANSI Z210.1-1976. Approximate English or in some cases customary unit equivalents are included in parentheses following SI units. In some of the illustrations which are extracted from referenced papers, measurement units used by the authors are retained, and no conversion to SI or English units, as the case may be, are provided. A list of abbreviations for names of units used in this survey is presented in Table I.

E. Terminology

A glossary of terms frequently used in nondestructive testing has been prepared by Weismantel (Ref. 1). One section of this glossary deals with ultrasonic nondestructive evaluation terminology. This document is cited for the benefit of readers who may not have working familiarity with nondestructive testing terms.

II. AUTOMATED ULTRASONIC INSPECTION SYSTEMS

A. General

As technology develops, systems tend to increase in complexity and degree of automation. Ultrasonic nondestructive inspection technology has followed this trend. For example, most early ultrasonic nondestructive inspection systems comprised a "home-made" or commercial pulser-receiver-display unit and a hand-held transducer which was manually scanned over the part to be inspected. Now, with recent, rapid decreases in cost, size, and power requirements of general-purpose digital computers, highly automated, computer-based systems are appearing in the field of ultrasonic nondestructive inspection. Although some automated systems are used in the laboratory for conducting experiments in ultrasonic inspection, many systems are working on the production line yielding high-volume, high-quality inspection of basic material forms (i.e., plates, billets, and forgings) and fabricated structures (e.g., pipe, tubing, and welded joints). Many automated systems provide hard-copy records which are becoming progressively more important as demand increases for high-quality, 100-percent inspected materials with traceability.

The remainder of this section discusses and illustrates automated systems which have been reported in the literature in recent years.

B. Plate, Billet and Forging Inspection

Many researchers have shown that nonmetallic inclusions degrade mechanical properties of high-strength materials. Degree of material property degradation is related to quantity and size distribution of such inclusions. Harlan *et al.* (Ref. 2) assembled an automated apparatus to inspect billets of high-strength steel and to compute a "cleanliness index."

The billet to be inspected was submerged in a large water tank, and a motorized scanner under computer control moved an ultrasonic transducer over a prescribed path around the specimen. A standard ultrasonic instrument, equipped with special range gating features, facilitated inspection at various depths into the billet. Electrical output of the ultrasonic instrument was linearly quantized into 16 categories corresponding to inclusion size. Equipment was operated first in the RECORD mode in which the number of echoes in each of the 16 categories was counted and stored. Following scanning of the billet, the apparatus was used in the REPORT mode to print out an inclusion-size distribution and to calculate the cleanliness index which was, in effect, a summation of the number of inclusions in each size category weighted by a factor related to the material-property degradation characteristics of inclusions in that category.

Also reported by Harlan *et al.* were experiments to establish validity of the cleanliness index approach and to define specific material properties which were most significantly affected by changes in cleanliness index. About 40 specimens of type 4340 steel were cut from billets prepared by various steel-making processes. Each billet was ultrasonically inspected, and observed inclusions of various categories were intentionally included in the highly stressed areas of test pieces. Test specimens were cycled to failure in a standard fatigue-testing machine. Conclusions drawn from these tests indicated that ductility, as measured by area reduction, was sensitive to material cleanliness. Also, a relationship between the weighted cleanliness index and the number of cycles to failure was observed.

German steel mills have been using ultrasonics for plate testing since 1952. Since that time, the quantity of plate which could be tested per day has increased to 12,000 m^2 (130,000 ft^2). An automatic ultrasonic plate testing system with an on-line computer was reported by Kuenne (Ref. 3). The system incorporated 80 transducer assemblies mounted on 50-mm (2-in.) centers so that a maximum plate width of 4 m (160 in.) could be inspected. Plate thickness up to 40 mm (1.6 in.) could be accommodated by the apparatus. Figure 1 illustrates one-half of the on-line apparatus and shows 20 transducer assemblies and part of the water circulation apparatus. The system employed through transmission with the transmitting transducers mounted below the plate being inspected and the receiving transducers above. Figure 2 illustrates schematically how the ultrasonic portion of the system functions. A plate (d) was passed through the inspection area on rollers. Transmitting transducers (a) were coupled to the plate through water jets (b). Ultrasonic energy traveled through satisfactory plate material (f) to the opposite side where coupling to receiving transducers (e) was accomplished through water jets (c). If the plate being tested contained a lamination

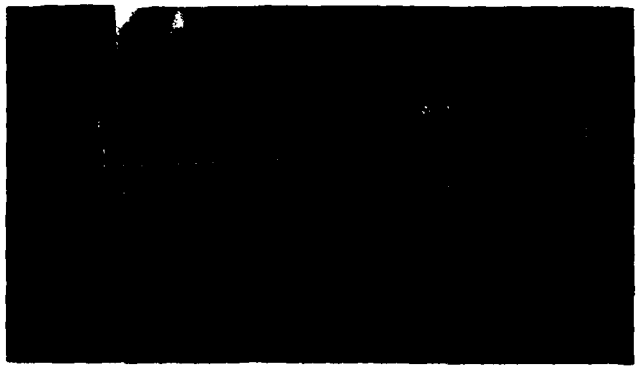

FIGURE 1. PHOTOGRAPH OF PLATE INSPECTION APPARATUS
(From Ref. 3, Reproduced by permission of The American Society for Nondestructive Testing, Inc., Columbus, OH)

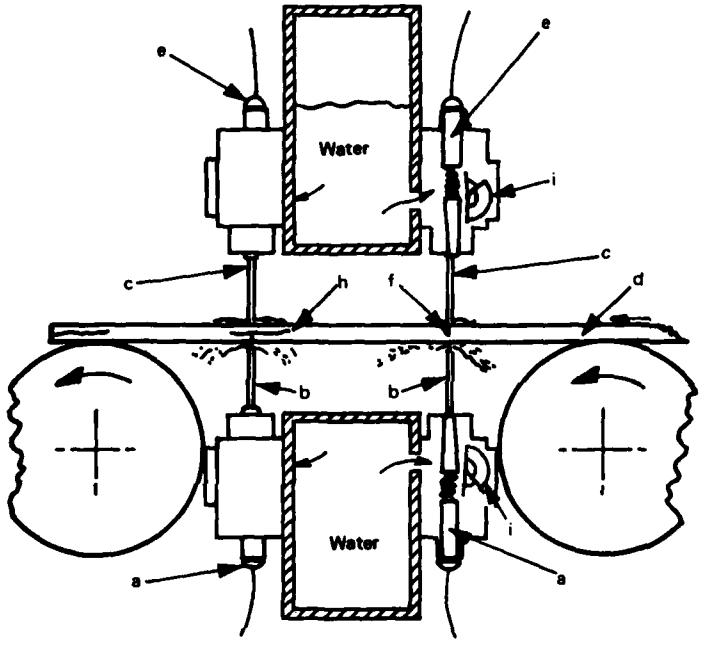

FIGURE 2. SCHEMATIC DIAGRAM OF PLATE INSPECTION SYSTEM ILLUSTRATED IN FIGURE 1 (From Ref. 3, Reproduced by permission of The American Society for Nondestructive Testing, Inc., Columbus, OH)

(h), ultrasonic transmission was interrupted, and the corresponding receiving transducer did not receive a signal. Flap valves (i) were provided for shutting off water jets which lay beyond the edges of the particular plate being inspected to conserve water. Interruptions of the ultrasonic beam were recognized and recorded by an on-line computer which classified defects according to a specification and printed out instructions for cutting the plate for maximum yield in terms of current orders for specific plate sizes and qualities.

Another on-line ultrasonic instrument for detecting inclusions and doublings in sheet material passing through a pickling line was reported by Ploegaert (Ref. 4). This device used a Sperry wheel to couple Lamb waves into sheet material in the thickness range of 1.5 to 6 mm (0.06 to 0.25 in.).

One of the most elaborate automated ultrasonic inspection systems reported in the literature was developed by Yee *et al.* (Refs. 5 & 6). Most automated inspection systems work only with flat or cylindrical shapes, but the system developed by Yee and his associates was intended to inspect aircraft forgings which may have compound curves. The specimen to be inspected was immersed in a water tank, illustrated in Figure 3, which was sufficiently large to contain a 1360-kg (3,000-lb) forging. A five-degree-of-freedom scanning unit moved the transducer over the surface of the specimen to be inspected and maintained the transducer axis normal to the test specimen surface. A carriage attached to the water tank provided translational scanning in two axes or polar coordinate scanning for surfaces of revolution. The transducer manipulator performed vertical, rotational and tilt movements of the transducer. Horizontal scanning of the transducer was accomplished either manually or by computer control, whereas vertical, rotational and tilt motions were accomplished either manually, automatically (i.e., under servo control for contour following) or by computer command.

A general-purpose minicomputer (1) controlled peripheral hardware which included (a) a disk memory, (b) a paper tape system, (c) a teletype console, and (d) a graphic terminal with hard-copy capability and (2) performed arithmetic, logic and instruction-decoding operations. The computer program had five operational phases including (1) initialization, (2) calibration, (3) data acquisition, (4) display generation, and (5) report generation.

In the initialization and calibration phases of operation, the operator entered a limited quantity of scanner control data and the test conditions to be included in the report. The apparatus automatically calibrated

itself using a flat-bottom hole for a reference standard. In the data acquisition phase, the ultrasonic transducer was scanned over the part to be inspected in the contour-following mode so that the transducer axis was maintained normal to the surface of the part being inspected. The system could, if desired, manipulate the transducer in a commanded mode similar to that used in numerically controlled machine tools. During data acquisition either compressional or shear waves in pulse-echo or Delta-scan modes could be used.

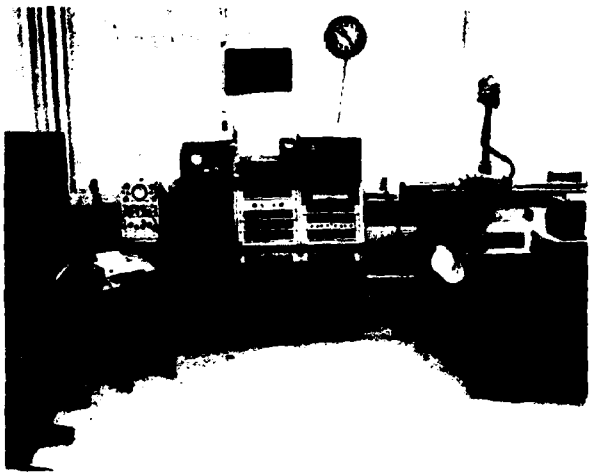

FIGURE 3. PHOTOGRAPH OF AUTOMATED SYSTEM FOR INSPECTION OF AIRCRAFT FORGINGS (From Ref. 6, Reproduced by permission of IIT Research Institute, Chicago, IL)

The system recorded in radio-frequency form all signals which exceeded 20 percent of the calibration level. This facilitated a wide range of post-inspection data analysis including the most recent techniques for flaw characterization.

Data were displayed on the graphic terminal after each scan. In addition, data above a prescribed threshold level from a particular flaw could be displayed for detailed examination. A specific advantage of this computerized system was the capability of storing large quantities of data in compact form; for example, data storage on magnetic disk or magnetic tape provided permanent records which could be re-entered into a computer at a future time for data review, examination of specific flaws or additional signal processing.

C. Pipe and Tube Inspection

Apparatus for inspecting thin-wall tubing intended for nuclear reactor fuel element enclosures was reported by Boulanger *et al.* (Ref. 7). Although the reported system also employed eddy current testing, only the ultrasonic portion, illustrated in Figure 4, will be discussed here. The apparatus was primarily intended to inspect 2-m (79-in.)-long tubing, 6.5 mm (0.25 in.) in diameter having 0.45-mm (0.018-in.) wall thickness, but it was designed to accommodate 5- to 20-mm (0.2- to 0.8-in.)-diameter tubing in lengths up to 5 m (197 in.). A laminar-flow leaking water tank, through which the tube to be inspected was fed with helical motion, contained five ultrasonic transducers, two of which were oriented to produce longitudinal waves, two of which were angled to produce transverse waves, and one of which was used to continuously monitor tube wall thickness. Mechanical fixtures loaded a tube into the inspecting apparatus, drove it past the inspection station, and placed it in a bin corresponding to tube quality. Commercially available electronic units provided for transmission, reception and threshold detection of ultrasonic signals.

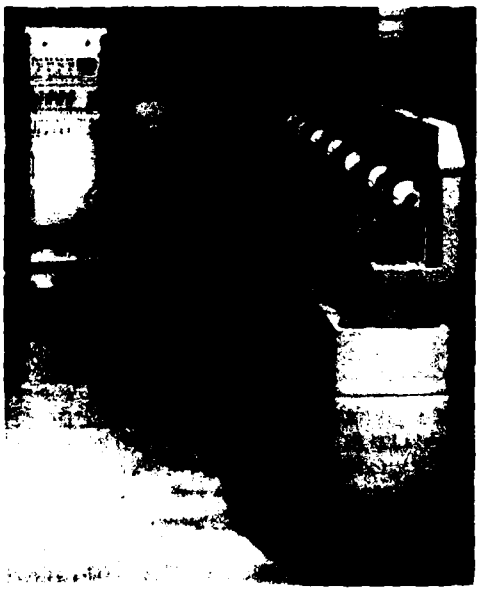

FIGURE 4. APPARATUS FOR ULTRASONIC INSPECTION OF THIN-WALL TUBING (From Ref. 7, Reproduced by permission of The American Society for Nondestructive Testing Inc., Columbus, OH)

Data processing functions included in the system produced statistical information for production control purposes and specific information on each tube for research purposes. Data were punched in cards to provide permanent, reusable records of inspection results.

Another automatic machine for testing tubes was reported by Kyte and Whittington (Ref. 8) to accomplish

inspection of tubes at production line speed. Twenty-four fixed transducers mounted on a ring which surrounded the tube to be inspected, were pulsed in sequence at the rate of 8,000/s while the tube was rotated about its axis at 277 rev/min. With this pulse rate and tube rotation speed, the entire periphery of the tube was inspected. Axial inspection speeds on the order of 0.67 m/s (2.2 ft/s) were practical.

A mechanical system, which could accommodate tubing diameters ranging from 12.5 to 50 mm (0.5 to 2.0 in.), provided for (1) moving tubes one at a time through the test head with the required helical motion, (2) marking the position of a defect, and (3) transferring the tube to an acceptance or rejection rack. Electronic circuitry handled sequential pulsing of transmitting transducers, reception of signals from corresponding receiving transducers, flaw signal detection, and alarm output. A paint-spray system operated by the alarm circuitry made a permanent record on the tube of flaw location and extent.

Lewis and Cornforth (Ref. 9) described another automatic tube inspection system designed to accommodate tubing in the diameter range of 170 to 460 mm (6.7 to 18 in.) and in the wall thickness range of 5 to 25 mm (0.2 to 1 in.). In this apparatus, eight transducers were mounted on a test head which rotated at 100 rev/min about the tube to be inspected. Linear tube speed up to 0.5 m/s (1.6 ft/s) was possible. Each transducer was coupled to the tube surface by a water jet. Four of the transducers monitored tube wall thickness and indicated laminar defects; the other four transducers detected radially oriented defects. Two electronic units separately processed laminar and radial signals. Both visible and audible alarms were provided when a defect was detected, and a paint mark was made on the tube in the area of a defect. Permanent records in the form of strip charts were prepared by the system. Figure 5 is an overall view of the rotary probe system installed in a tubing plant, and Figure 6 is a close-up view of the rotary inspection head.

FIGURE 5. OVERALL VIEW OF TUBE INSPECTION SYSTEM INSTALLED IN AN OPERATING PLANT (From Ref. 9, Reproduced by permission of IPC Science and Technology Press, Ltd., Guildford, England)

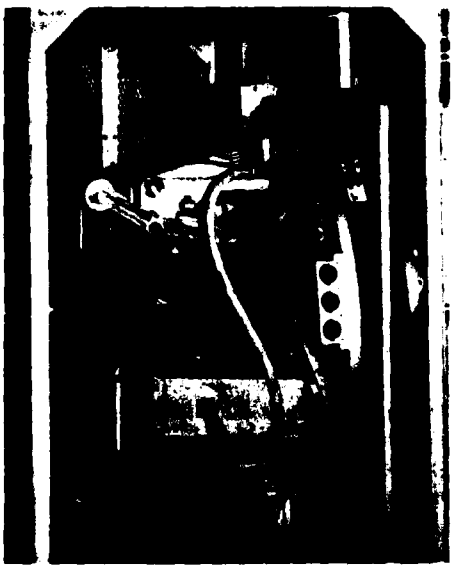

FIGURE 6. CLOSE-UP VIEW OF ROTARY TRANSDUCER HEAD IN TUBE INSPECTION SYSTEM (From Ref. 9, Reproduced by permission of IPC Science and Technology Press, Ltd., Guildford, England)

Winters and his colleagues (Refs.,10-14) have developed an automated crack position and depth measurement device for use on cannon tubes. Cracks in cannon tubes generally initiate at the root of the rifling and grow radially outward. The apparatus, illustrated in Figure 7, employed a single transducer which was scanned over the external surface of the cannon tube. Transducer position was continuously monitored, and crack depth and transducer location were recorded on digital magnetic tape at each detected maximum of crack depth. A computer routine

translated raw data into a crack map, such as that illustrated in Figure 8, which represents the developed exterior surface of a short length of cannon tube (shown to the left of the equipment in Figure 7). The angle coordinate of the map corresponds to angular position about the axis of the cannon tube in a plane perpendicular to the axis. The distance coordinate of the map refers to length along the cannon tube parallel to the axis. Numbers printed on the map represent maximum crack depth in inches measured from the interior surface of the cannon tube at that point. When a series of such numbers appear in a straight line as shown in Figure 8, they represent extended cracks in the cannon tube wall. Since cracks tend to follow the roots of the rifling and since rifling is helical, crack lines appear slanted in the developed map of Figure 8.

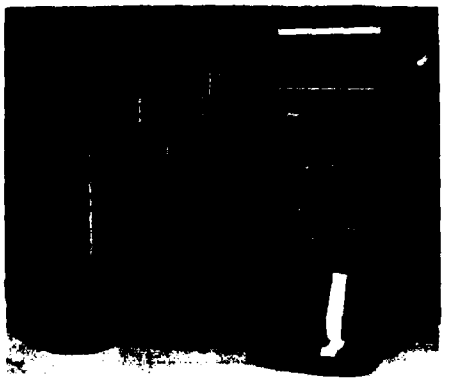

FIGURE 7. PHOTOGRAPH OF CANNON-TUBE CRACK MEASUREMENT SYSTEM
(From Ref. 13, Reproduced by permission of U.S. Army Watervliet Arsenal, Watervliet, NY)

D. Weld Inspection

Thousands of feet of weld joints in the tanks of a large liquified petroleum gas (LPG) tanker required inspection. In the past,

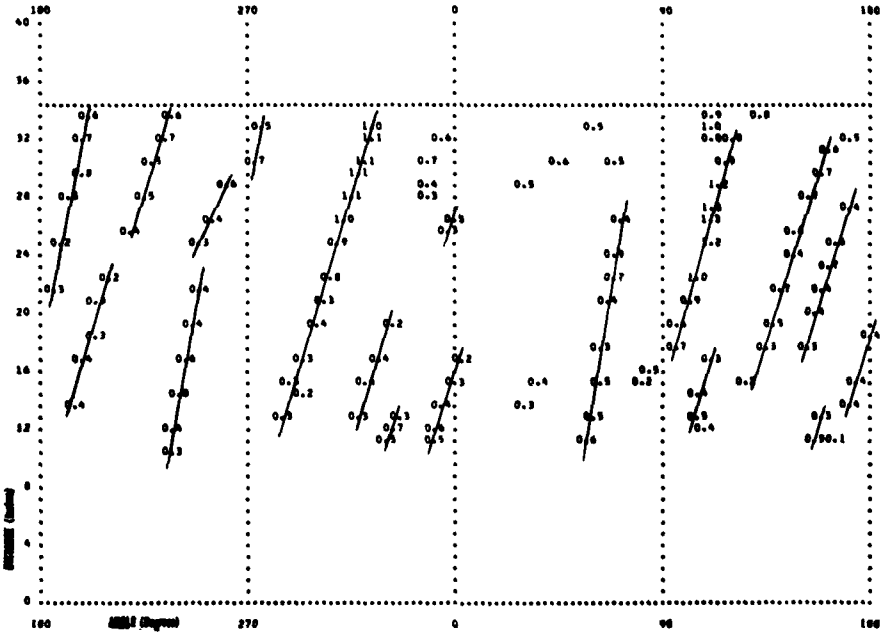

FIGURE 8. MAP OF CRACKS IN A CANNON TUBE (From Ref. 10, Reproduced by permission of U.S. Army Watervliet Arsenal, Watervliet, NY)

100-percent radiographic inspection was employed. Because this technique was very expensive and slow, Suzuchi and Kikuchi (Ref. 15) developed an automated ultrasonic device for inspecting welds in steel plate 6 to 30 mm (0.25 to 1.25 in.) thick. A mechanized probe traveler followed the weld and carried two or three angle transducers at a speed of 1.7 to 40 mm/s (0.07 to 1.6 in./s). Supporting electronics, mounted in a portable cart, provided transducer excitation and defect recording functions. Strip chart records of flaws detected by the ultrasonic probes were generated by the electronics package. It was reported that during early use of the automated ultrasonic weld-inspection device, radiographs were made of the same areas inspected ultrasonically; it was found that no defects were missed by the ultrasonic system, so further radiography was abandoned.

E. Experiment Supervision

In the laboratory where frequent ultrasonic nondestructive evaluation experiments are conducted, a *dedicated* automated inspection system normally cannot be justified because of cost. However, Gieske (Ref. 16) and Stiefeld (Ref. 17) have reported a "roll-around" computerized nondestructive evaluation experiment supervision system which was built around a minicomputer, as illustrated in the block diagram of Figure 9, coupled with a variety of peripheral units. The system was packaged in a pair of relay racks as shown in Figure 10, and the racks were mounted on a dolly for portability. The computer interface contained signal-conditioning apparatus, analog-to-digital and digital-to-analog converters, relays and other functional interface devices required to facilitate interconnection between the computer system and experimental apparatus and to provide control over certain *functions of the experiment. Figure* 11 illustrates the peripheral panel through which connections to experimental apparatus were made. Multi-pin connectors were provided so that frequently conducted experiments could be quickly and repeatably connected to the computer system; banana plug connectors were provided for infrequent *experiments where the cost of* preparing a cable and connector was not justified. In addition, the banana plug connectors provided simple means of adding connections not included in the cable.

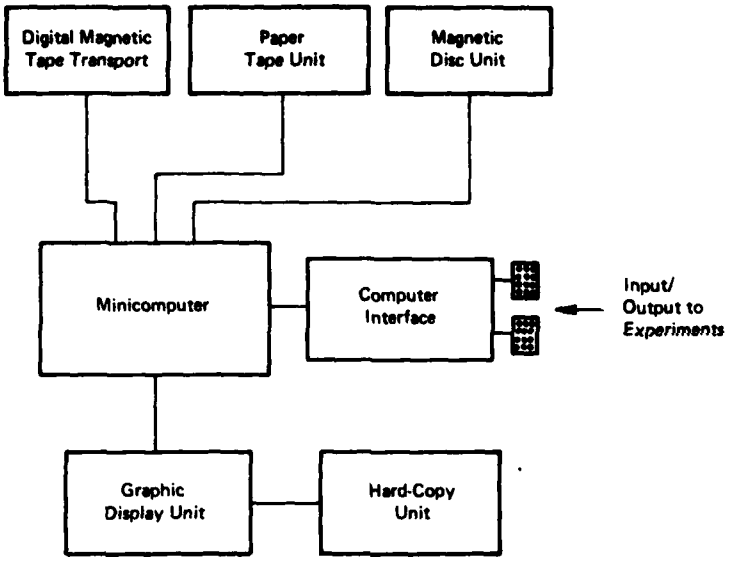

FIGURE 9. BLOCK DIAGRAM OF COMPUTER-CONTROLLED EXPERIMENT SUPERVISION SYSTEM (From Ref. 16, Reproduced by permission of IIT Research Institute, Chicago, IL)

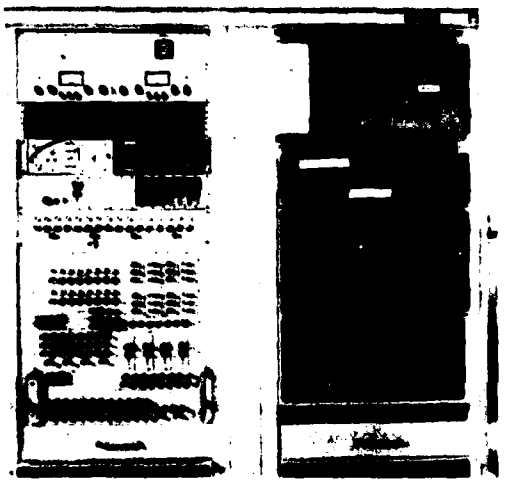

FIGURE 10. COMPUTER-CONTROLLED EXPERIMENT SUPERVISION AND DATA ACQUISITION SYSTEM HARDWARE (From Ref. 17, Reproduced by permission of The American Society for Nondestructive Testing, Inc., Columbus, OH)

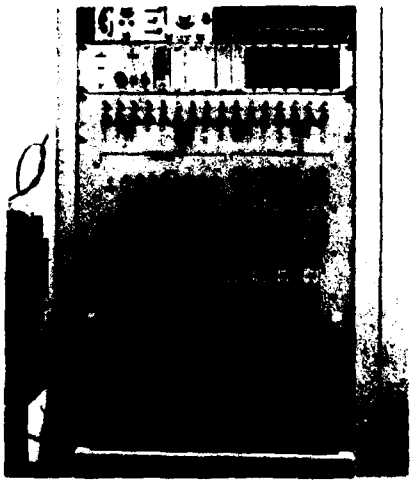

FIGURE 11. CLOSE-UP OF COMPUTER-CONTROLLED EXPERIMENT SUPERVISION SYSTEM INTERFACE PANEL (From Ref. 17, Reproduced by permission of The American Society for Nondestructive Testing, Inc., Columbus, OH)

The system was designed so that personnel relatively inexperienced in computer technology could easily prepare programs for data acquisition and processing. Data could be recorded on digital magnetic tape or paper tape for future display or for subsequent signal processing on the minicomputer contained in the experiment supervision system or on another computer. A variety of data display formats could be generated using the computer and the graphic terminal.

III. TECHNIQUES

A. Signal Processing

1. General

As demand for increased material performance has developed, requirements for more detailed information about nondestructively detected defects have increased. In the early days of nondestructive evaluation, it may have been adequate to merely note the existence of a defect or flaw, but the need for precise definition of flaw location quickly became evident. Now, in many cases, even precise flaw location is not sufficient information; defect size, shape, orientation and composition have been added to the list of flaw characteristics which should be defined so that the effects of the flaw on material properties can be estimated. For very large defects, some of these characteristics can be measured or estimated by transducer scanning; however, for smaller, but still important defects, less direct methods of flaw characterization are required. Electronic signal processing applied to radio-frequency (i.e., not rectified or filtered) ultrasonic echo signals shows promise as a means of accomplishing flaw characterization. Signal averaging, filtering and correlation have been used to extract weak signals from incoherent noise; deconvolution has been applied to improve system resolution; and deconvolution and spectral analysis have been used together to elicit flaw characterization information from ultrasonic echoes.

A number of general applications of signal processing to ultrasonic nondestructive evaluation have been listed by Erikson *et al.* (Ref. 18), Kennedy and Woodmansee (Ref. 19), and Rose and Meyer (Refs. 20 & 21). The work of Erikson *et al.* (Ref. 18) is an exhaustive review of ultrasonics as applied to medicine, and it covers not only signal processing, but many other areas of ultrasonics. This particular paper contains an extensive bibliography of 376 references, many of which are of interest to persons engaged in nondestructive evaluation work.

2. Spectral Analysis

Gericke (Ref. 22) first suggested use of spectral analysis (or spectroscopy) of ultrasonic pulses as a means of eliciting flaw geometry information. He showed that spectral energy distribution of an ultrasonic pulse is influenced by geometry of the defect from which it was reflected.

In implementing spectroscopy for nondestructive evaluation, it is necessary to use a wideband transmitting transducer excited by a short-duration (i.e., broadband) signal. Echo signals from the receiving transducer are passed through a wideband amplifier into a spectrum analyzer. If desired, the reflected signal waveform may be simultaneously displayed as a time function on an oscilloscope. A reference spectrum, which contains the frequency response characteristics of the transducers and the receiving system and the spectral characteristics of the transmitted pulse, is determined by analysis of the back echo from a test block on which the transducer is temporarily placed. The transducer is then transferred to a test specimen, and the spectrum of the echo from a flaw or a group of flaws is determined. In some cases, particularly where only a comparison is desired, the spectrum thus obtained may be used directly; more frequently, however, where quantitative results are desired, it is necessary to subtract the reference spectrum from the spectrum of an unknown defect. If the spectra of a family of similar defects (e.g., a series of flat-bottom holes of various diameters) are known, then the spectrum of the unknown defect may be compared with known spectra, and a certain characteristic of the unknown defect (to continue the example, the unknown diameter of a flat-bottom hole) may be determined.

There is a significant body of literature related to ultrasonic spectroscopy. Papers by Gericke (Refs. 22 through 25), Whaley *et al.* (Refs. 26 through 30), Seydel and Frederick (Ref. 31), Papadakis (Ref. 32), Yee *et al.* (Ref. 33), and Baryshev (Ref. 34) describe a wide range of nondestructive evaluation applications of spectroscopy.

Figure 12 (Ref. 24) shows the spectra associated with three grades of steel having markedly different microstructures. The spectra exhibit decreasing energy content above 8 MHz as grain size increases.

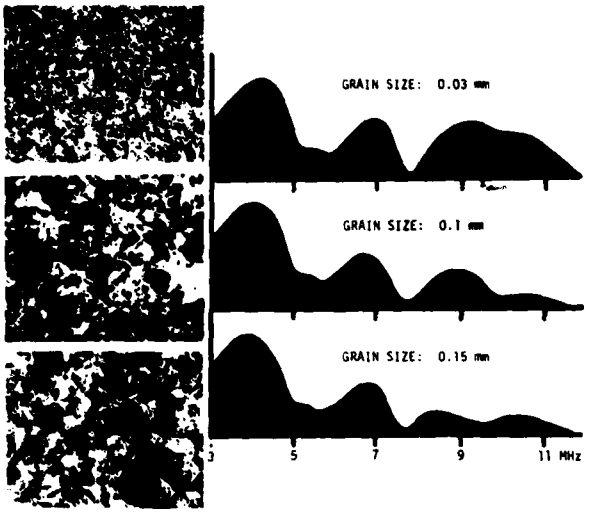

FIGURE 12. SPECTRA ASSOCIATED WITH VARIOUS GRAIN SIZES IN STEEL. (From Ref. 24, Reproduced by permission of the American Institute of Mining, Metallurgical and Petroleum Engineers, Inc., New York, NY)

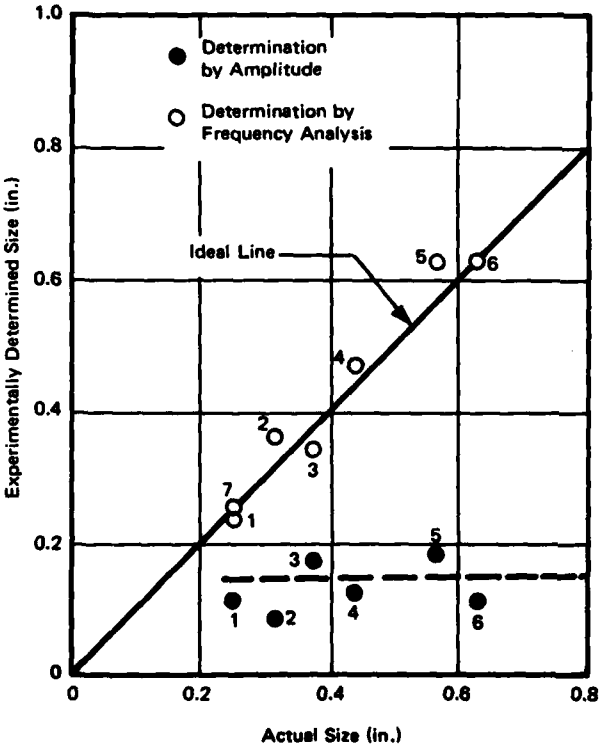

FIGURE 14. COMPARISON OF TWO METHODS OF MEASURING HOLE SIZE (From Ref. 28, Reproduced by permission of Noordhoff International Publishing, Leyden, The Netherlands)

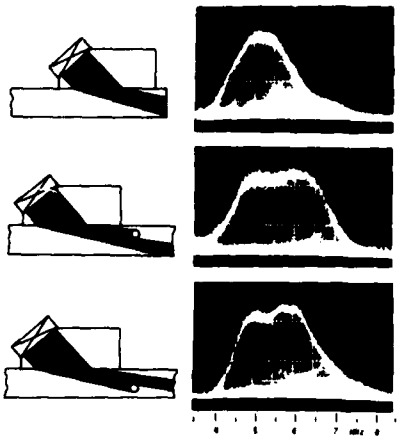

FIGURE 13. SPECTRA OBTAINED WITH A 30° ANGLE-BEAM PROBE GENERATING TRANSVERSE ULTRASONIC WAVES IN A 1.5-INCH-THICK ALUMINUM PLATE. Top Trace: Spectrum of Echo Reflected from Edge; Middle and Bottom Traces: Spectra of Echoes Reflected from Cylindrical Holes of 0.040 Inch Diameter Located in Different Positions. (From Ref. 25, Reproduced by permission of The American Society for Nondestructive Testing, Inc., Columbus, OH)

Figure 13 (Ref. 25) illustrates the effect of varying positions of a defect within an ultrasonic beam. The upper spectrum in Figure 13 was the reference spectrum, whereas the remaining two spectra indicated the effects of an artificial defect in two locations in the beam. Presence of the defect introduced significant spectral content in the vicinity of 6 MHz, and position of the defect within the beam altered the magnitude of the 6-MHz spectral peak and changed the slope of the high-frequency skirt of the spectrum.

Figure 14 (Ref. 28) compares two methods of measuring the diameters of flat-bottom holes oriented at various angles to the surface of a test block. Estimates of hole diameter made from echo amplitude measurements are represented by filled dots in the figure; hole sizes measured by this method were relatively constant and consistently incorrect. It is readily apparent that hole sizes measured by spectral (frequency) analysis techniques, represented by open circles in Figure 14, agreed satisfactorily with true hole sizes (i.e., spectral analysis points lay near the ideal line).

Figure 15 (Ref. 30) illustrates the effect on echo spectrum of slightly different wall thicknesses in a thin-wall tube. A variation of approximately 10 percent in wall thickness shifted the prominent spectral valley by one megahertz.

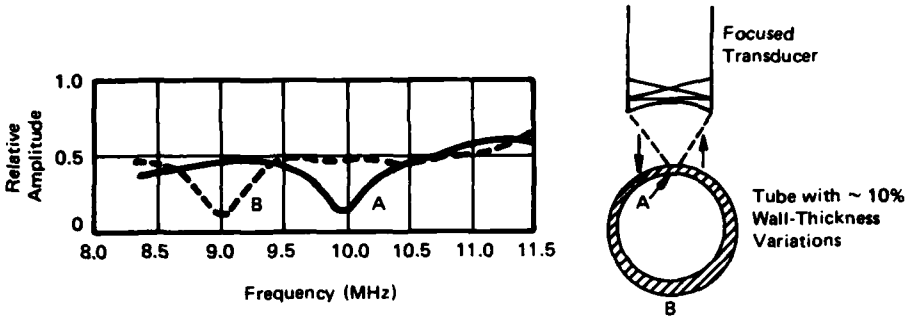

FIGURE 15. SPECTRA OBTAINED FROM TWO LOCATIONS ON A TUBE HAVING WALL-THICKNESS VARIATIONS (From Ref. 30, Reproduced by permission of The American Society for Nondestructive Testing, Inc., Columbus, OH)

The spectra of Figure 16 (Ref. 32) were generated in a study of ultrasonic double refraction in worked metals. Transverse (shear) waves of three nominal frequencies (1.0, 2.25, and 5.0 MHz, respectively) were propagated in directions transverse to and parallel with the material orientation axis induced by rolling, and at 45 degrees between these two directions. For the 45-degree propagation direction, nulls in the spectrum were evident. From these nulls it was possible to calculate the fractional velocity difference between orthogonally polarized waves propagating in the material. For aluminum with moderate texture the fractional velocity difference was determined to be 0.021.

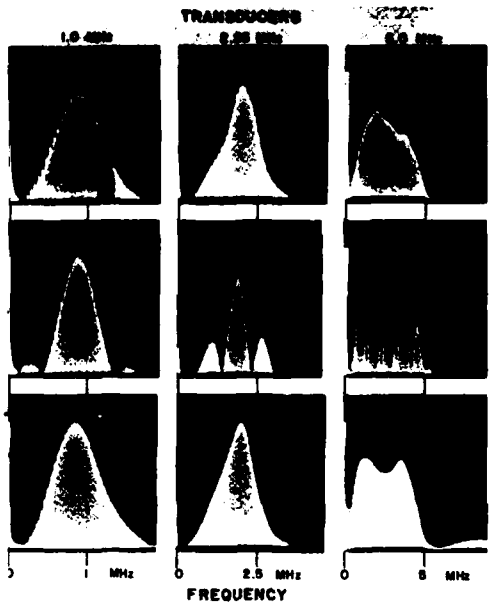

FIGURE 16. SPECTRA OF FIRST ECHOS FROM SPECIMEN AT THREE TRANSDUCER NOMINAL FREQUENCIES AND AT THREE POLARIZATIONS WITH RESPECT TO THE ROLLING DIRECTION (From Ref. 32, Reproduced by permission of the American Institute of Physics, New York, NY)

3. Signal Averaging

Signal averaging is a process by which a recurrent signal can be extracted from incoherent noise even though the initial signal-to-noise ratio is quite poor. The principle behind signal averaging is that a coherent, repetitive signal synchronously added to itself n times increases in amplitude by a factor of n, while incoherent noise added to itself n times increases by a factor of only $\sqrt{n}$. Thus, after n iterations, the signal-to-noise ratio will be improved by a factor of $\sqrt{n}$. Limitations of the process include (1) the signal must be repetitive and (2) coherent noise (e.g., stray reflections in an ultrasonic nondestructive evaluation system) is not reduced by signal averaging. In spite of these limitations, signal averaging does facilitate extension of inspection range in large specimens or highly attenuating materials. Kennedy and Woodmansee (Ref. 19) have used signal averaging to enhance clarity of flaw indications in an electron-beam weld. Additionally, these investigators have used signal averaging to improve signal-to-noise ratio in through-transmission inspection of honeycomb composites. McSherry (Ref. 35) has used signal averaging with other techniques to improve image quality obtained from conventional ultrasonic scanners.

4. Correlation

Correlation is a mathematical process which indicates waveform similarity between two functions which, in ultrasonic nondestructive evaluation applications, are usually electrical signals. The process involves (1) introducing a variable time delay between the two signals (which, incidentally, may be the same signal, in which case the process is called "autocorrelation," or different signals, in which case the process is called "cross correlation,"),

(2) multiplying the first signal by the delayed second signal, and (3) averaging the product over a long time period. The result of this process is referred to as the "correlation function." Magnitude of the correlation function is directly related to the degree of similarity between the two signals; that is, the correlation function is normalized to unity for signals of identical waveform. Zero correlation indicates totally unrelated signal waveforms. The value of delay corresponding to a peak in the correlation function is the amount by which one signal must be shifted in time with respect to the other to produce maximum waveform similarity. For example, the autocorrelation function of a sinusoid is a cosinusoid; that is to say, at zero delay and at delays corresponding to integral multiples of 180 degrees (i.e., the positive and negative peaks of the cosine function), maximum similarity occurs between the sinusoid and a delayed replica of itself. A negative peak indicates the same degree of similarity as a positive peak of equal magnitude, but implies that the two correlated functions are inverted replicas of each other.

Waidelich (Ref. 36) has applied correlation to extracting a signal from uncorrelated random noise. Random noise has zero autocorrelation for all values of delay except near zero. Thus, at points removed from zero delay, the correlation function of a periodic signal plus noise equals (nearly) the periodic signal. Although Waidelich applied correlation to signals from eddy current testing, validity of correlation is independent of signal source, so a similar approach can be applied to ultrasonic signals.

If a signal of approximately known waveform is buried in noise, time location of that signal is possible by correlating the noisy signal with a signal of similar waveshape (e.g., the transmitted signal). Such a technique is useful in ultrasonic inspection of highly attenuating materials where received signals may be hidden in receiver noise.

Newhouse and his associates (Refs. 37 and 38) developed a correlation technique which achieved significantly greater signal-to-noise ratio than was possible with conventional pulse-echo methods. In this system, a block diagram of which is presented in Figure 17, a wideband transmitting transducer was

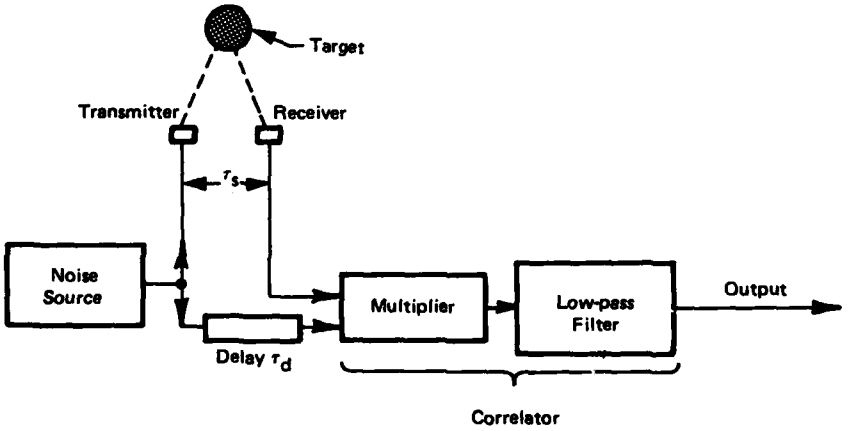

FIGURE 17. BLOCK DIAGRAM OF RANDOM NOISE SIGNAL PROCESSING
(From Ref. 37, Reproduced by permission of IPC Science and Technology Press, Ltd., Guildford, England)

excited by a random-noise source. Echoes from a target (i.e., a flaw in a material specimen) were converted by an identical receiving transducer to electrical signals. The received signal was then correlated with a delayed sample of the transmitted signal as shown in the block diagram. Because the transmitted signal was random, correlation between the transmitted and received signals occurred only at a value of delay corresponding to the total signal propagation time from transmitting transducer to target to receiving transducer. Since this system could transmit almost continuously, relatively low peak-to-average transmitted power ratio was possible. Signal-to-noise ratio enhancement obtained in wideband systems employing correlation techniques should be particularly suitable for application to highly attenuating materials where weak return signals are often encountered.

Correlation techniques have been applied by Kennedy and Woodmansee (Ref. 19) in detection of artificial flaws in a titanium test block. A single transducer insonified an artificial flaw, and four receiving transducers, all aimed at the same elemental volume in the test specimen, received energy scattered from the defect. As expected, signals received by various transducers from artificial flaws were not of equal strengths. Cross correlation of various combinations of receiving transducer outputs equalized responses from different sizes and types of flaws and improved signal-to-noise ratio.

An analog technique for computing approximate auto- and cross-correlation functions of ultrasonic echoes was reported by Yamshchikov and Nosov (Ref. 39). With the aid of block diagrams, this paper described (1) a noise generator, (2) an analog spectrum analyzer, and (3) an analog correlation analyzer. The reasons cited for use of analog rather than digital computation were reductions in weight, size, and power consumption. The noise generator was intended to drive a wideband transmitting transducer which launched a random wave into the material being inspected. A single wideband receiving transducer, followed by suitable amplification, fed the analog spectrum analyzer. Two wideband receiving transducers, each followed by suitable amplification, drove the two inputs of the analog correlator. Flaws in such materials as rock and concrete could be detected by this system.

Koryachenko (Ref. 40) described a potential difficulty in systems employing correlation. Normally, correlation rejects random (i.e., uncorrelated) noise. However, noise resulting from reverberation of the ultrasonic signal within the specimen being inspected is not necessarily uncorrelated. Reverberation noise, then, may interfere significantly with signal-to-noise ratio enhancement by correlation methods. Koryachenko reported that signal-to-reverberation-noise ratio could be enhanced by a factor of 10 to 15 by (1) frequency modulating transmitted ultrasonic pulses, (2) using pulses having a small product of bandwidth and duration, and (3) separating the axes of the transmitting and receiving transducers by an angle between 20 and 30 degrees. These actions tended to decorrelate reverberation noise and thereby minimized interference from that source.

5. Filtering

In many cases signal-to-noise ratio in ultrasonic systems can be improved by rejecting certain portions of the received signal spectrum. For example, receiver noise increases in proportion to the square-root of bandwidth; thus, it is evident that excessive bandwidth will result in increased noise and, hence, degraded signal-to-noise ratio. If the transmitted pulse is a coherent burst containing several cycles of the carrier frequency, then most of the useful energy is contained in a relatively narrow band centered about the carrier frequency. Thus, signal-to-receiver-noise ratio can be maximized by limiting receiver bandwidth to that required to adequately pass the ultrasonic pulse.

More sophisticated types of filters (in the broadest sense of the word) can be matched to a particular set of signal and noise conditions to achieve maximum signal-to-noise ratio. In addition, systems involving computers can be made to learn the characteristics of one or more classes of defects and then classify an unknown defect in accordance with the pattern it has learned. Although such learning networks or filters are relatively recent innovations, interest in them is developing, and some experimental work (described in a later paragraph) is in process.

McSherry (Ref. 35) used a digital band-pass filter through which radio-frequency echo signals were passed to improve the appearance of a display and to reveal details in displayed signals which were originally masked by low-frequency components. In the example cited by this author, a 40-kHz to 1-MHz, 19-point digital filter with high and low rejection slopes of 3 dB per 4 kHz was used to process echo signals from a diseased heart valve. Rejection of high frequencies reduced general clutter in the display, and rejection of low frequencies reduced dynamic range and improved discrimination of detail.

Waidelich (Ref. 36) briefly described use of passive low-, high-, and band-pass filters to reject noises which interfered with signal interpretation. Of course, to obtain benefit from such filtering, it was necessary that frequencies of interfering noises were not the same as desired signal frequencies. In the case of a system employing a number of frequencies, a "comb" filter, comprising a number of relatively narrow band-pass filters, was used to advantage.

In the more common case, undesired noise has components in the same frequency range as the signal. In this case, a special filter, referred to as a "matched filter," can be designed to incorporate known characteristics of the signal and of the noise in such a way as to approximately maximize signal-to-noise ratio.

Low-pass, high-pass and band-pass filter functions can be programmed on a digital computer. Thus, if ultrasonic echo signals are available in digitized form, then digital filtering can be employed.

Adaptive nonlinear learning networks constitute a class of digital filters which can be "taught" to recognize the signature of a certain type of defect and to give quantitative indication of some defect parameter. A typical adaptive learning network measures a wide range of echo signal parameters, including, for example, amplitude, time delay, frequency spectrum, autocorrelation function, power density spectrum, and special functions or parameters derived from any combination of these. The network is taught by inputting echo signals from a range of similar defects (called the "fitting set") which vary in one characteristic. A digital computer operates on the measured parameters of the echo signals and upon the known characteristics of the fitting set of defects to, in effect, fit a complex equation to the available data. A second set of known defects, called the "selection set", is used to refine the adaptive learning network by eliminating those echo signal parameters which have small effect. After completion of the learning and refinement processes, the network may be fed the echo signal from an arbitrary flaw of the same general type used in training. The network then computes the value of the specific defect characteristic which it was trained to recognize and quantify.

Mucciardi *et al.* (Ref. 41) reported use of an adaptive nonlinear learning network to measure diameters of flat-bottom holes drilled to uniform depths in metallic test blocks. Ultrasonic pulse-echo signals were used as inputs to the network. Three sets of test blocks were used in developing the network; these were called the "fitting," "selection," and "evaluation" sets whose purposes were, respectively, (1) to train the network initially, (2) to refine the network and eliminate relatively insignificant variables, and (3) to test the trained network. Out of 96 candidate waveform parameters, 15 were found to contain information about flat-bottom hole diameter. These included parameters related to shape, area and frequency content of certain parts of the received signal. It is interesting to note that echo amplitude, which is often used to estimate defect size, was not significant in the adaptive learning network for flat-bottom hole diameter measurement. The resulting adaptive learning network implemented an eighth-degree function of the 15 input waveform variables. The reported synthesized nonlinear adaptive learning network correctly measured the diameters of 46 out of 48 flat-bottom holes in the evaluation set.

6. Deconvolution

Deconvolution is a process for removing the effects of signal path characteristics from a received signal. It is, in effect, a process of inverse filtering. For example, if a complex signal passes through an amplifier with deficient high-frequency response, alteration of the signal waveform will result. But, if the frequency response characteristic of the amplifier is known, then signal distortion introduced by the amplifier can be removed from the signal, and the waveform of the signal, had the frequency response of the amplifier been adequate, can be determined. Deconvolution can be a time-domain process, or by means of the Fourier transformation, can be a frequency-domain process. In the frequency domain, deconvolution is a relatively simple multiplicative operation.

McSherry (Ref. 35) used a standard least-squares technique to design a deconvolution filter which increased resolution of closely spaced ultrasonic echo signals. Figure 18a illustrates a typical test apparatus in which the target was a group of 0.3-mm (0.012-in.)-diameter wires, the first of which was 40 mm (1.6 in.) from the transducer. The two wires nearest the transducer were approximately 1 mm (0.040 in.) apart, and the third and fourth were 10 and 20 mm (0.4 and 0.8 in.), respectively, from the first wire. Figure 18b compares the original data and the deconvolved data. It is apparent that the first two wires were not resolved in the original data, whereas separate echoes from the first and second wires were evident in the deconvolved data.

Seydel and Frederick (Ref. 31) implemented frequency-domain deconvolution as a means of improving ultrasonic pulse-echo inspection system resolution. The ultrasonic echo signal occurring inside of a time gate was processed by a spectrum analyzer, the digital output of which was sent to a digital computer. The computer, in turn, performed the necessary point-by-point multiplication and inverse Fourier transformation required to accomplish deconvolution. The authors presented experimental verification of the system and showed how complex echoes from closely spaced targets could be resolved by this technique.

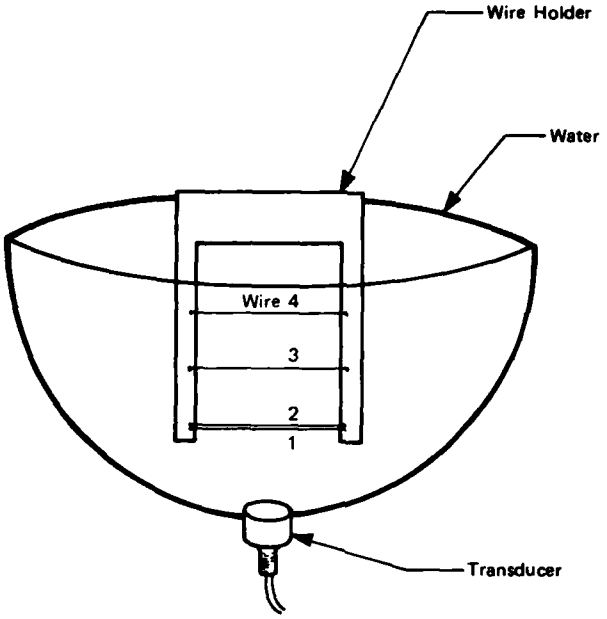

a. Apparatus

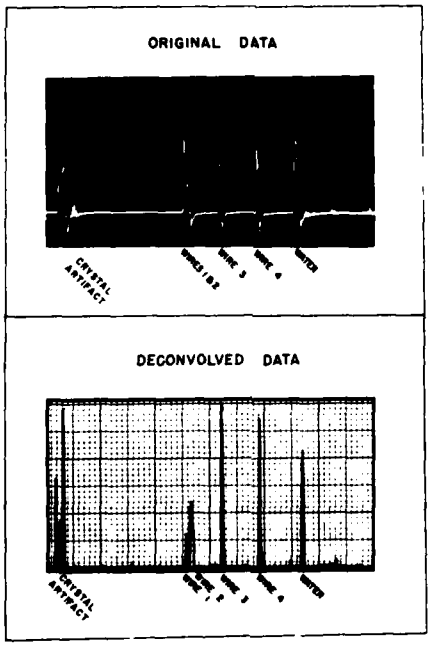

b. Data

FIGURE 18. ILLUSTRATION OF USE OF DECONVOLUTION TO IMPROVE DATA RESOLUTION (From Ref. 35, Reproduced by permission of the Institute of Electrical and Electronics Engineers, Inc., New York, NY)

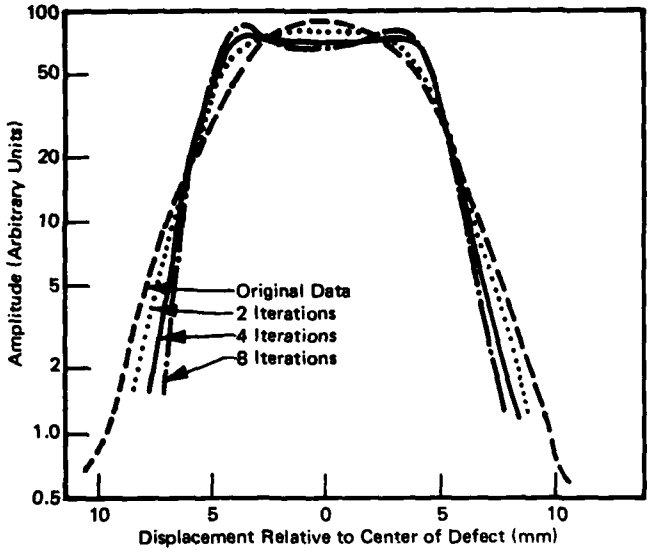

FIGURE 19. EFFECT ON DEFECT RESOLUTION OF MULTIPLE ITERATIONS OF THE DATA-UNFOLDING (DECONVOLUTION) PROCESS (From Ref. 42, Reproduced by permission of IPC Science and Technology Press, Ltd., Guildford, England)

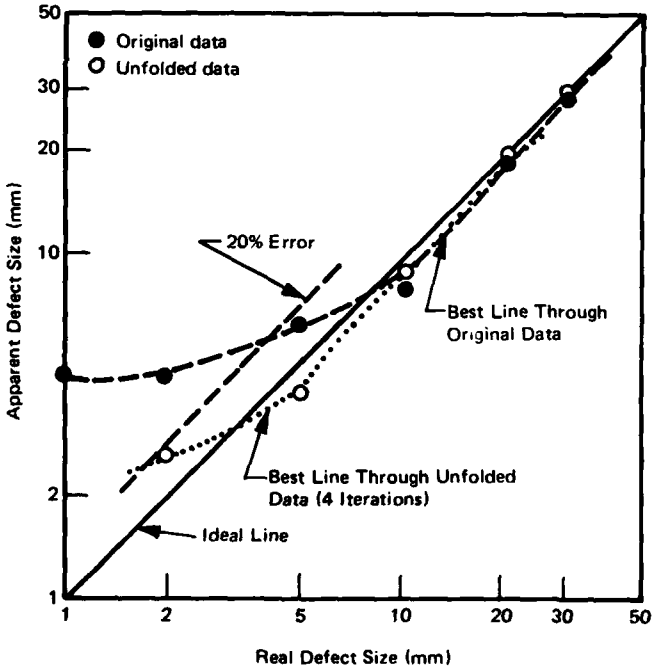

FIGURE 20. BENEFIT OF USING DATA UNFOLDING (DECONVOLUTION) IN ESTIMATING SIZES OF SMALL DEFECTS (From Ref. 42, Reproduced by permission of IPC Science and Technology Press, Ltd., Guildford, England)

Silk and Lidington (Ref. 42) have applied deconvolution (referred to as "data unfolding" by these authors) to increasing resolution in an ultrasonic system. They noted that the response observed in an ultrasonic inspection was the convolution of (1) the ideal response to a particular defect and (2) the response of the experimental system. A series of artificial defects ranging in width from 1 to 10 mm (0.04 to 0.40 in.) were scanned with an ultrasonic probe. Echo amplitude data were recorded at various positions of the transducer as it scanned the object. Because of beam spread and other effects, definition of the smaller defects was poor. Using the scan of the 1-mm (0.04-in.) defect as a definition of system response, an iterative solution of the deconvolution problem in matrix form was carried out on a computer. Typical results are shown in Figure 19 for the 10-mm (0.40-in.) defect located 200 mm (8 in.) from the transducer. The original data plotted as a relatively rounded curve which gave very poor definition of the edges of the defect. After eight iterations of the deconvolution process, skirts of the curve were significantly steeper, and edges of the defect were more clearly defined.

Figure 20 compares graphically the effects of data unfolding or deconvolution on estimating defect sizes. The diagonal straight line through the graph represents the ideal case where the measured defect size equals the true defect size. If data unfolding was not applied (i.e., the curve represented by filled circles) determination of defect size was in error by greater than 20 percent for defects smaller than 4 mm (0.16 in.) wide, whereas if data unfolding was applied (i.e., the curve represented by open circles), defects greater than approximately 1.7 mm (0.06 in.) wide were measured with less than 20 percent error. Thus, in the illustrated case, resolution improvement by a factor of 2.3 was achieved by application of iterative data unfolding (deconvolution).

B. Imaging

1. General

In all but the least sophisticated ultrasonic nondestructive inspection systems, information about size, shape, location, and character of a flaw is desired. One of the best means for conveying large quantities of information in an easily interpreted form is the picture or image. Because of the desirable properties of

an image, much research effort has been expended in developing ultrasonic imaging systems. Berger (Ref. 43) discussed a wide range of ultrasonic imaging methods capable of responding to intensities of 100 W/m^2 (10 mW/cm^2) or less. The primary emphasis of Berger's survey, however, was the Sokolov tube.

Erikson *et al.* (Ref. 18) surveyed a number of ultrasonic imaging methods used in medical diagnosis. Another survey by Jones (Ref. 44) described a variety of ultrasonic imaging methods with emphasis on acoustical holography. A very recent survey by Addison (Ref. 45) described a number of state-of-the-art ultrasonic imaging systems developed primarily for medical use. Addison pointed out that ultrasonic imaging systems developed for medical applications are significantly further advanced than corresponding systems used for nondestructive evaluation. Some of the advances in imaging techniques developed in the medical field should be applicable to nondestructive evaluation problems with little or no modification.

A number of specific ultrasonic imaging systems and techniques will be described in this section.

2. Sequenced Array

For purposes of this survey article, a sequenced array is a group of ultrasonic transducers arranged in a geometrical pattern (i.e., a line, a rectangle, a circle, etc.) with individual transducers used sequentially as transmitters, receivers, or both. This excludes phased arrays which are discussed in a later paragraph.

In many applications, a cross-section (B-scan) is required. Such a scan is often accomplished mechanically by moving the transducer in a line over the test specimen. Acquisition of data by this means generally requires a storage element in the system since the image is built-up relatively slowly as the transducer moves over the object. Digital memory or a storage oscilloscope can serve this function. However, in many medical applications, such as study and diagnosis of heart abnormalities, real-time B-scan display of a moving object is necessary. To avoid flicker, the image must be updated at the rate of about 30 frames per second. Bom *et al.* (Ref. 46) built a 20-element linear array transducer which could image a cross-section of the heart at a rate of 150 frames per second. Each element of the array had its own excitation and receiving circuitry. The image was presented on a standard cathode-ray-tube display.

Many ultrasonic imaging systems employ a lens to focus ultrasonic energy transmitted through or reflected from an object onto a receiving array. Harrold (Ref. 47) described one such system. A single transmitting transducer was used to insonify the object as illustrated in Figure 21a. Transmitted ultrasonic

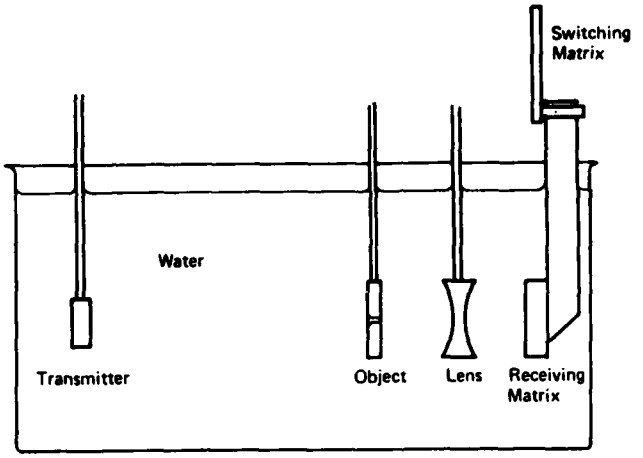

a. Apparatus

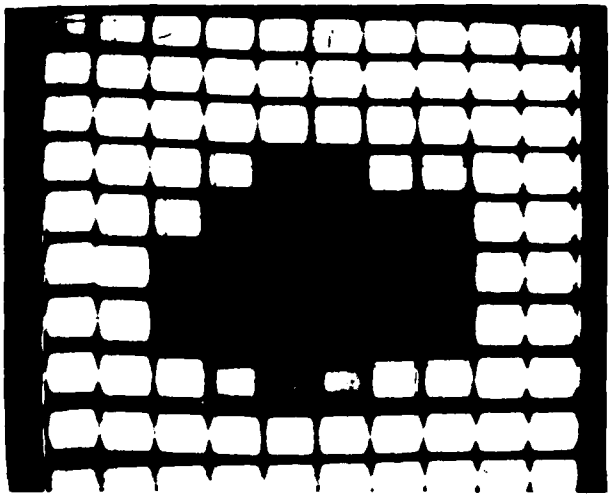

b. Image of 0.3-in. Diameter Hole in Aluminum Sheet

FIGURE 21. SEQUENCED ARRAY ULTRASONIC IMAGING SYSTEM (From Ref. 47, Reproduced by permission of IPC Science and Technology Press, Ltd., Guildford, England)

energy was focused by an acoustical lens on a 10 by 10-element array transducer. The effective aperture of the transducer was a 25-mm (1.0-in.) square. Each of the 100 elements was connected to a separate input of a 100-input, single-output switching matrix. A single channel of amplification and detection electronics followed. The referenced paper described in detail fabrication of the transducer array, design of the acoustical lens, and design of the electronic circuitry. An image produced by this system of a 7.6-mm (0.3-in.)-diameter hole in an aluminum sheet is shown in Figure 21b.

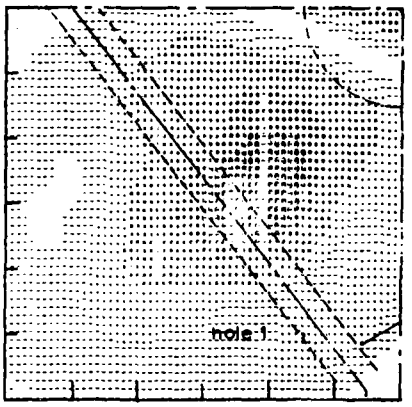

FIGURE 22. COMPUTER-PRINTED IMAGE SHOWING USE OF VARIOUS CHARACTERS TO PRODUCE GRAY-SCALE
(From Ref. 48, Reproduced by permission of The Institution of Electronic and Radio Engineers, London, England)

Maginness and Kay (Ref. 48) described a system employing a 12 by 12-element array transducer. The outputs of the transducer elements were digitized and stored on paper tape. After completion of data recording, computer processing was employed to generate an image of any chosen plane within the object. The visible image was generated on a standard computer line printer. Interpretation of the printed image was enhanced by using a series of characters of increasing ink coverage to display a few shades of gray as illustrated in Figure 22.

Maginness *et al.* (Ref. 49) fabricated an elaborate array transducer. The reported array was a 10 by 10-element structure made from a single plate of piezoelectric ceramic material backed with an array of silicon monolithic integrated-circuit field-effect transistor switches specially designed to handle high-level transducer excitation signals as well as low-level transducer output signals. With logic circuitry, a single element of the array could be addressed and used as transmitter and receiver in the pulse-echo mode. An acoustical lens, located between the object and the transducer array, focused the transducer array so that a single point in the interior of an object could be interrogated by a single array element. This approach minimized interaction among various elements of the array and signal degradation by stray reflectors in the acoustical path. To accompany this transducer, Maginness and his associates also designed analog signal processing circuitry including a high-power transmitter, receiving preamplifiers, swept-gain amplifiers, function generators, filters, gain compressors, and detectors. Additionally, a digital controller, which facilitated operation of the array in a variety of modes, was included.

Green *et al.* (Ref. 50) reported fabrication of an ultrasonic camera intended for soft-tissue examination. Either pulse-echo or through-transmission modes of operation were included. An acoustical lens system was used to form an image of the object on a horizontally oriented 192-element linear receiving array. Elements of the array were scanned sequentially to produce a single video line output. A pair of counter-rotating wedges located between lenses caused the ultrasonic image to be translated vertically past the line detector at a rate of 15 fields per second; thus, each scan of the linear array produced a new line of video information so that a two-dimensional image was displayed on a television monitor. Of course, the video signal could be recorded on magnetic tape for further review or processing. The reported system imaged with high resolution a field 150 by 150 mm (6 by 6 in.). A detection threshold of $0.1\mu W/m^2$ ($10pW/cm^2$) facilitated penetration of an appreciable thickness of tissue. Ultrasonic imaging portions of the system were mounted in a tubular structure which could be hand-held against the skin of the subject. Provision was included for focusing the image plane at various depths in the body being examined.

Knollman and Brown (Ref. 51) adopted a different approach to scanning the image field. A 100-element linear transducer array, sampled electronically, was used to generate one line of video data. Scanning in the vertical direction was accomplished by reflecting the image from an acoustical mirror which was rotated cyclically about an axis parallel to the linear transducer array. Mirror motion had triangular waveform so that the image was scanned first from top to bottom and then from bottom to top on the retrace. Vertical deflection was derived directly from mirror position by a linear variable differential transformer (LVDT).

Vertical and horizontal scans were not synchronized in this device. Details of construction, material selection, electronic circuitry, and performance specifications were presented in the referenced paper.

Knollman et al. (Ref. 52) reported another linear array transducer designed for underwater use in acoustical imaging and holography. This transducer was a 2.1-MHz, 16-element linear array sampled at 8000 elements per second to produce a line of video information. Images were obtained by translating or rotating either the array or the test specimen. Application of this transducer array in nondestructive evaluation was discussed.

Fabrication of a 256 by 256-element array of electrostatic transducers was reported by Alais (Ref. 53). Individual transducer elements in this array were miniature capacitor microphones which were polarized by an externally applied voltage. Scanning of the array was accomplished by switching the polarizing voltage to the particular element to be sampled at the proper time. This large array was used experimentally in acoustical holography and in acoustical imaging systems. Performance limitations were traced to noise in the multiplexing circuitry.

3. Focused

Because acoustical waves obey the same basic equations as optical waves insofar as imaging is concerned, it is possible to apply analogs of optical techniques in acoustical imaging. Perhaps the most obvious optical component to attempt to duplicate in acoustical form is the lens. As a matter of fact, many of the acoustical imaging systems mentioned in connection with sequenced array transducers employed acoustical lenses to form an image on the transducer (e.g., see Refs. 47, 49, and 50). There are other types of ultrasonic imaging systems employing lenses which use phenomena other than those normally employed in conventional transducers.

The principle of optical linearity, illustrated in Figure 23, has been translated by Hanstead (Ref. 54) into ultrasonic form. A three-dimensional *image* (represented by the points "A" through "I" on the left-hand side of the figure) of a three-dimensional *object* (represented by the points "A" through "I" on the right-hand side of the figure) is formed by a system of two confocal lenses (i.e., adjacent focal points coincident). The image is (1) inverted (that is, in Figure 23, the top row of points in the object appears in the bottom row of the image) and (2) pseudoscopic (that is, in Figure 23, the column of points nearest the lens in the object is farthest from the lens in the image and *vice versa*). In the optical case, the image can be viewed only from an axial position (P on the left-hand side of Figure 23).

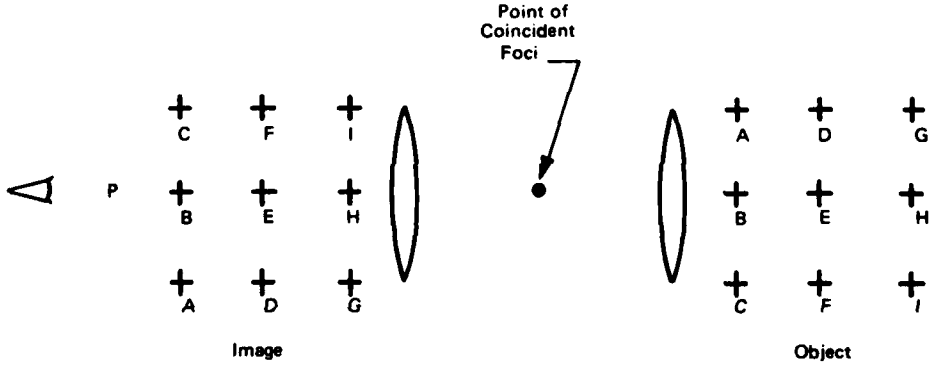

FIGURE 23. ILLUSTRATION OF OPTICAL LINEARITY (From Ref. 54, Reproduced by permission of The Institute of Physics, Bristol, England)

To make an ultrasonic imaging system using this principle, an object was insonified by a pulsed ultrasonic transducer as illustrated schematically in Figure 24. Reflected waves from boundaries of and defects in the object were imaged by an acoustical focusing system (a pair of confocal lenses) in an optically birefringent solid material labeled "imaging medium" in the figure. The acoustical focusing system was designed so that not only were acoustical waves brought to focus in the imaging medium, but so that the acoustical wavefronts which formed the image all arrived at their focal points simultaneously. Those points in the imaging medium where acoustic energy

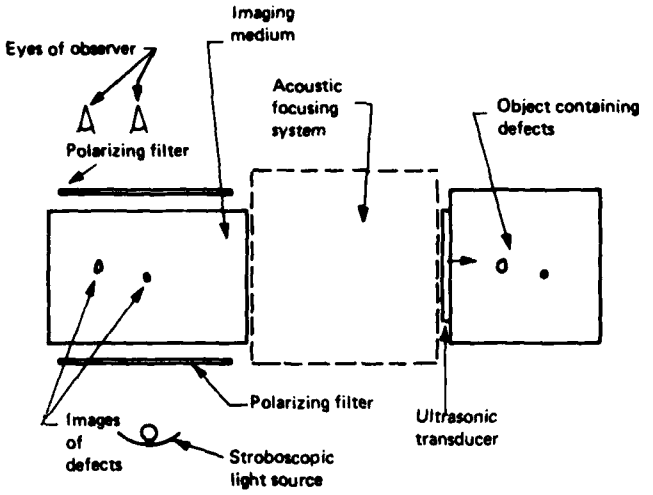

FIGURE 24. SCHEMATIC DIAGRAM OF ULTRASONIC IMAGING SYSTEM EMPLOYING PRINCIPLE OF LINEARITY (From Ref. 54, Reproduced by permission of The Institute of Physics, Bristol, England)

came to focus produced optical birefringent effects which were detected by viewing the imaging medium optically through crossed polarizers. Illumination for viewing was provided by a stroboscopic light source which was flashed at the instant that the acoustical wavefronts arrived at their focal points. Figure 25a illustrates a 25-mm (1-in.) cube of steel in which seven 1.5-mm (0.060-in.)-diameter holes had been drilled. Figure 25b illustrates the image of such a test block formed by the described imaging system. The two lines represent the transducer and the back face of the test block, respectively. The five dots are images of five of the drilled holes. The two outside holes do not show in the image since they were outside of the insonifying ultrasonic beam.

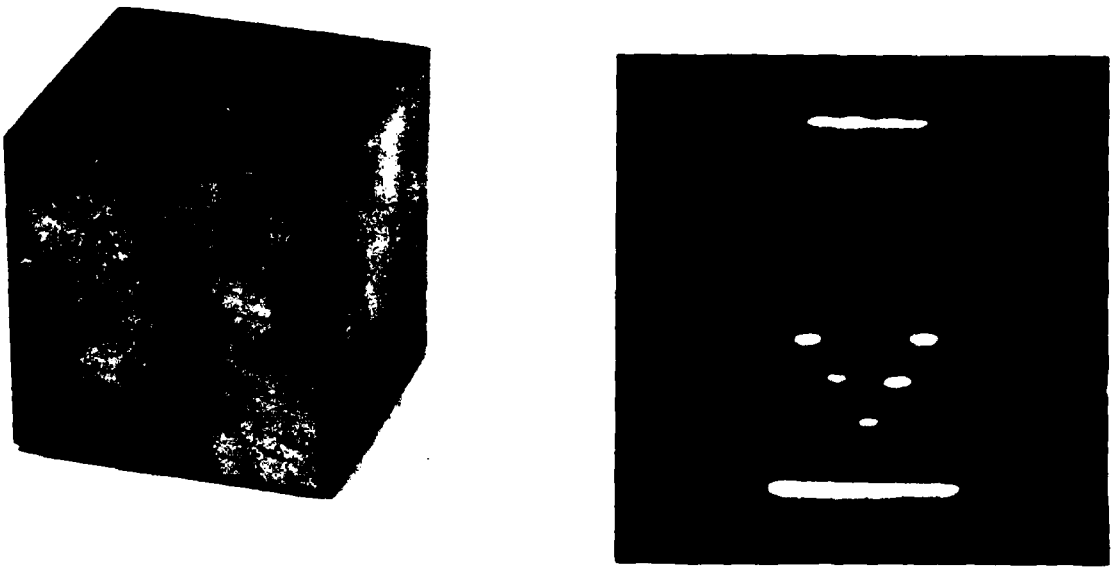

a. Original Object

b. Image

FIGURE 25. IMAGE OBTAINED WITH "LINEARITY" IMAGING SYSTEM (From Ref. 54, Reproduced by permission of The Institute of Physics, Bristol, England)

Mezrich *et al.* (Refs. 55 and 56) described another imaging system which utilized interaction between acoustical and optical waves. This system, shown schematically in Figure 26, employed an acoustical lens system to image ultrasonic waves passing through an object on a thin, metallized plastic film approximately 6 μm (240 μin.) thick. The film was immersed in the acoustical propagation medium which in this case was water. Passage of acoustical waves through the water medium displaced not only water molecules, but also localized areas of the thin metallized plastic film (called a "pellicle"). At an acoustic intensity level of 10 mW/m^2 (1 μW/cm^2), displacement amplitude of 1.5-MHz waves was on the order of 10 pm (0.1 Angstrom unit or 4×10^{-10} in.). Each point of the pellicle followed almost exactly the displacement amplitude of the wave at that point in the propagation medium.

To detect these very small motions, the metallized face of the pellicle was made the reflector in one arm of a Michaelson interferometer. A lens system and beam deflector provided for scanning the pellicle, which could have a diameter as large as 150 mm (6 in.). Even a minute displacement of the pellicle caused a phase shift in the reflected optical wave which was compared with a wave reflected from a plane mirror (the reference mirror) in the other arm of the interferometer. Illumination for the interferometer was provided by a laser. Changes in phase of the optical wave reflected from the pellicle produced small changes in intensity of the interferometer output, and such intensity changes were detected by a photodiode, the output of which was amplified and displayed on an oscilloscope.

In an optical interferometer, maximum sensitivity and linearity are obtained when the two interfering waves are 90 degrees out of phase. However, drift in optical interferometers can be substantially greater than the magnitude of displacements to be detected. To provide stability sufficient for detection of sub-Angstrom-unit displacements of the pellicle, Mezrich and his associates introduced cyclic vibratory motion of the reference mirror (referred to in Figure 26 as the "wiggler"). Frequency of wiggler motion was adjusted so that one full cycle of mirror vibration occurred for each picture element. Since maximum sensitivity occurred when the two interfering beams were in quadrature, peak output from the photodiode occurred at the point in the wiggler cycle at which quadrature existed. Peak detection in the photodiode circuit eliminated from consideration those parts of the signal for a particular picture element which were below maximum. Thus, only the peak signal for each picture element appeared in the display. This approach to system stabilization permitted detection of displacement amplitudes as small as 0.7 pm (0.007 Angstrom units or 28×10^{-12} in.) with a 15-mW helium-neon laser. At a frequency of 1.5 MHz, a displacement amplitude of 0.7 pm (28×10^{-12} in.) corresponded to an acoustic intensity of 50 μW/m^2. With a 1-W argon-ion laser, sensitivity could be increased to 0.1 μW/m^2 which is comparable with the most sensitive transducer systems presently available.

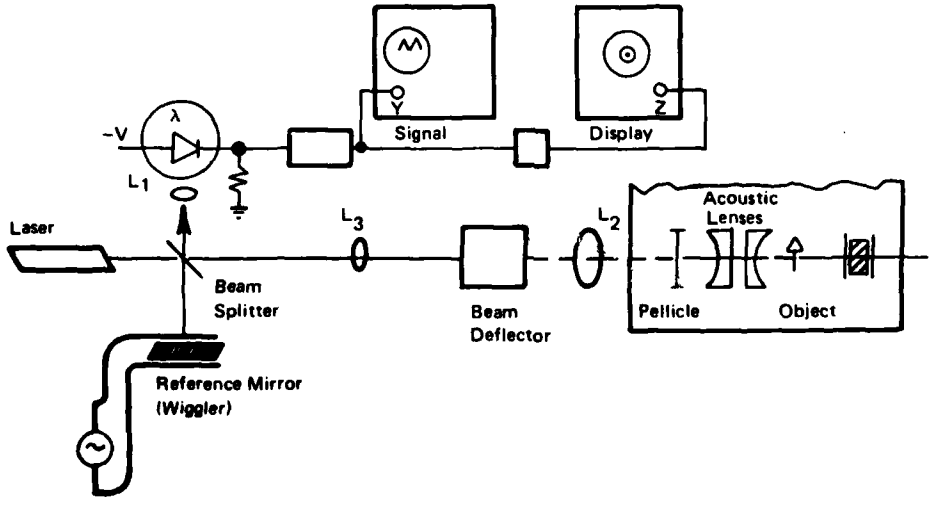

FIGURE 26. SCHEMATIC DIAGRAM OF ACOUSTICAL-OPTICAL INTERACTION IMAGING SYSTEM
(From Ref. 56, Reproduced by permission of the Institute of Electrical and Electronics Engineers, Inc., New York, NY)

4. Liquid-Surface Levitation

Liquid-surface levitation as an acoustical imaging technique was first proposed by Sokolov in 1929. Subsequently, liquid-surface levitation has been used in a number of acoustical imaging applications, and more recently has been used as a method of generating acoustical holograms. Because acoustical holography is a separate heading in this state-of-the-art survey, holographic applications of liquid-surface levitation are discussed later.

Acoustical waves reaching the surface of a liquid propagation medium exert a radiation pressure of sufficient magnitude to locally elevate the surface. Gravity and surface tension act as restoring forces. In a stationary acoustical system, equilibrium between radiation pressure forces and restoring forces is reached, and a stationary deformation pattern is established on the liquid surface. Degree of deformation is proportional to local acoustic intensity. The resulting optical phase object can be converted into a visible image by reflecting light from or refracting light through the deformed surface.

Gericke and Grubinskas (Ref. 57) reported a liquid-surface levitation ultrasonic imaging system which was applied as illustrated in Figure 27a to solid specimens containing defects. A shallow vessel, the bottom of which

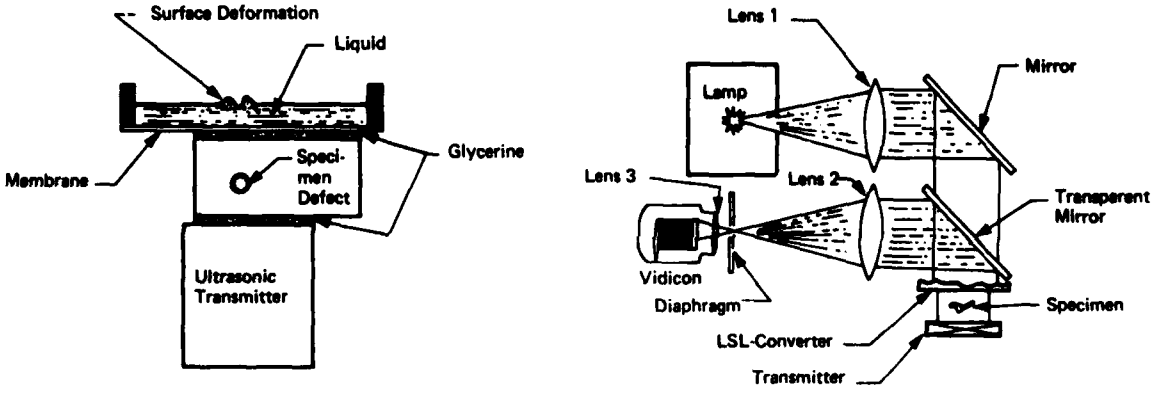

a. Ultrasonic Apparatus

b. Viewing Optics

FIGURE 27. LIQUID-SURFACE LEVITATION (LSL) ACOUSTICAL IMAGING SYSTEM
(From Ref. 57, Reproduced by permission of the American Institute of Physics, New York, NY)

was a thin membrane, contained a layer of liquid. The membrane bottom of the vessel was coupled ultrasonically to the specimen which, in turn, was coupled on its opposite side to an ultrasonic transmitting transducer. Scattering and diffraction of the ultrasonic wave caused by the defect produced a characteristic deformation pattern on the liquid surface. A viewing system, illustrated in Figure 27b, included a light source to illuminate the liquid surface and a television camera to observe the reflected optical pattern. Typical images produced by the system are shown in Figure 28. The objects of the presented images were plastic blocks with embedded steel balls of 6- and 12-mm (0.25- and 0.50-in.) diameter, respectively. Images for both objects for pulsed, frequency-modulated, and continuous-wave ultrasonic excitation are shown. Gericke and Grubinskas concluded that continuous-wave excitation produced the best results, and frequency-modulated and pulsed excitation produced approximately equal results.

Green (Ref. 58) used the system illustrated schematically in Figure 29. An acoustical lens was employed to focus ultrasonic energy, transmitted through the object of interest, on the surface of a liquid contained within a shallow barrier near the surface of a water tank. An ultrasonic grating, located just below the surface, added a high-frequency spatial carrier to the liquid-surface deformation pattern. Laser light reflected from the deformed liquid surface was converted into an electrical signal by a television camera. Components of the television camera

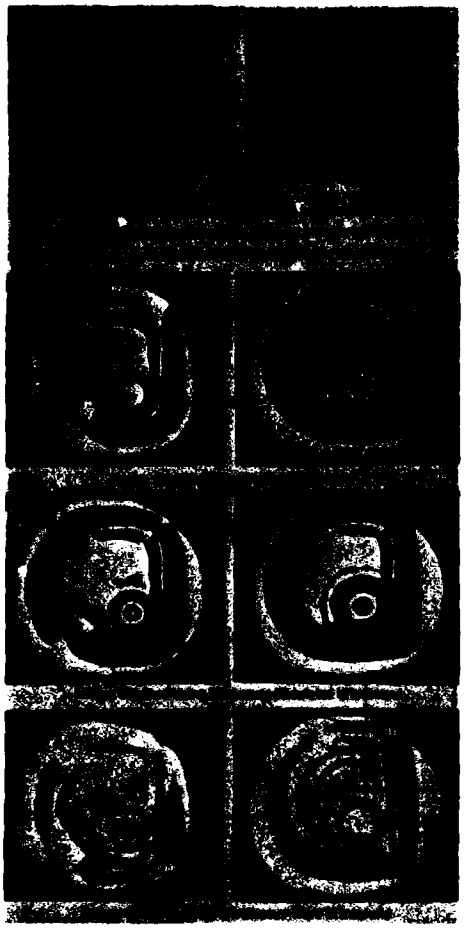

FIGURE 28. IMAGES PRODUCED BY LIQUID-SURFACE LEVITATION SYSTEM (From Ref. 57, Reproduced by permission of the American Institute of Physics, New York, NY)

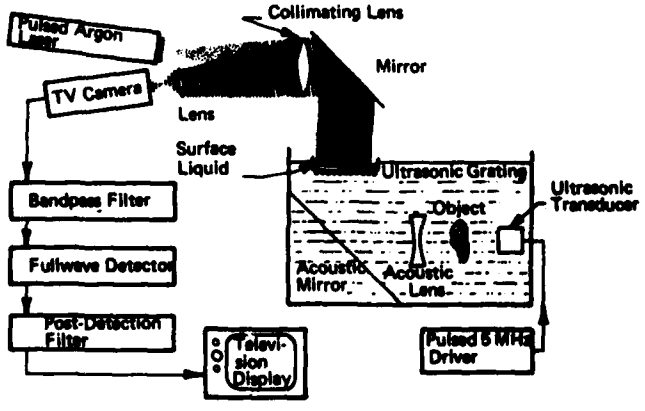

FIGURE 29. LIQUID-SURFACE LEVITATION ULTRASONIC IMAGING SYSTEM EMPLOYING A GRATING BELOW LIQUID SURFACE (From Ref. 58, Reproduced by permission of Plenum Publishing Corporation, New York, NY)

video output signal corresponding to the spatial carrier frequency and its sidebands were transmitted by a band-pass filter to a full-wave detector followed by a low-pass filter. The output of the latter filter was displayed on a television monitor. This system of introducing a high-frequency spatial carrier eliminated the need for a reference wave and the consequent system aperture limitation imposed by a reference wave requirement. A typical image produced by the grating system is illustrated in Figure 30.

5. Acoustical Holography

a. General

As previously mentioned, acoustical waves are described by the same mathematics as optical waves; therefore, it should be possible to translate optical techniques into analogous acoustical techniques. Development of optical holography with its high-resolution, three-dimensional images stimulated interest in attempting analogous techniques in acoustics. Images produced so far by acoustical holographic techniques have not shown the high degree of detail characteristic of optical holographic images because (1) ultrasonic wavelengths at commonly used frequencies are significantly greater than optical wavelengths, (2) the effects of inhomogeneities in the propagation medium are more pronounced for acoustical waves than for optical waves in air, and (3) methods of recording the acoustical hologram so that it can be reconstructed optically generally do not have resolution equivalent to the photographic process used for optical holography. In spite of these limitations, useful images are being obtained from acoustical holograms.

Holography is a two-step process involving (1) recording of an interference pattern, and (2) reconstruction of an image. Figure 31a illustrates the relative positions of system components used in optical holography. System configuration for acoustical holography is similar. In the recording step of holography, a beam of coherent energy illuminates an object (represented by P in Figure 31a). Incident energy is scattered and diffracted by each point P of

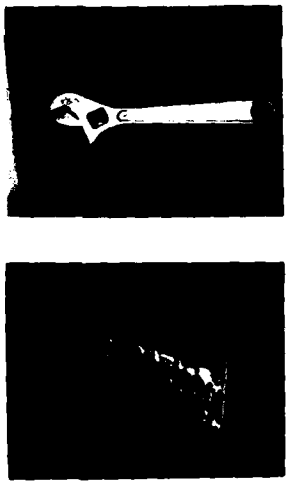

FIGURE 30. WRENCH OBJECT AND ACOUSTICAL IMAGE PRODUCED BY LIQUID-SURFACE LEVITATION SYSTEM EMPLOYING A GRATING (From Ref. 58, Reproduced by permission of Plenum Publishing Corporation, New York, NY)

the object to form a field (called the "object beam") which contains both amplitude and phase information about the object. Optical recording media (i.e., photographic emulsions) respond only to intensity of the incident field and, hence, do not record phase, so that significant image information is lost. To avoid loss of phase information, an off-axis reference beam, coherent with the beam of energy used to illuminate the object, is caused to fall upon the photographic plate in the same area as the object beam. Because the object and reference beams are mutually coherent, they produce an interference pattern which can be recorded on an intensity-sensitive recording medium (i.e., such as the photographic emulsion used in optical holography) which introduces square-law detection of the combined energy field. Such detection, in effect, causes phase information to be translated into intensity information which can be recorded.

Once the characteristic pattern of the combined field formed by the object and reference beams has been recorded, the record (or hologram) is transferred to a reconstruction configuration as illustrated in Figure 31b. A beam of coherent light is caused to impinge upon the hologram at the same angle as the reference beam used during recording. A virtual image of the object (P1 in Figure 31b) of the corresponding object point is formed. A real image (P2 in Figure 31b) is also formed. Because the reference beam was at an angle to the object beam during recording, the real and virtual images are separated in the reconstruction process so that they do not interfere with each other.

In acoustical holography, the process is basically the same as described for optical holography; however, in the recording step, acoustic rather than optic energy must be used, and the reference signal can be introduced either acoustically or electronically. In addition, a recording medium sensitive to acoustic intensity must be employed. In the reconstruction step, optic energy is used to illuminate the hologram in much the same way as in optical holograpy. Sometimes in acoustical holography, the recording medium does not produce a permanent record; in such cases the recording and reconstruction steps may be combined so that essentially real-time imaging results. Brenden (Ref. 59), Collins and Gribble (Ref. 60), Erikson *et al.* (Ref. 18), Hildebrand (Ref. 61), and Intlekofer *et al.* (Ref. 62) presented introductions to acoustical holography and described a number of specific methods and applications of techniques.

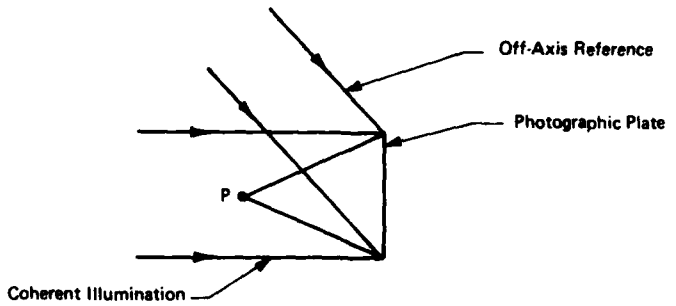

a. Recording Hologram

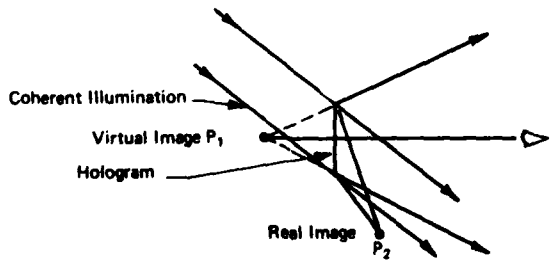

b. Image Reconstruction

FIGURE 31. BASIC CONFIGURATIONS OF HOLOGRAPHY (From Ref. 59, Reproduced by permission of the American Society for Testing and Materials, Philadelphia, PA, Copyright 1971)

A typical, practical set-up described by Intlekofer *et al.* (Ref. 62) is shown in Figure 32. Two transducers, one to illuminate the object and one to provide the reference beam, were immersed in a water tank. A thin film of liquid crystal applied to a vinyl substrate was used as a detector. A helium-neon laser beam was used to illuminate the liquid crystal film. Ultrasonic energy absorbed in the vinyl sheet caused localized temperature increases which, in turn, caused substantial local shifts in the scattering peaks of the liquid

crystals; that is, areas receiving low acoustic energy reflected a greater percentage of the red laser beam than those areas which received greater acoustic intensity. The resulting pattern of bright and dark areas appearing on the liquid crystal surface was photographed, and an image was reconstructed from the photograph. A typical transmission object and corresponding reconstructed image are shown in Figures 33a and 33b, respectively.

b. Scanned Transducer

One way of recording intensity variations of an acoustical field is to mechanically scan a transducer through the field and record the transducer output in a suitable medium. Collins and Gribble (Ref. 60) described a variety of scanning systems involving single and dual focused and unfocused transducers. In addition, both acoustical and electronic injection of the reference signal were discussed.

Knollman and Weaver (Ref. 63) reported use of a linear transducer array which was sampled electronically while the array was translated mechanically. Signals received from the transducer were processed to produce acoustical holograms. Both rectilinear and oscillating-mirror (cylindrical) scans were employed. In all cases, the reference was introduced electronically. Such systems employing only n transducers were capable of producing aperture and resolution equal to those of an n by n-element array.

A system of recording an acoustical sound field for holographic purposes using a square array of transducers was reported by Marom *et al.* (Ref. 64). The system used a 20 by 20-element receiving array in conjunction with a 5 by 5-element transmitting array. One element of the transmitting array was used at a time, and the receiving array was electronically scanned in its entirety for each transmitting element used. Ultimately a 100 by 100-element receiving array will be fabricated, and output signals of that device, when used to control a coherent-light area modulator, will provide a real-time holographic viewing system.

Ying *et al.* (Ref. 65) reported an acoustical holographic system in which a single focused transducer was used for both transmitting and receiving. As illustrated schematically in Figure 34, the transducer was scanned mechanically in x-y fashion over the object to be imaged. Electronic

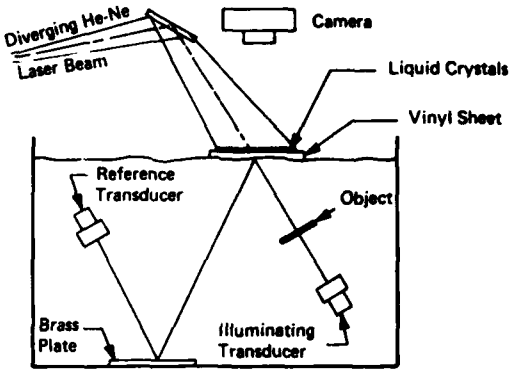

FIGURE 32. LIQUID-CRYSTAL METHOD OF RECORDING AN ACOUSTICAL HOLOGRAM (From Ref. 62, Reproduced by permission of the Society of Photo-optical Instrumentation Engineers, Palo Alto, CA)

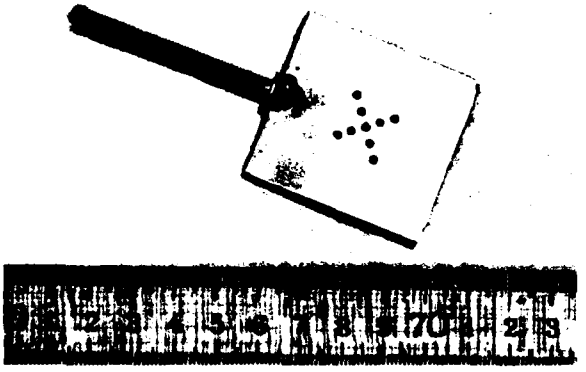

a. Object

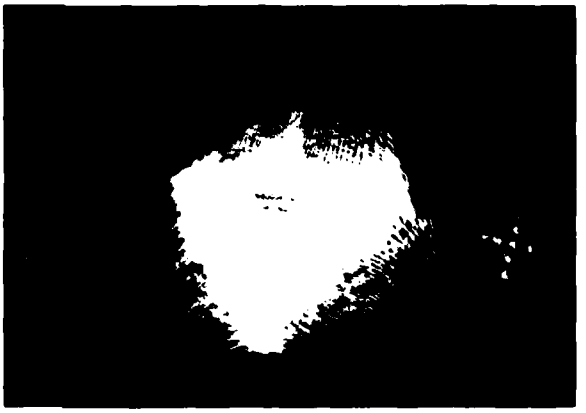

b. Reconstructed Image

FIGURE 33. IMAGE OBTAINED FROM LIQUID-CRYSTAL ACOUSTICAL HOLOGRAPHY SYSTEM (From Ref. 62, Reproduced by permission of the Society of Photo-optical Instrumentation Engineers, Palo Alto, CA)

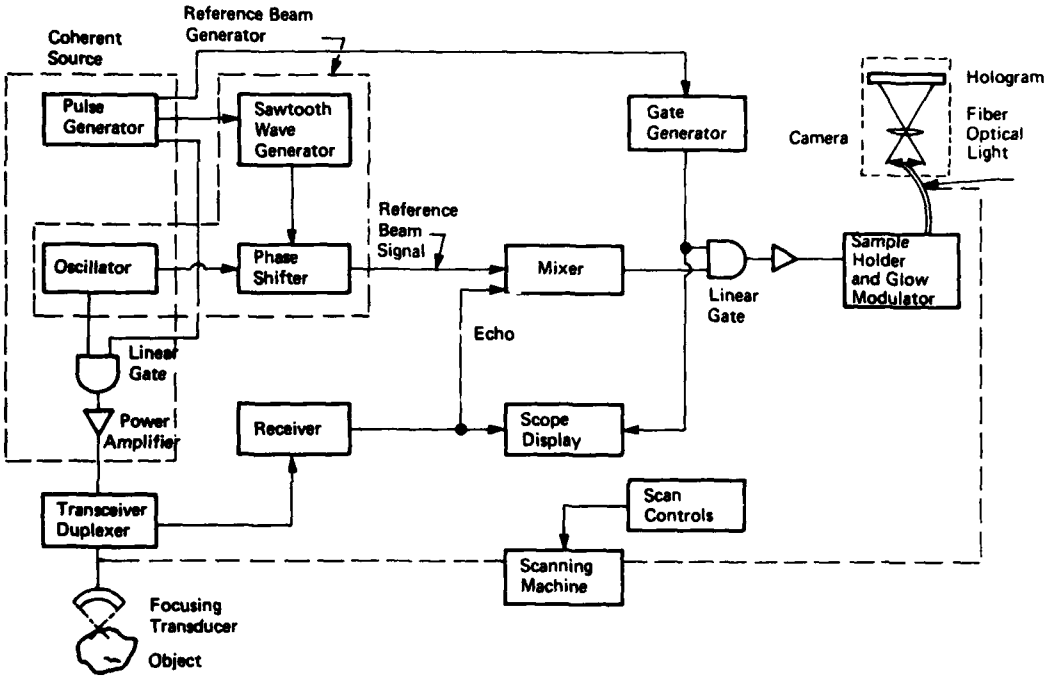

FIGURE 34. BLOCK DIAGRAM OF SCANNED-TRANSDUCER ACOUSTICAL HOLOGRAPHIC SYSTEM
(From Ref. 65, Reproduced by permission of the Quality Assurance Systems and Engineering Division, Southwest Research Institute, San Antonio, TX)

reference signal injection was used. Processed echo signals were applied to a glow modulator which produced light, the intensity of which was proportional to echo amplitude. A light pipe, one end of which was scanned over a piece of photographic film in synchronism with the focused-transducer motion, conducted light from the glow modulator to the film. Thus, as the transducer scanned, a hologram was built up point-by-point on photographic film. Hologram reconstruction was accomplished by conventional techniques using coherent illumination.

c. *Liquid-Surface Levitation*

Liquid-surface levitation as applied to direct acoustical imaging systems has already been discussed. Similar techniques, however, can be used in acoustical holography to generate a real-time holographic viewing system. The major difference between conventional and holographic applications of liquid-surface levitation is the introduction of a reference beam for holography. Hildebrand (Ref. 61) stated in his survey of current and potential uses of acoustical holography that the liquid-surface levitation method is nearest to routine use in acoustical holography and is the closest analog to optical holography. Pille and Hildebrand (Ref. 66) performed a rigorous analysis of the liquid-surface levitation method of acoustical holography, including (1) response of the liquid surface to time and space variations in radiation pressure and (2) effect of a "mini-tank" as a means of isolating the detecting surface from environmental disturbances.

Brenden (Ref. 59) described an acoustical holographic system, illustrated schematically in Figure 35a, employing liquid-surface levitation in a "mini-tank". An acoustical transducer insonified a transmission object, and an acoustical lens imaged the object on the liquid surface. A second acoustical transducer generated the reference beam which struck the liquid surface at an angle to the object beam. All of the acoustical apparatus was submerged in a large tank of liquid, but the area in which the object and reference beams reached the surface was enclosed in a small tank or "mini-tank" which isolated surface response in that area from disturbances existing in the liquid medium of the main tank. The deformation pattern on the liquid surface was an acoustical hologram of the object. Reconstruction was accomplished by illuminating the liquid surface with a coherent source and then viewing light reflected from the surface through appropriate optics. Figure 35b is a typical image formed by acoustical holography. In this case the object was a plastic block with a variety of side-drilled holes.

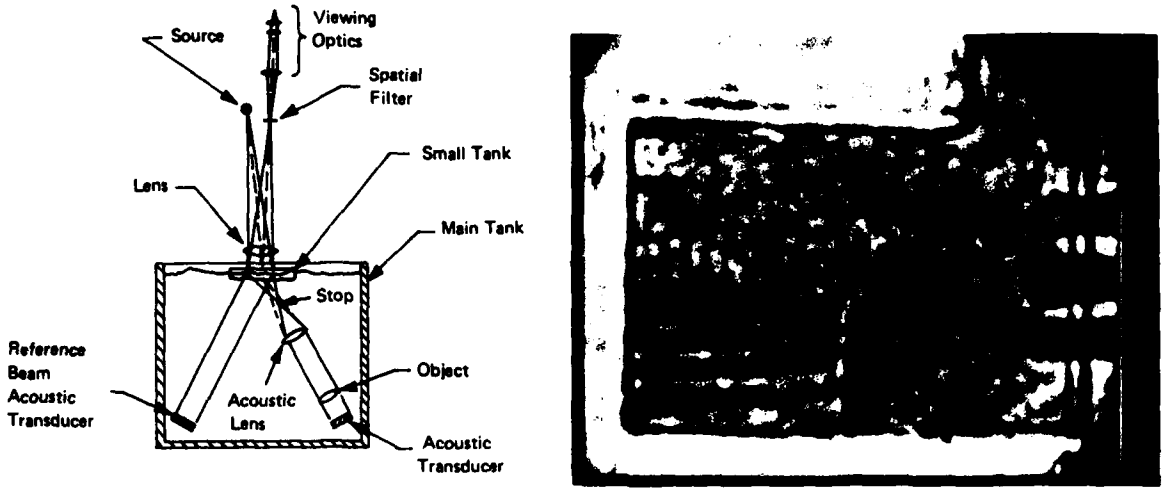

a. Apparatus

b. Image of Plastic Block with Side-Drilled Holes

FIGURE 35. ACOUSTICAL HOLOGRAPHY SYSTEM EMPLOYING LIQUID-SURFACE LEVITATION WITH A SMALL ISOLATION TANK (From Ref. 59, Reproduced by permission of the American Society for Testing and Materials, Philadelphia, PA, Copyright 1971)

d. Synthetic-Aperture

The synthetic-aperture method of imaging is derived from synthetic-aperture side-looking radar technology. In the radar case, excellent images of almost photographic quality are obtainable. Ultrasonic synthetic-aperture imaging has not yet developed to the same degree of perfection as radar technology, but application of the synthetic-aperture principle to ultrasonics is relatively new; it does, however, show great promise.

In conventional B-scan, a reflecting point, such as P in Figure 36, is displayed as a line segment, the length of which is equal to the width of the ultrasonic beam at the range of the reflecting point. Thus, resolution in the range coordinate is quite good, but resolution in the lateral direction is rather poor. Lateral resolution in conventional B-scan can be improved by using a focused transducer, but only at the expense of limited depth of focus.

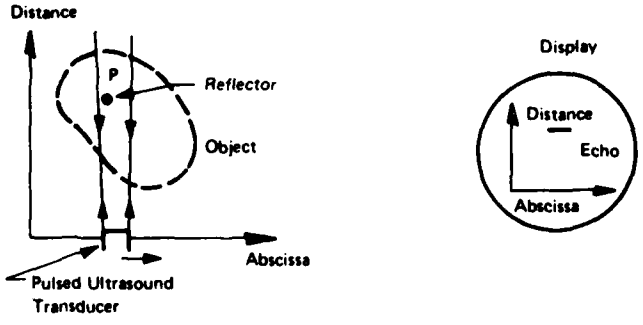

FIGURE 36. PRINCIPLE OF B-SCAN (From Ref. 67, Reproduced by permission of the Institute of Electrical and Electronics Engineers, Inc., New York, NY)

In the synthetic-aperture case, illustrated in Figure 37a, the transducer is scanned linearly past the object which in the figure is represented by points P and Q. A much wider beam than would be used in B-scan is used for synthetic-aperture imaging. The output of the transducer, when used as a receiver, is multiplied by a coherent reference signal as illustrated in the block diagram of Figure 38. Output of the multiplier controls intensity of a cathode-ray-tube display while the cathode-ray spot is deflected linearly in the y-direction representative of time

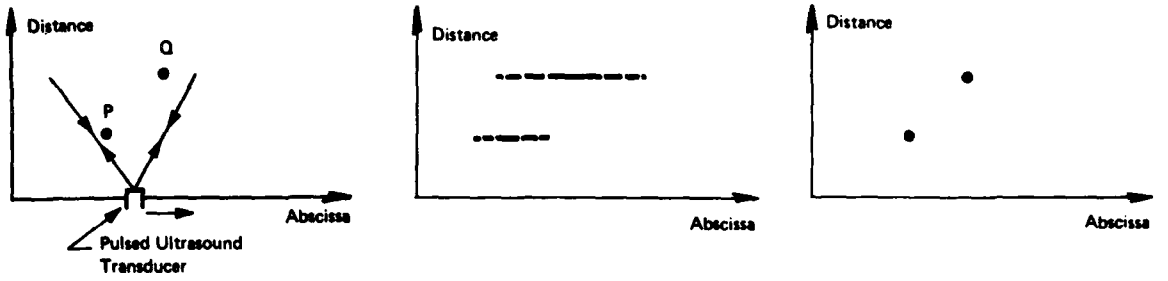

a. Recording Configuration b. Unprocessed Record c. Processed Image

FIGURE 37. PRINCIPLE OF SYNTHETIC-APERTURE IMAGING (From Ref. 67, Reproduced by permission of the Institute of Electrical and Electronics Engineers, Inc., New York, NY)

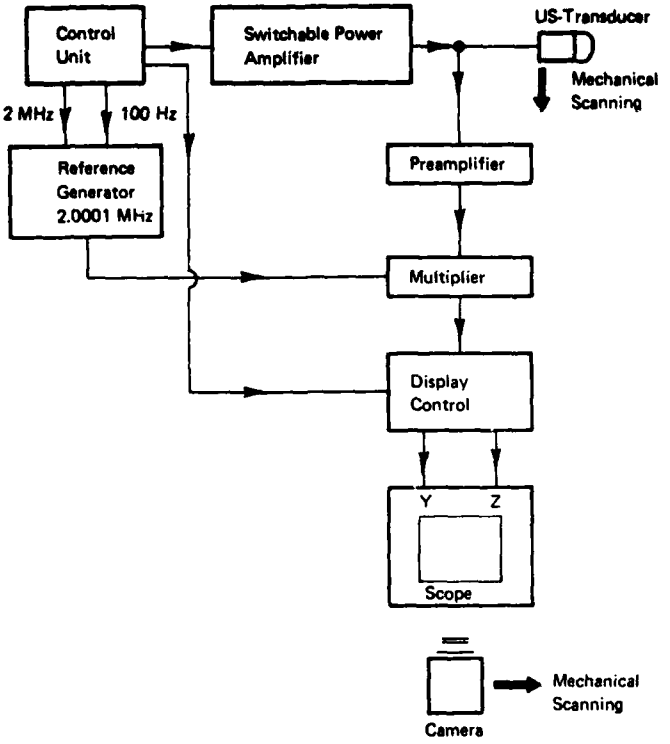

FIGURE 38. BLOCK DIAGRAM OF TYPICAL SIGNAL-PROCESSING FOR SYNTHETIC-APERTURE SYSTEMS (From Ref. 68, Reproduced by permission of Plenum Publishing Corporation, New York, NY)

of flight. A camera, focused on the cathode-ray-tube screen, is mechanically scanned in synchronism with transducer motion. The resulting photographic record for a two-point object is illustrated in Figure 37b. The two structures shown in this figure are caused by successive constructive and destructive interference between (1) reflected signals received from the object points and (2) the coherent reference signal.

The record of Figure 37b is , in effect, a hologram in which the structures shown are one-dimensional zone plates. When a zone plate is illuminated coherently, it acts as a lens and focuses the illuminating energy to a point; thus, the processed image of Figure 37c shows the result of illuminating the photographic record with coherent light. One of the principal features of the synthetic-aperture approach is that lateral resolution is independent of range for a properly processed signal, whereas in conventional ultrasonic systems, resolution *is* a function of range.

Burckhardt *et al.* (Refs. 67 and 68) reported an ultrasonic synthetic-aperture imaging system operating at 2 MHz. Figure 39 illustrates an image obtained with their system. The object for this image was two wire grids mounted at a distance of 70 mm (2.75 in.) from each other in the range coordinate. Each grid had a number of groups of three copper wires strung at different pitches. All wires were 0.3 mm (0.012 in.) in diameter. The image shown is a cross-section through the object. Going from left to right in the top grid of Figure 39 and from right to left in the bottom grid, the spacings between wires in the various groups of three are as follows: 10 mm (0.40 in.), 5 mm (0.20 in.), 4 mm (0.16 in.), 3 mm (0.12 in.), 2 mm (0.08 in.), 1.5 mm (0.06 in.) and 1 mm (0.04 in.). It is apparent in the figure that the top grid wires spaced 2 mm (0.08 in.) apart were resolved, and in the bottom grid, wires having a spacing of 3 mm (0.12 in.) were resolved. Burckhardt *et al.* (Ref. 67) pointed out that these values of resolution were near those theoretically expected and were about one order of magnitude better than those of a conventional B-scan system working at the same frequency.

Prine (Ref. 69) presented some of the theory of synthetic-aperture ultrasonic imaging systems and also gave some practical design information. Prine also reported construction and test of an ultrasonic synthetic-aperture imaging system.

6. Image Processing

Images created in various ways can be altered by processing to emphasize or clarify a certain feature or to change the point of view. Processing of ultrasonic images is usually done electronically by either analog or digital means.

FIGURE 39. ULTRASONIC SYNTHETIC-APERTURE IMAGE OF TWO WIRE GRIDS (From Ref. 67, Reproduced by permission of the Institute of Electrical and Electronics Engineers, Inc., New York, NY)

Becker and Trantow (Ref. 70) described an analog method of presenting conventional C-scan images in isometric form. Image restructure was accomplished by a special-purpose analog computer which solved conventional equations for rotation of axes. A system block diagram is given in Figure 40. The system received x- and y-information from the transducer scanning apparatus and obtained z-information from time of flight. A visual image was formed on a cathode-ray-tube display. Controls were provided in the analog circuitry so that the point of view could be changed. The authors suggested that original data could be recorded on tape and played back at high speed so that an operator could adjust the point of view for optimum display of a particular image

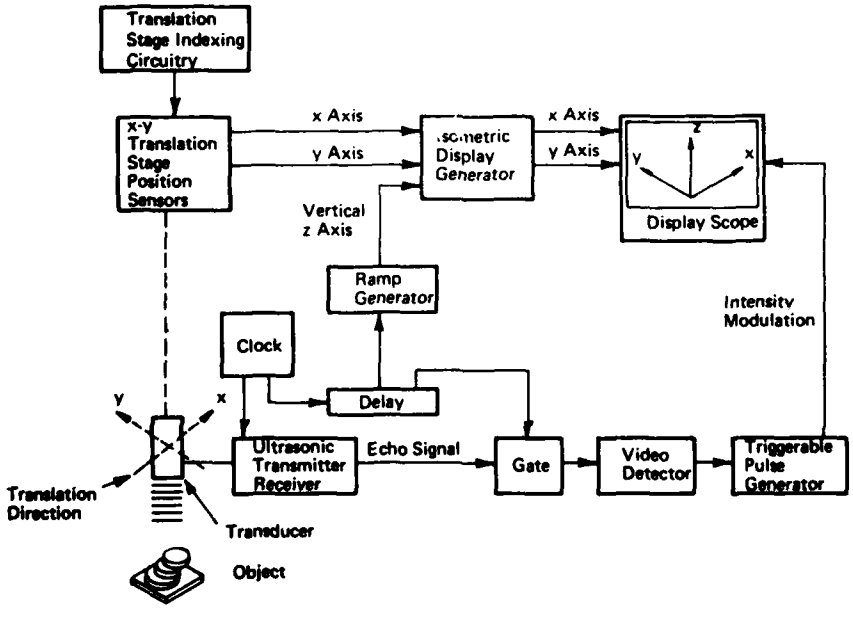

FIGURE 40. BLOCK DIAGRAM OF "ISO-SCAN" SYSTEM FOR GENERATION OF ISOMETRIC C-SCAN IMAGES (From Ref. 70, Reproduced by permission of the Society of Photo-optical Instrumentation Engineers, Palo Alto, CA)

feature. Photographs of typical objects, their conventional C-scan images, and corresponding isometric (i.e., "Iso-scan" in the authors' words) images are shown in Figures 41a and 41b. The Iso-scan images clearly have the appearance of depth, whereas conventional C-scan images appear to be flat.

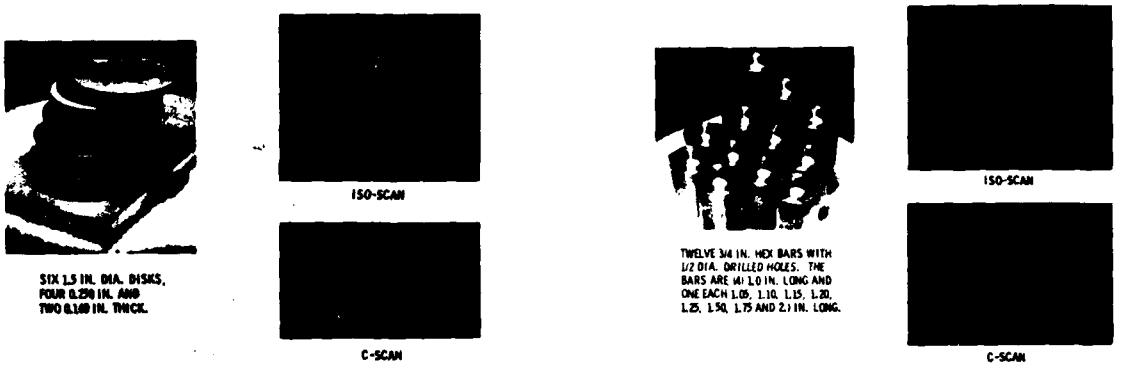

a. Stacked Disks

b. Hexagonal Bars

FIGURE 41. ISO-SCAN IMAGES COMPARED TO ORIGINAL OBJECTS AND CONVENTIONAL C-SCANS
(From Ref. 70, Reproduced by permission of the Society of Photo-optical Instrumentation Engineers, Palo Alto, CA)

Lee and his colleagues (Refs. 71and 72) have used digital computation to perform a wide range of enhancement operations on acoustical images obtained from a 25-MHz Bragg-diffraction cell. Images were digitized into 256 by 256 picture elements with 8-bit resolution. Processing in the spatial domain, the frequency domain, and the sequency domain (i.e., based on the Walsh transform which is similar to a frequency spectrum, but is based on square waves rather than sine waves) was used to accomplish density stretching, density equalization, inverse filtering, low- and high-pass filtering, correction of geometrical distortion, and signal averaging. Figure 42a is an original image of a tropical fish. It is apparent that this image is poorly exposed, and it is difficult to distinguish the fish. By applying density equalization, in which optical density or darkness of the image is increased in light areas and decreased in dark areas, the processed image of Figure 42b

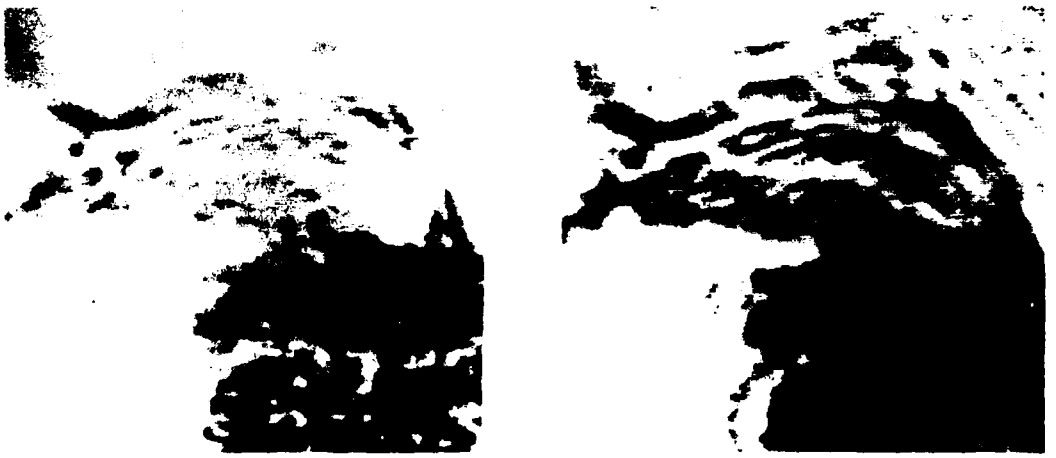

a. Image of Tropical Fish Before Processing

b. Image After Density Equalization

FIGURE 42. EXAMPLE OF IMAGE ENHANCEMENT BY DIGITAL PROCESSING
(From Ref. 71, Reproduced by permission of the Institute of Electrical and Electronics Engineers, Inc., New York, NY)

results. In the processed image it is possible to distinguish some of the structure of the tropical fish. In Figure 43a the unprocessed image of a hook after digitization is shown. Figure 43b is the same image after correction for shading, and Figure 43c shows the image after removal of unwanted noise (i.e., the concentric elliptical rings of the previous pictures). It is evident from these examples that the quality of an acoustical image can be improved by application of suitable processing.

7. Acoustical Microscopy

Ultrasonic imaging systems are capable of resolution commensurate with optical methods if frequency is sufficiently high. Of course, at very high frequencies attenuation is high, limiting such high-resolution techniques to relatively thin objects. Frequencies in the range of 400 MHz to 2 GHz are used in special configurations to produce acoustical images of microscopic structures. Kessler (Ref. 73) surveyed the field of acoustical microscopy and listed four imaging methods currently being used: (1) acoustical waves emerging from the specimen are interacted in bulk with a light beam (i.e., Bragg-diffraction imaging); (2) acoustical waves from the specimen deform an optically reflective surface which is scanned by a focused light beam; (3) acoustical waves from the object act upon a thin layer of suspended particles which, in turn, alter transmission of a light beam; and (4) acoustical waves from the object strike a piezoelectric photoconductor material which can be read-out by a scanned focused light beam.

Lemons and Quate (Ref. 74) described a special through-transmission, focused-transducer acoustical microscopy cell which is illustrated schematically in Figure 44. A piezoelectric transmitting transducer was coupled through a rod with a specially shaped end into a water cell which contained the object. A similar rod coupled transmitted acoustic energy into a receiving piezoelectric transducer. The object was scanned through the focal point of the cell in two perpendicular directions. An image was formed by translating the acoustic energy transmitted by the object into intensity modulation of a synchronized raster on a cathode-ray-tube display. The reported system operated at 400 MHz and demonstrated resolution of 3 μm (120 μin.). Typical images produced by this acoustical microscopy system (left-hand column) are compared with corresponding optical

a. Image of Hook After Digitization, but Before Processing

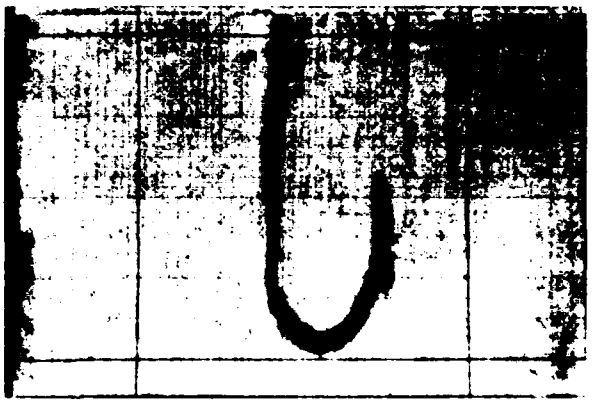

b. Image After Correction for Shading

c. Image After Removal of Unwanted Noise (the Concentric Elliptical Rings in a above)

FIGURE 43. CHANGES IN AN ACOUSTICAL IMAGE AS VARIOUS PROCESSING STEPS ARE APPLIED (From Ref. 72, Reproduced by permission of Plenum Publishing Corporation, New York, NY)

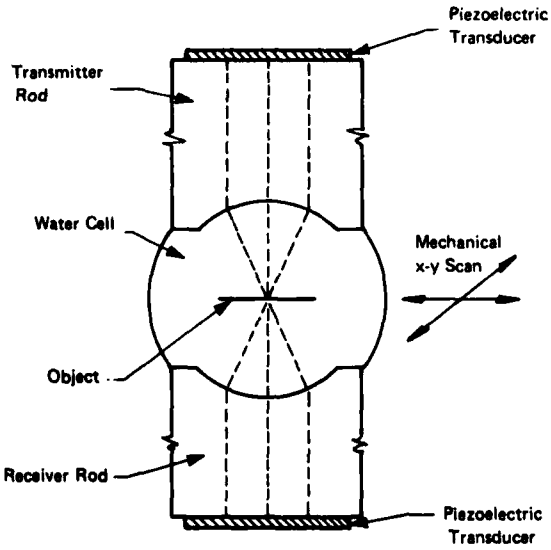

FIGURE 44. SCHEMATIC DIAGRAM OF ACOUSTICAL MICROSCOPY SYSTEM (From Ref. 74, Reproduced by permission of the Institute of Electrical and Electronics Engineers, Inc., New York, NY)

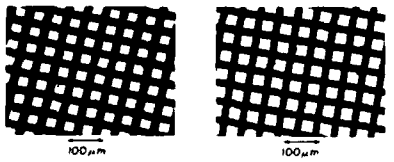

a. Comparison of the Acoustic (left) and Optical (right) Images of a 500-Mesh Nickel Grid

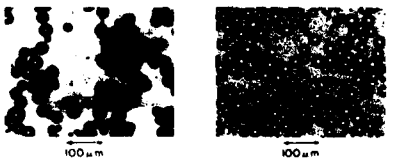

b. Comparison of the Acoustic (left) and Optical (right) Images of Polystyrene Particles

c. Comparison of the Acoustic (left) and Optical (right) Images of Human Red Blood Cells

FIGURE 45. IMAGES OBTAINED BY ACOUSTICAL MICROSCOPY (Left Column) AND OPTICAL MICROSCOPY (Right Column) (From Ref. 74, Reproduced by permission of the Institute of Electrical and Electronics Engineers, Inc., New York, NY)

images (right-hand column) in Figure 45. Figure 45a shows images of a 500-mesh nickel grid, Figure 45b shows images of small polystyrene particles, and Figure 45c shows images of human red blood cells. These image comparisons show clearly that acoustical images of microscopic objects compare favorably with optical images and, in some cases, may reveal features of the object to which optical microscopy is insensitive.

8. Other Imaging Methods

The Sokolov tube is a well known device for imaging acoustical fields; however, it has had a history of difficulties which include limited aperture, limited acceptance angle, and a tendency to implode. Operation of the Sokolov tube is indicated schematically in Figure 46. A piezoelectric plate is coupled on one side to the acoustical propagation medium (often water), and the other side is exposed to the interior of a high-vacuum chamber. Acoustical waves impinging on the outside of the piezoelectric plate generate on the inside of the plate a charge pattern proportional to field strength. A focused electron beam, generated by a conventional electron gun, raster scans the inside of the piezoelectric plate. Secondary electrons are emitted from the vacuum side of the piezoelectric plate, and their energies are modulated by the local charge on the plate. Secondary electrons are collected in an electron multiplier and yield a video output from the tube which can be used to intensity modulate a cathode-ray display.

Addison (Ref. 75) reported fitting a Sokolov tube with a metal-fiber faceplate which eliminated many of the difficulties characteristic of Sokolov tubes. The faceplate was fabricated by fusing many parallel, glass-coated wires to form a vacuum-tight mass. A photomicrograph of a small region of such a faceplate is illustrated in Figure 47. Wire diameter was 0.05 mm (0.002 in.), and average center-to-center spacing was 0.15 mm (0.006 in.). The faceplate was exposed to vacuum on one side and to the back of the piezoelectric plate on the other. Use of a metal fiber faceplate increased the usable aperture to 140 mm (5.5 in.) because of its greater strength, permitted greater selection of piezoelectric material, and did not degrade resolution. Figure 48 illustrates the acoustical image of a perforated aluminum plate obtained with a metal-fiber faceplate Sokolov tube using 5-MHz acoustical waves; in Figure 48 the small holes are about 1.5 mm (0.06 in.) in diameter.

Jacobs and Peterson (Refs. 76 and 77) reported use of discrete, shaped matching devices bonded to the faceplate of a Sokolov tube to improve (1) impedance match between the coupling medium (usually

water) and the sensing plate of the tube, (2) acceptance angle, and (3) resolution. Small hemispherical domes of quarter-wavelength (or odd multiples thereof) radius made of copper-loaded casting material were screened on the face of a Sokolov tube in a rectangular grid pattern. A photograph of a quartz faceplate with discrete matching elements applied is presented in Figure 49. Normal field of view of a Sokolov tube is about 2 degrees; however, with hemispherical matching elements applied, an acceptance angle of approximately 30 degrees was achieved. Figure 50 is an image produced by a Sokolov tube having shaped acoustical matching elements. The smallest dimension resolved in this image was approximately 1.2 mm (0.048 in.).

Lund and Jensen (Ref. 78) described an interesting method of visualizing

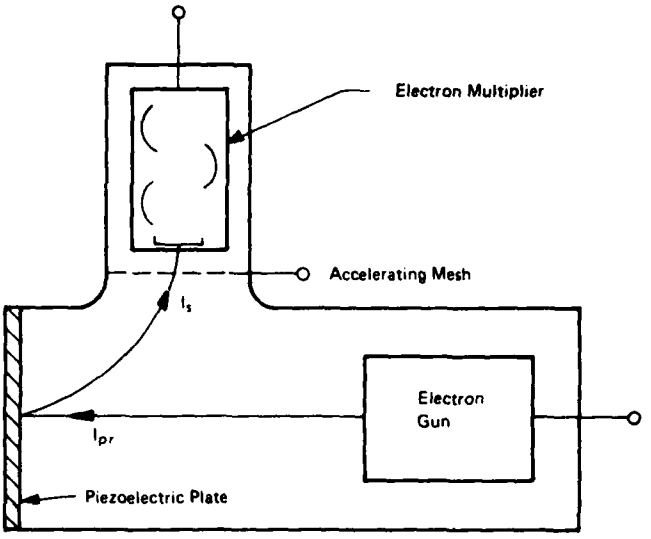

FIGURE 46. SCHEMATIC DIAGRAM OF SOKOLOV TUBE (From Ref. 77, Reproduced by permission of Plenum Publishing Corporation, New York, NY)

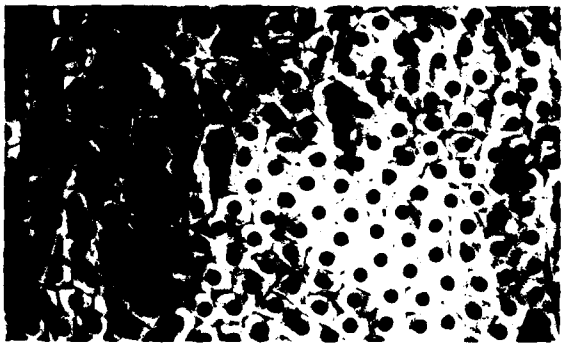

FIGURE 47. PHOTOMICROGRAPH OF METAL-FIBER FACEPLATE FOR SOKOLOV TUBE (From Ref. 75, Reproduced by permission of Plenum Publishing Corporation, New York, NY)

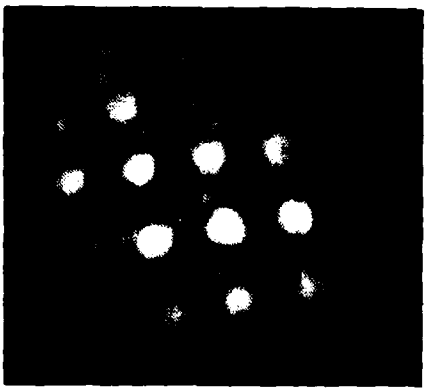

FIGURE 48. IMAGE OF PERFORATED METAL PLATE USING METAL-FIBER-FACEPLATE SOKOLOV TUBE (From Ref. 75, Reproduced by permission of Plenum Publishing Corporation, New York, NY)

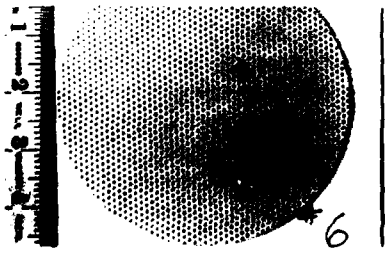

FIGURE 49. QUARTZ FACEPLATE FOR SOKOLOV TUBE WITH DISCRETE MATCHING SECTIONS APPLIED (From Ref. 77, Reproduced by permission of Plenum Publishing Corporation, New York, NY)

FIGURE 50. IMAGE PRODUCED BY SOKOLOV TUBE HAVING DISCRETE MATCHING SECTIONS APPLIED TO FACEPLATE (From Ref. 77, Reproduced by permission of Plenum Publishing Corporation, New York, NY)

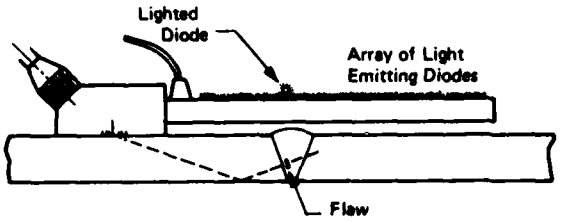

a. Detail of Apparatus

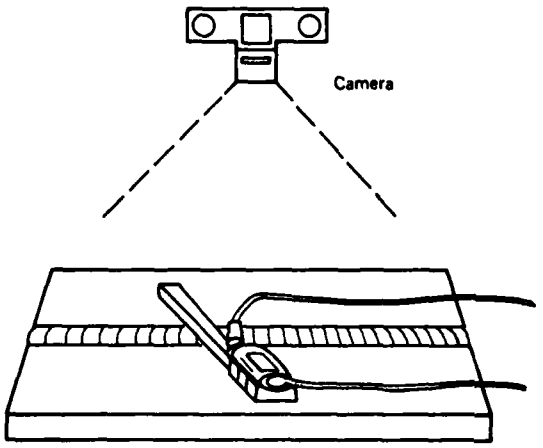

b. Typical Recording Configuration

FIGURE 51. APPARATUS FOR PROJECTION SCAN
(From Ref. 78, Reproduced by permission of IPC Science and Technology Press, Ltd.,Guildford, England)

defects in welds which they referred to as "projection scan." Their system is illustrated schematically in Figure 51a. An angle transducer was used to launch an ultrasonic wave into the parent material. Projecting from the angle block of the transducer was a small cantilever beam on which a linear array of light-emitting diodes was mounted. The line of diodes was arranged so that it lay above and parallel to the ultrasonic beam path in the material being inspected. An electronic circuit detected the presence of an echo from a flaw in the weld and illuminated the light-emitting diode just above the flaw as illustrated in Figure 51a. A typical method of recording the results is illustrated in Figure 51b. The probe assembly rested on the surface of the parent material with the cantilever beam projecting over the weld. A camera, mounted above the plane of the material, photographed the illuminated light-emitting diodes. If this operation were carried out in the dark and a second exposure of the film in normal light were made, the resulting photographic record would include not only images of defects, but a representation of the material surface. Figures 52a, 52b, and 52c are records obtained by this method from the same weld, but at three different levels of sensitivity, Figure 52a being for high sensitivity, Figure 52b for medium sensitivity, and Figure 52c for low sensitivity.

Use of liquid crystals for acoustical imaging has already been mentioned in connection with acoustical holography (Ref. 62). A non-holographic acoustical imaging system employing liquid crystals was described by Sproat and Cohen (Ref. 79). The system is illustrated in Figure 53. A viscoelastic absorber was placed in contact with a thin steel diaphragm which had been previously coated with a thin layer of cholesteric liquid crystal material. An ultrasonic transducer, located in a water bath, was used to insonify a transmission object. Acoustic energy passing the object impinged upon the absorber causing localized temperature rises. The water in the tank was preadjusted to the change-threshold temperature of the liquid crystal material so that differential heating caused by absorbed ultrasonic energy produced in the liquid crystal layer color changes which could be observed visually. The image of a corkboard mask in the form of a profile of an airplane is shown in Figure 54. Although response of the system was relatively slow (1 to 10 s required to produce an image) and sensitivity was relatively low (1 MW/m^2 [100 W/cm^2] at 1 MHz), images produced were relatively good.

A means of making surface elastic waves visible was developed by Adler *et al.* (Ref. 80) and was later applied by Alers *et al.* (Ref. 81). The principle of the system is illustrated in Figure 55a. A laser beam incident upon a material surface is reflected at an angle which differs from the quiescent value by twice the instantaneous tilt of the surface. A portion of the beam in its static position was obstructed by an opaque knife edge. The remainder of the beam was detected by a photodiode. As a surface wave propagated along the material, the reflected laser beam was deflected through a small angle which changed the fraction of the beam which reached the photodetector and, hence, modulated the photocurrent. A display representing a surface wave propagating over an area was formed by scanning the light beam in synchronism with scanning of a cathode-ray spot while the amplified photocurrent modulated spot intensity. This system was useful for detecting surface and near-surface defects in materials. An example of an image formed by this system is

a. High Sensitivity

b. Medium Sensitivity

c. Low Sensitivity

FIGURE 52. TYPICAL IMAGES OF A WELD MADE BY PROJECTION SCAN SYSTEM (From Ref. 78, Reproduced by permission of IPC Science and Technology Press, Ltd., Guildford, England)

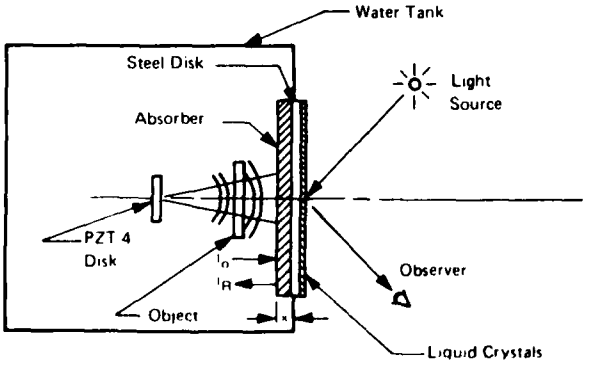

FIGURE 53. LIQUID-CRYSTAL ACOUSTICAL IMAGING SYSTEM (From Ref. 79, Reproduced by permission of The American Society for Nondestructive Testing, Inc., Columbus, OH)

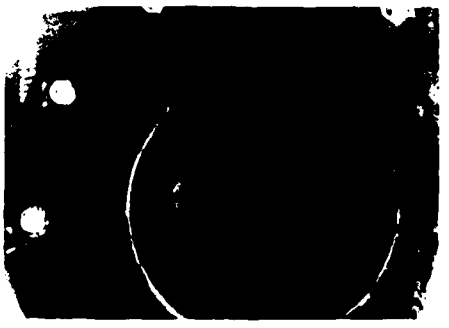

FIGURE 54. IMAGE OBTAINED WITH LIQUID-CRYSTAL SYSTEM (Note: Original was in color) (From Ref. 79, Reproduced by permission of The American Society for Nondestructive Testing, Inc., Columbus, OH)

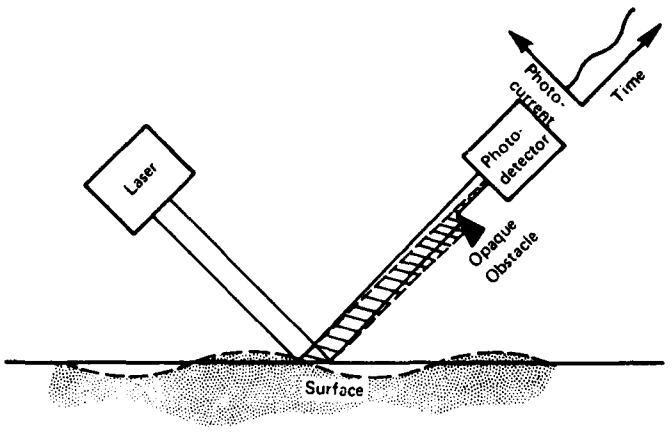

a. System Principle

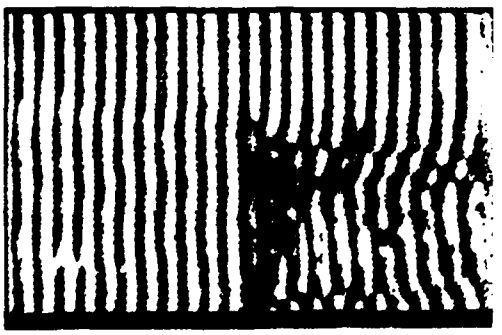

b. Wavefront Disturbance by Small Slot in a Steel Plate

FIGURE 55. SURFACE-WAVE VISUALIZATION SYSTEM (From Ref. 81, Reproduced by permission of IPC Science and Technology Press, Ltd., Guildford, England)

given in Figure 55b. The defect in this case was a 3-mm (0.12-in.)-long by 0.3-mm (0.012-in.)-deep slot in steel. The approaching wavefront is undisturbed to the left of the defect, but the effects of the slot are readily visible in the disturbed pattern to the right.

Bragg diffraction cells are often used as acoustical imaging devices. In these cells, an acoustical wave is propagated through a medium which is usually a liquid, but may be a solid. Compressions and rarefactions of the acoustical wave make small changes in the optical properties of the propagation medium. The wavefront of a collimated beam of coherent light also propagating through the medium is disturbed by localized alterations of propagation medium optical properties. This interaction between acoustical and optical waves produces a real-time acoustical imaging system which eliminates the need for receiving transducers and other display producing devices. Aprahamian and Bhuta (Ref. 82) and Keyani *et al.* (Ref. 83) reported use of Bragg-diffraction cells for acoustical imaging. Keyani *et al.* (Ref. 83) described some of the problems associated with multiple acoustical reflections within a low-frequency (3.58-MHz) cell and discussed a variety of special absorbers designed to eliminate undesired stray reflections.

Greenleaf *et al.* (Ref. 84) reported use of an algebraic reconstruction technique to derive spatial distributions of acoustic absorption within an object. The technique required multiple C-scans of the object from a number of points of view. The result of each C-scan was, in effect, a one-dimensional shadowgram in which received intensity was related to acoustical absorption in the object along the selected C-scan path. Transmitting and receiving transducers were scanned past the object using a computer-controlled arm which moved both transducers simultaneously. The through-transmission mode of operation was used. Output signals from the receiving transducer were digitized, and those signals lying within a range gate were used in computation. Multiple scans from various points of view were achieved by rotating the object a few degrees between successive scans. A set of linear algebraic equations derived for this situation were solved on a computer to determine the two-dimensional distribution of acoustical absorption on a planar cross-section of the object. The system of equations solved produced a 64 by 64-picture-element cross-section of the object.

In theory, this method is limited to situations in which the intensity at a point in the shadow is directly related to the total absorption experienced by a ray traveling through the object from the source to that point; however, when the transmitted energy is acoustic, there are (1) losses caused by reflections at acoustic-impedance interfaces, and (2) refraction effects resulting from acoustic impedance gradients within the object which cause the intensity in the shadow to no longer be related to absorption. However, it was shown that this technique works reasonably well even though these effects degrade accuracy slightly.

Greenleaf *et al.* (Ref. 85) also reported a method of plotting spatial distributions of acoustic velocity using algebraic reconstruction techniques similar to those previously mentioned. In this case, rather than using received intensity as the input for computation, time-of-flight of pulsed acoustic energy was used instead. Time-of-flight was measured from a number of points of view, first through the object and then through water. Times-of-flight through the specimen were normalized to those through water so that the resulting 64 by 64-picture-element plot was based on absolute rather than relative velocity. Use of time-of-flight eliminated the two major objections to the previously mentioned system based on acoustic absorption because (1) time-of-flight was easily and accurately measured, and (2) the first pulse to arrive at the receiver probably had traveled the shortest distance, meaning that minimal reflection and refraction interference were present.

C. Inference of Material Properties from Ultrasonic Measurements

The primary thrust of nondestructive evaluation of materials is location and identification of flaws or defects. However, in some cases it is necessary to measure quantitatively and nondestructively a particular material parameter (e.g., longitudinal modulus). Critical angle, velocity, attenuation, acoustic impedance, and scattering coefficient can be related to a variety of material constants. Various applications of these techniques are discussed in subsequent paragraphs.

In pulse-echo ultrasonic inspection, two maxima occur in the reflected signal as the angle of incidence of the ultrasonic beam is increased, one at the critical angle for longitudinal waves and another at the critical angle for transverse waves. Between these two peaks, there is a sharp minimum in reflected intensity. Lees (Ref. 86) related the angle of incidence at which this minimum occurs to material elastic parameters. The various material moduli were expressed in terms of the longitudinal modulus obtained from critical-angle measurement. Lees derived equations relating the desired moduli to observable quantities and presented a computer program in BASIC for reducing observed data to the parameters of interest.

Alers (Ref. 87) has used measurements of ultrasonic surface-wave velocity at various frequencies to deduce hardness *versus* depth contours in induction-hardened steel. Penetration of elastic surface waves into a solid is inversely proportional to frequency; thus, measuring elastic surface-wave velocity as a function of frequency facilitates determination of such properties as residual stress, chemical composition, hardness, etc. Alers presented a mathematical analysis of the problem of determining hardness gradients by surface-wave velocity measurements and discussed experimental verification of the technique in the case of measuring hardness *versus* depth contours.

Moran *et al.* (Ref. 88) have used electromagnetic-acoustic transducers for accurate measurement of acoustic velocity and attenuation. Attenuation was related to the presence of defects, and velocity, determined by a phase-comparison system, was related to residual and induced strain. Preliminary experiments indicated that good sensitivity to such strains could be achieved.

Noronha *et al.* (Ref. 89) have devised a means of measuring residual stress in metals using ultrasonic shear waves. In an isotropic material, shear-wave velocity is independent of polarization and direction of propagation. Application of stress, however, causes anisotropy so that orthogonally polarized shear-wave components no longer travel at equal velocities. A constant, called the "total stress acoustic constant (TSAC)," related to shear-wave velocity change, may be determined for a material. With a previously calibrated material, Noronha and his associates were able to determine stress in a material sample by measuring the degree of anisotropy. Experiments to determine the variation of total stress acoustic constant of aluminum and steel as functions of grain size, heat treatment, composition, and preferred orientation were reported.

Hsu and Sachse (Ref. 90) have used a rotatable shear-wave transducer to make attenuation measurements along various symmetry directions of a single crystal and acoustical birefringence measurements in anisotropic solids. Acoustical birefringence experiments using the rotatable shear-wave transducer showed that (1) velocity of a shear wave propagating parallel to the direction of applied compressive stress increased in proportion to magnitude of stress and (2) velocity of a shear wave propagating perpendicular to the stress direction remained relatively unchanged or decreased slightly.

Ultrasonic spectroscopy was used by Papadakis (Ref. 32) to measure the fractional shear-wave velocity difference in worked aluminum. Using this measurement technique as a basis, a system for measuring texture in worked materials was proposed.

Green (Ref. 91) has shown that early detection of onset of fatigue failure can be accomplished by measurement of ultrasonic attenuation. A substantial increase in ultrasonic attenuation was observed in various fatigue test specimens an appreciable time before formation of detectable cracks. A typical graph of ultrasonic attenuation *versus* number of fatigue cycles for an aluminum test bar is presented in Figure 56. An increase in attenuation was observed at 3.13 million cycles, and it was not until 3.39 million cycles that acoustic emission, surface waves, or bulk waves were able to detect presence of a crack.

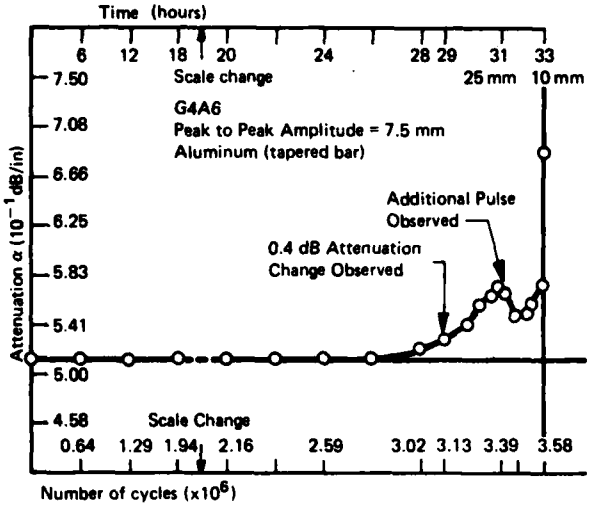

FIGURE 56. ULTRASONIC ATTENUATION *VERSUS* NUMBER OF CYCLES FOR A TYPICAL ALUMINUM FATIGUE SPECIMEN (From Ref. 91, Reproduced by permission of IPC Science and Technology Press, Ltd., Guildford, England)

A new method of measuring specific acoustic impedance has been developed by Jones (Ref. 92). The technique, referred to as "impediography," employed two ultrasonic transducers as illustrated in Figure 57. The source or transmitting transducer radiated an acoustical impulse of specified shape designated "incident wave" in Figure 57. This impulse traveled past the receiver and entered the test object. Reflections from the test object were converted by the receiving transducer into an electrical signal designated "reflected wave" in the figure. Deconvolution (cf.III.A.6) applied to the reflected and incident waves produced the system impulse response. Integration of the impulse response yielded a curve of acoustic impedance as a function of depth into the material. An example impedance graph is illustrated in Figure 58 for a multi-layer structure comprising two layers of glass-reinforced plastic (GRP) with a layer of rubber sandwiched between and with the entire structure immersed in saline solution. Acoustic impedances of various layers are clearly indicated in the graph. This technique facilitates accurate measurement of specific acoustic impedance at an arbitrary position within a test object.

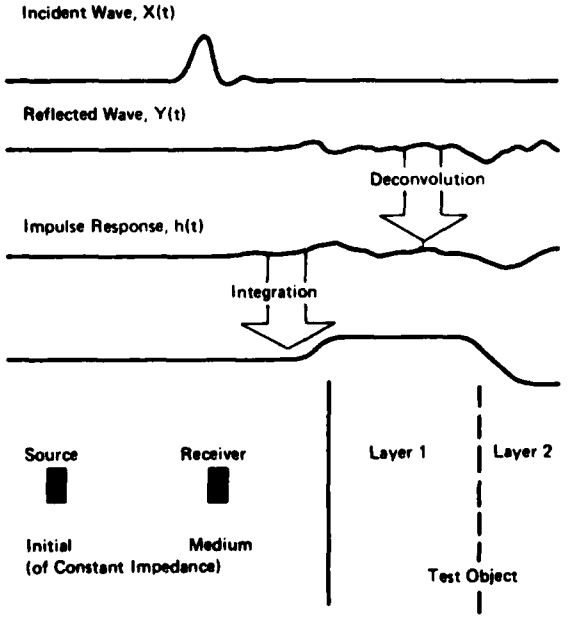

FIGURE 57. PRINCIPLES OF IMPEDIOGRAPHY (From Ref. 92, Reproduced by permission of IPC Science and Technology Press, Ltd., Guildford, England)

Tittmann (Ref. 93) reported attempts to correlate strength parameters of titanium alloy specimens with the scattering properties of an array of voids and defects in the material. It was found that ductility, as expressed by percent elongation, could be correlated with the ultrasonic scattering coefficient and spectral content of the scattered wave (See also II.B). Other strength parameters (i.e., yield stress and ultimate tensile stress) were not satisfactorily correlated with ultrasonic scattering data.

D. Delta Technique

The Delta technique (which derives its name from the triangular juxtaposition of the transmitting transducer, the receiving transducer, and the material flaw) is a new approach to ultrasonic detection of defects in materials. The technique, developed by Cross *et al.* (Ref. 94 and 95), detects reradiation from the defect of interest rather than directly reflected or scattered waves detected by conventional ultrasonic test configurations. Various ways in which ultrasonic energy from a transmitting transducer (T) can reach a receiving transducer (R) by way of a defect in a material specimen are shown in Figure 59. Direct reflection, mode conversion by a direct path, mode conversion by an indirect path, and reradiation from each of (1) a smooth vertical defect, (2) a spherical defect, and (3) an irregular defect are illustrated. It is apparent from these figures that certain types of defects fail to couple energy to the receiving transducer in certain test configurations. The Delta technique relies on reradiation (Figure 59d) which transmits energy to the receiving transducer independently of the shape and orientation of the defect. Figure 60 shows the typical configuration employed in the Delta technique; a transmitting transducer is arranged to launch an angle beam into the material under test, and a receiving transducer aimed normal to the material surface is oriented so that its capture region coincides with the volume insonified by the transmitter. Tests reported by Cross *et al.* (Ref. 94) indicated that for a variety of weld defects including (1) lack of penetration, (2) lack of fusion, (3) porosity greater than 0.25 mm (0.01 in.), (4) porosity less than 0.25 mm (0.01 in.), (5) cracks, and (6) microfissures, correlation between results of Delta inspection and results of destructive tests was very high. Correlations between (1) 60-degree angle-beam tests and destructive tests and (2) radiographic tests and destructive tests were in all cases, except one, poorer than correlations obtained by Delta inspection. The one case in which Delta inspection did not yield the highest correlation was porosity greater than 0.25 mm (0.01 in.), in which case 60-degree angle-beam inspection achieved greatest correlation.

E. Stress Enhancement of Fatigue Crack Detection

As metal fatigues, small cracks develop at the surface, usually initiated by a small surface

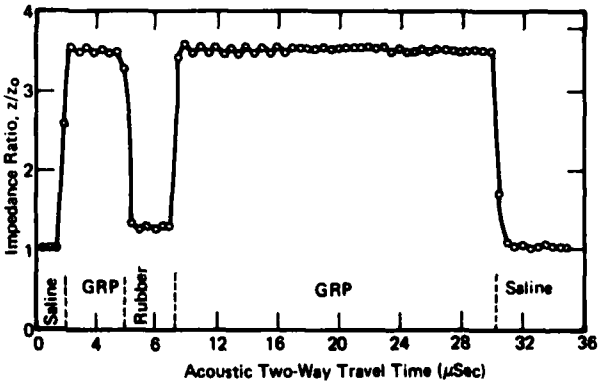

FIGURE 58. IMPEDIOGRAM OF MULTI-LAYER STRUCTURE IMMERSED IN SALINE SOLUTION (From Ref. 92, Reproduced by permission of IPC Science and Technology Press, Ltd., Guildford, England)

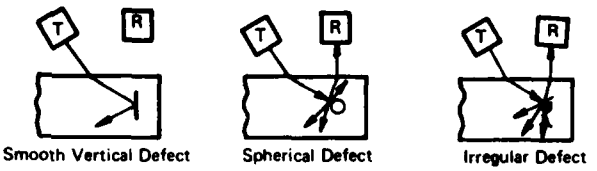

a. Reflected Energy

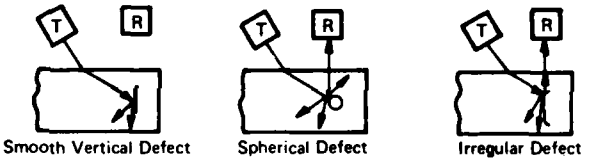

b. Mode Converted Energy (Direct)

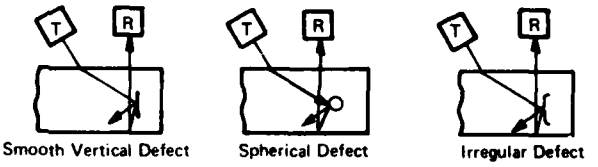

c. Mode Converted Energy (Indirect)

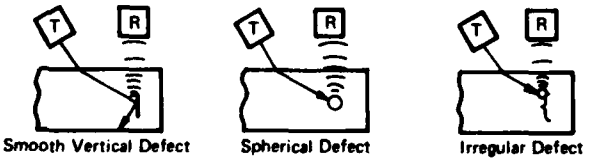

d. Reradiated Energy

FIGURE 59. VARIOUS MODES OF PROPAGATION OF ULTRASONIC ENERGY FROM A TRANSMITTER (T) TO A RECEIVER (R) BY WAY OF A DEFECT (From Ref. 95, Reproduced by permission of National Aeronautics and Space Administration, Marshall Space Flight Center, AL)

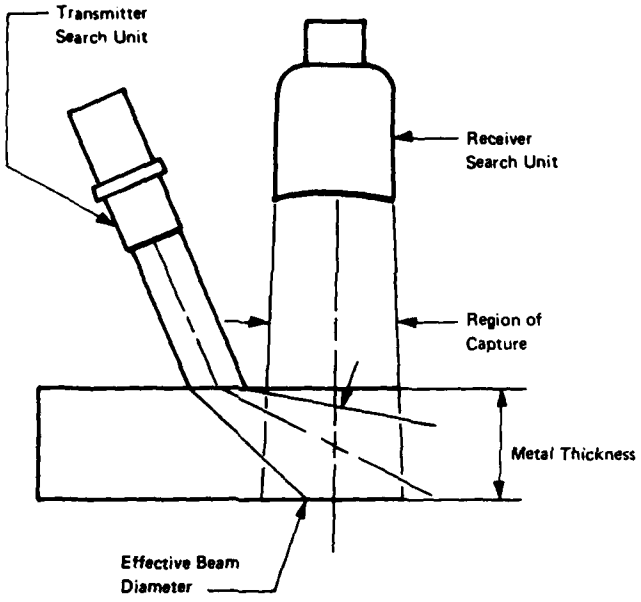

FIGURE 60. BASIC DELTA-INSPECTION CONFIGURATION
(From Ref. 95, Reproduced by permission of National Aeronautics and Space Administration, Marshall Space Flight Center, AL)

defect or subsurface inclusion. Once a fatigue crack starts it acts as a stress concentrator, and because of increased localized stress the crack grows rapidly until failure occurs. Often when a fatigue crack has reached an appreciable length, it may be undetectable by visual microscopic examination or by normal nondestructive inspection techniques. Figure 61a shows a region near the base of a turbine-engine compressor blade in which there is a tightly closed, invisible crack. Barton and Leonard (Ref. 96) have shown that such tightly closed fatigue cracks can be rendered visible and detectable by applying stress to the component under inspection. Figure 61b shows the same region of the same compressor blade with a load applied at the blade tip. The 1-mm (0.040-in.)-long fatigue crack is clearly visible when opened by application of stress.

The technique of stress enhancement of fatigue crack detection is particularly applicable in automated inspection of components in which such cracks may occur. A device employing this principle has been reported by Lake *et al.* (Ref. 97) for automatic in-place inspection of jet-engine compressor blades. A photograph of the apparatus mounted on a T-53 jet engine is presented in Figure 62. The instrument carried out multiple ultrasonic surface-wave inspections of compressor blades in both unstressed and stressed conditions. Defects noted during the unstressed inspection were classified as surface damage, and corresponding defect signals were digitized and committed to memory in the apparatus for future reference. New defects which appeared during stressed inspection were classified as fatigue cracks. A number of useful features were incorporated in the apparatus including (1) built-in check for proper ultrasonic coupling, (2) digital display of blade position number and defect code, (3) aural and visual alarms and interruption of test sequence when a defect was detected or when coupling failure occurred, and (4) automatic shut-down when all blades on the compressor disk had been inspected.

a. Photograph of Unstressed Compressor Blade with Fatigue Damage

b. Photograph of Compressor Blade with Load Applied to Accentuate Fatigue Damage

FIGURE 61. STRESS ENHANCEMENT OF FATIGUE CRACK DETECTION (From Ref. 97, Reproduced by permission of the Tenth Symposium on Nondestructive Evaluation, San Antonio, TX)

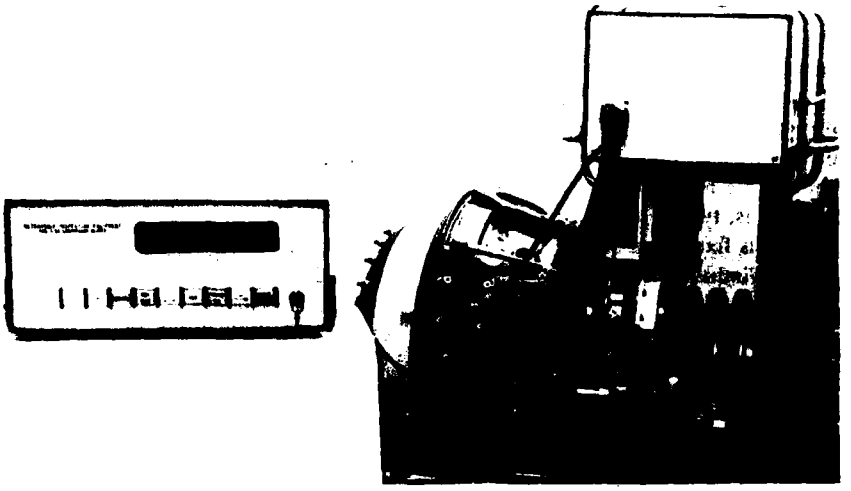

FIGURE 62. PROTOTYPE STRESS ENHANCED ULTRASONIC COMPRESSOR BLADE INSPECTION SYSTEM (From Ref. 97, Reproduced by permission of the Tenth Symposium on Nondestructive Evaluation, San Antonio, TX)

IV. SYSTEM COMPONENTS

A. Transducers

1. General

In ultrasonic nondestructive evaluation systems the transducer is the key link between the object being inspected and all of the electronic, signal processing, imaging and control functions of the system. Although new devices and techniques are being developed, the transducer is at present one of the least flexible components of an inspection system; that is, typical transducers usually operate efficiently at a single frequency, damping is not easily changed, beam pattern is fixed, and aiming must be accomplished mechanically. New technologies reported in this section are seeking to eliminate some of these restrictions on transducers. Use of new transducer techniques will add flexibility and versatility to future ultrasonic nondestructive evaluation systems.

2. Phased Array

Phased arrays have been used in electromagnetic antenna technology to dynamically control antenna pattern both in shape and principal aiming direction. Similar phased-array technology is now being applied to ultrasonic transducers to produce electronically steerable and focusable beams. The advantages of such an approach are (1) elimination of mechanical scanning apparatus, thereby increasing speed of operation, (2) increased inspection resolution over a greater depth range than possible with fixed-focus transducers, and (3) easy control of transducer operating parameters by a computer or other electronic device.

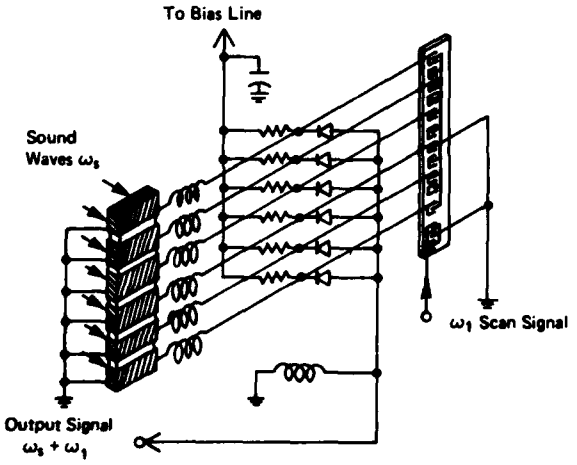

FIGURE 63. METHOD OF SCANNING A RECEIVING PHASED TRANSDUCER ARRAY (From Ref. 98, Reproduced by permission of the Institute of Electrical and Electronics Engineers, Inc., New York, NY)

Kino and his associates (Ref. 98 and 99) have developed a phased-array transducer with a unique method of addressing the individual elements in a receiving array. Outputs of the individual piezoelectric elements of a linear array were connected to individual diode modulators as shown in Figure 63. Also connected to the diode modulators were the multiple outputs of a tapped acoustic-surface-wave delay line. There were as many equally spaced taps on the delay line as there were elements in the linear transducer array. A signal, typically on the order of 50 MHz, was injected into the delay line, and a delayed version of this signal appeared sequentially at each of the diode modulators. If an output from a particular transducer element was present at the time the corresponding delay line output was energized, nonlinear mixing between the two signals occurred, thereby generating sum and difference frequencies. The outputs of all mixers were added on a common line, and either the sum frequency or the difference frequency was passed by a filter into the output circuit. If a chirped (i.e., linearly frequency modulated) signal were applied to the delay line, dynamic focusing of the array could be accomplished.

Various imaging system configurations are possible using the dynamically focused linear phased array as a receiver in conjunction with (1) a line transmitter array and (2) mechanical scanning of both transmitting and receiving arrays. Additionally, a group of line transmitters may be used to project a focused line of acoustic energy which passes through the specimen to a line-array receiver which is focused on the transmitted line. Also, a line array may be used to transmit and then later receive in the pulse-echo mode. A typical image produced by such a system is illustrated in Figure 64. Resolution on the order of 1mm (0.04 in.) was achieved with a transducer-to-object distance of 250 mm (10 in.).

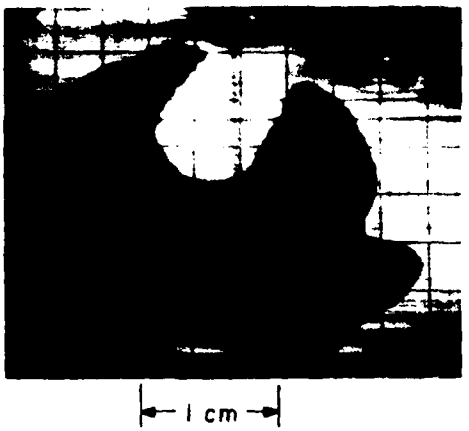

FIGURE 64. IMAGE OF WRENCH MADE WITH PHASED ARRAY SYSTEM (From Ref. 98, Reproduced by permission of the Institute of Electrical and Electronics Engineers, Inc., New York, NY)

FIGURE 65. IMAGE OF SIX MONOFILAMENTS MADE BY A PHASED ARRAY SYSTEM (From Ref. 100, Reproduced by permission of Plenum Publishing Corporation, New York, NY)

Thurstone and von Ramm (Ref. 100) used a linear array of ultrasonic transducers to produce high-resolution sector B-scans. Dynamic focusing during transmission was achieved by delayed pulsing of array elements according to an aspheric curve. Dynamic focusing in the receive mode was achieved by passing the received signals through switchable delay lines. The receiving focal point was made to track the focal point of the transmitted burst. A dedicated digital computer programmed phasing of the array on both transmission and reception and provided flexible interactive control of scan format and imaging parameters. Figure 65 is a typical image produced by this system. The object was six nylon monofilaments supported in a rectangular grid with spacings of 6 and 12 mm (0.25 and 0.50 in.). The image shown in the figure is a cross-section through the array of monofilaments.

Pappalardo (Ref. 101) reported design, fabrication, and test of a phased transducer array intended for beam steering. The array was composed of a number of line elements arranged side-by-side to form a plane rectangular radiating surface. Various phasing functions were applied to produce main-lobe steering and side-lobe reduction. Electronically controlled beam scanning was accomplished with this array by application of properly selected time-varying phase functions. A typical test array achieved 24-degree deflection (to one side) of the main-lobe center line with the worst case side lobe being 13 dB below the main lobe.

Yamshchikov *et al.* (Ref. 102) presented theoretical and experimental evaluation of a system for achieving virtual beam steering by cross correlation of the output signals from two spaced transducers. It was shown that to avoid distortion of the correlation diagram, (1) phase and amplitude characteristics of both transducer-amplifier channels must be identical and (2) spacing of the transducers should be on the order of a half wavelength. Directivity diagrams presented by the authors indicated that as the main lobe rotated, its shape changed and that strong side lobes appeared at certain angles of main-lobe rotation.

3. Focused

Focused transducers are often employed to increase ultrasonic inspection system resolution; however, increased resolution is obtained at the expense of depth of field. Thus, an unfocused transducer can inspect a volume of material with a certain range-dependent resolution, but a focused transducer inspects with significantly increased resolution a relatively thin slab of material while virtually ignoring portions of the material volume outside the focal region. Of course, increased focal depth can be achieved by increasing transducer focal length, but doing so increases spot size and, hence, decreases resolution.

Burckhardt *et al.* (Ref. 68) designed an annular transducer which gave good resolution over an unusually long focal range. The transducer actually was an annular array of 12 transducer elements which were excited sequentially with pulses having successively increasing phase delays. Received signals were

(1) delayed similarly, (2) digitized, (3) stored in a shift register, (4) reconverted to analog form, and (5) subtracted from the next-received echo signal. Sequential subtractions of this type reduced side-lobe contributions and emphasized main-lobe response. Focal depth of 200 mm (8 in.) with lateral resolution of 2 to 3 mm (0.08 to 0.12 in.) throughout the focal region was reported.

Burckhardt *et al.* (Ref. 103) also reported a transducer arrangement which was the ultrasonic analog of the optical axicon lens. The axicon lens is conical in form and focuses an incident collimated beam into a focal line as illustrated in Figure 66a. Detailed construction of the ultrasonic axicon is illustrated in Figure 66b. Acoustic energy from a commercial transducer was focused by an acrylic plastic lens, and the divergent beam on the far side of the focal point was incident upon a small conical mirror. Acoustic energy reflected from the small conical mirror was redirected and focused by a large annular mirror to form a 200-mm (8-in.)-long focal line as illustrated in Figure 66b. The annular mirror had two functions: (1) to effectively collimate the highly divergent incident acoustical beam, and (2) to act as the acoustical equivalent of the optical axicon. The surface of the large mirror was generated by rotating a circle around the device axis with the center of the generating circle not lying on the axis. The surface so generated was a combination of a cone and a sphere. A typical image produced by scanning a grid of wires is illustrated in Figure 67. The object used to generate this image was described in detail in Section III.B.5.d of this survey (See Ref. 67).

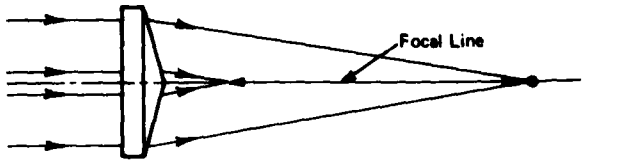

a. Geometry and Focal Properties of Axicon Lens

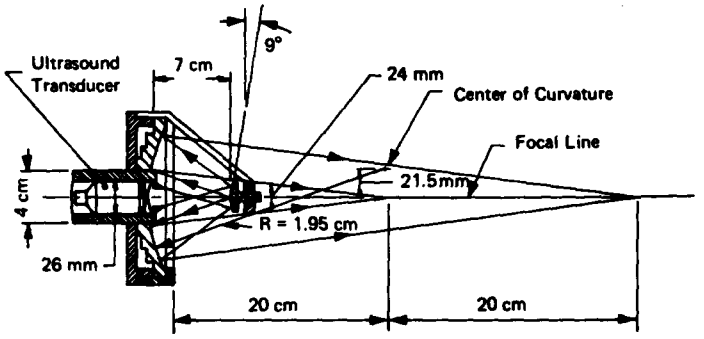

b. Details of Ultrasonic Axicon Lens

FIGURE 66. ULTRASONIC AXICON LENS (From Ref. 103, Reproduced by permission of the American Institute of Physics, New York, NY)

FIGURE 67. IMAGE OF TWO WIRE GRIDS MADE WITH ULTRASONIC AXICON (From Ref. 103, Reproduced by permission of the American Institute of Physics, New York, NY)

Hurwitz (Ref. 104) developed a transducer in which individual piezoelectric elements were mounted in a circular arc. The goal of this device was to produce an acoustical beam approximately 0.3 degrees wide which would resolve a patch 1.5 mm (0.06 in.) square at a depth of 300 mm (12 in.) in the specimen. Experimental devices, such as the one illustrated in Figure 68, were built with 38- and 75-mm (1.5- and 3-in.) arc radii for operation at either 2.5 MHz or 5 MHz. Beam widths ranging from 0.3 degrees in water to 1.5 degrees in steel were achieved. One problem associated with fabricating focused arc transducers is that the individual piezoelectric elements must be closely matched to achieve the required degree of phase coherence over the

large aperture. Hurwitz developed a rapid and relatively inexpensive method of accomplishing the required match by making a series of measurements from a plot of the logarithm of magnitude *versus* phase angle of transducer element terminal impedance.

Vilkomerson (Ref. 105) presented an analysis of an annular aperture as applied to acoustical imaging. Resolution for such an aperture was the same as for a full circular aperture of the same diameter. Phase and amplitude data obtained from various points on the annulus were processed to produce an acoustical image. Additionally, processing could be altered to achieve both focusing and beam steering.

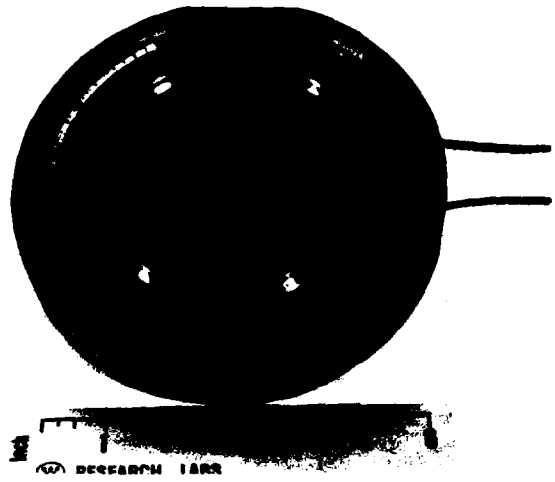

FIGURE 68. UNDERSIDE OF CONTACT-TYPE FOCUSED-ARC TRANSDUCER (From Ref. 104, Reproduced by permission of Defense Advanced Research Projects Agency, Arlington, VA)

4. Electromagnetic

The electromagnetic acoustic transducer (EMAT) is a new approach to acoustical transducer design. The EMAT offers a completely non-contacting means for generation and detection of ultrasonic waves. A radio-frequency coil is placed near the surface of an electrically conductive material in the presence of a strong, static magnetic field. Eddy currents induced in the conductor by radio-frequency excitation of the coil interact with the material through electron-ion collisions to produce ultrasonic waves which propagate into or along the surface of the material. Detection is accomplished by the reverse process; that is, in the presence of a static magnetic field, an acoustical wave produces eddy currents which are detected by a coil located near the surface. Although electromagnetic acoustic transducers have much lower electrical-to-acoustical power-conversion efficiency than conventional piezoelectric transducers, coils usually have less inherent noise than piezoelectric devices, so that signal-to-noise ratio comparable to that obtained in a conventional system is often realized. In spite of lower conversion efficiency, electromagnetic acoustic transducers have some unique application features including inspection of (1) moving objects, (2) liquid or powdered conductors, (3) materials at high temperatures, and (4) materials with rough or coated surfaces. In addition, because the EMAT is non-contacting, it does not require the usual coupling media which may prove advantageous in certain applications. Beissner (Ref. 106) has prepared an extensive state-of-the-art survey of electromagnetic acoustic transducer technology; this survey includes discussions of the basic physics of the process and EMAT design and application.

Burstein and his associates (Refs. 107 and 108) presented an extensive theoretical study of generation and detection of surface elastic waves on conducting solids using electromagnetic acoustic transducers and also by electromagnetic waves at microwave frequencies striking a wavelength-periodic grating scribed in the material surface. These authors also discussed experimental results with flat coil and meander-line electromagnetic acoustic transducer configurations. Surface elastic waves were generated and detected on aluminum at frequencies to 11.5 MHz. It was observed that when coils were used, surface waves were accompanied by bulk waves.

Maxfield and Hulbert (Ref. 109) have investigated various electromagnetic acoustic transducer coil configurations and the mode patterns which they produce. Their calculated results for spiral coils taking diffraction effects into consideration reportedly agreed satisfactorily with experimental mode-pattern measurements.

Thompson (Ref. 110) also presented a description and analysis of non-contacting electromagnetic acoustic transducers. Control of magnetic field strength and coil-pitch-to-ultrasonic-wavelength ratio facilitated excitation of various modes of propagation. Thompson reported, as a specific example of EMAT use, a "pig" for inspection of buried gas pipe incorporating electromagnetic acoustic transducers operating at 130 kHz.

5. Other Types

Although conventional piezoelectric transducers are most frequently used for ultrasonic nondestructive evaluation, there are other types and other configurations of transducers which may be used in certain special cases. Such devices are discussed briefly under this subheading.

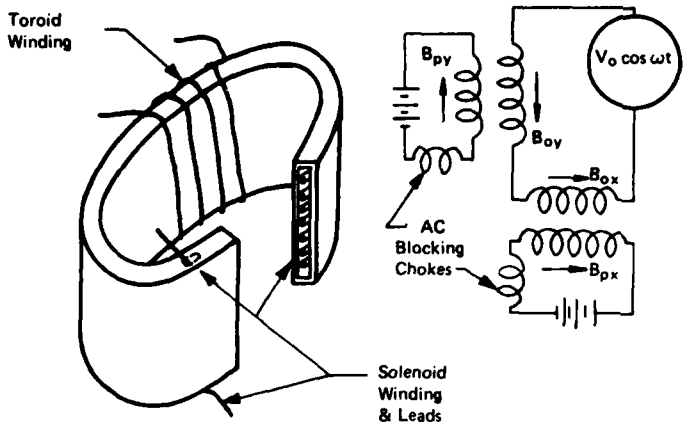

FIGURE 69. CONSTRUCTION AND EXCITATION OF A CROSSED-COIL MAGNETOSTRICTIVE TRANSDUCER (From Ref. 111, Reproduced by permission of the American Institute of Physics, New York, NY)

Edson and Huston (Ref. 111) presented a detailed mathematical analysis of a novel magnetostrictive transducer illustrated in Figure 69. Analysis showed that at low levels of operation, it was desirable to have magnetic excitation parallel to the axis of mechanical output. However, for high-level outputs where saturation may take place, increased output can be obtained by using off-axis excitation. The crossed-coil structure illustrated in Figure 69 was prepared by placing two solenoidal windings inside a tube of magnetostrictive material and two toroidal windings around the outside of the tube. One coil from each set of windings was used for direct-current bias, and the other coil in each set was excited with alternating current. Adjustment of field strengths produced by the various coils permitted the desired off-axis excitation. This configuration increased efficiency, strain amplitude, and coupling coefficient and reduced distortion.

Legros and Lewiner (Ref. 112) developed a theoretical model of electrostatic (i.e., capacitance) ultrasonic transducers using foil electrets. Experimental devices were fabricated using polyester and polypropylene dielectric films of approximately 10-μm (400-μin.) thickness to separate the plates of the capacitor. Such devices were operated experimentally to generate and receive ultrasonic signals at frequencies ranging from 10 to 200 MHz.

Alais (Ref. 53) has also built electrostatic transducers for ultrasonic applications. Performance details of these transducers were discussed in Section III.B.2. An interesting feature of the electrostatic transducers produced by Alais was the method of fabrication. Electrodes in the form of 256 parallel stripes of electrically conducting material were prepared by printed circuit techniques on both sides of a piece of thin dielectric film. The electrode stripes on one side were arranged horizontally and those on the other side, vertically. Individual electrostatic transducer elements were thus created at the intersections of the conducting stripes. Use of this device for acoustical imaging is discussed in an earlier section of this document.

Ultrasonic inspection of low-acoustic-impedance, highly attenuating, porous materials, such as polyfoam and fibrous silica ceramic, is difficult because of the high degree of acoustic impedance mismatch between the material to be inspected and typical transducer materials. Thompson and Alers (Ref. 113) have fabricated a transducer specifically intended for inspection of such difficult materials. The transducer, a cut-away view of which is shown in Figure 70, was made of 25 lead zirconate titanate (PZT) extensional-mode elements connected in parallel both mechanically and electrically. Strips of neoprene were bonded to each side of each transducer element to introduce mechanical damping. In addition, external electrical damping was applied to increase effective bandwidth of the transducer assembly. Using this device, detection of the back-surface echo from a 60-mm (2.4-in.)-thick slab of polyurethane foam was reported.

Wideband operation of piezoelectric ultrasonic transducers is usually achieved by use of a low-Q material such as lead metaniobate or by incorporation of mechanical and electrical damping. Korolev (Refs. 114 and 115)

observed that mechanical strain-wave generation in a piezoelectric transducer excited by a short electrical pulse occurred at the electroded surfaces. Ringing was caused by the strain waves so generated reflecting back and forth inside the transducer. An aperiodic transducer (i.e., one which has no resonant frequency) was fabricated by (1) depolarizing one end of a piezoelectric ceramic bar and (2) adding an acoustical absorber to that end of the transducer. The configuration is illustrated in Figure 71 in which variation of piezoelectric material polarization *versus* length is also illustrated by a graph. Upon application of a short pulse of electrical excitation to a transducer of this configuration, a corresponding pulse of mechanical strain was produced at the end of the transducer opposite the absorber where piezoelectric polarization was high. The wave thus generated coupled partially into the propagation medium (to the left in Figure 71), and the remainder propagated through the piezoelectric material into the absorber where it was dissipated; thus, no ringing occurred. Such a transducer proved excellent for generating unipolar acoustical pulses and other acoustical waveshapes requiring a wide-band transducer.

FIGURE 70. ARRAY TRANSDUCER INTENDED FOR ULTRASONIC INSPECTION OF LOW-ACOUSTIC-IMPEDANCE MATERIALS (From Ref. 113, Reproduced by permission of The Tenth Symposium on Nondestructive Evaluation, San Antonio, TX)

In cases where it is necessary to detect flaws very near the material surface or to measure thickness of relatively thin materials, interference from the "main bang" usually results. This problem can be overcome by incorporating an acoustical delay line between the transducer and the material being inspected. Korolev and Galkin (Ref. 116) reported fabrication of a transducer of this type. A delay line in the form of a brass cylinder (having a thread cut in the cylindrical surface to reduce radial-mode vibrations) was made an integral part of a transducer assembly intended for an ultrasonic thickness gage. The device was reported to have a round-trip transfer constant 225 times greater than that of a similar device with a plastic delay line.

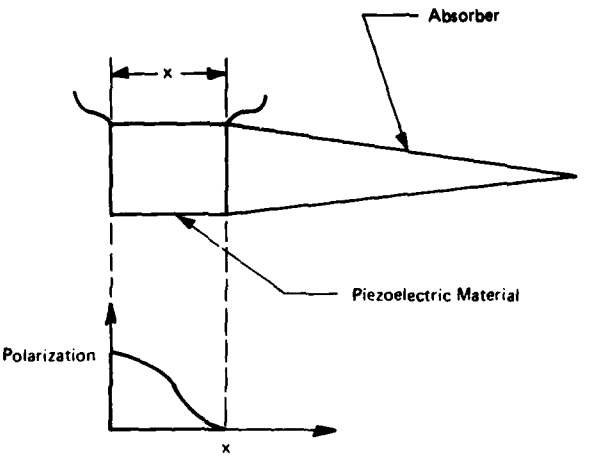

FIGURE 71. APERIODIC TRANSDUCER CONSTRUCTION (From Ref. 115, Reproduced by permission of Plenum Publishing Corporation, New York, NY)

6. Coupling

Since ultrasonic energy in the megahertz range is highly attenuated by even a short air path, it is essential that a couplant be provided between the face of the transducer and the surface of the material being inspected. Couplants are usually liquids, although in special cases other material forms can be used. Canella (Ref. 117) has studied both theoretically and experimentally the effects of couplant thickness in ultrasonic testing. Water, glycerin, lubricating oil, and penetrating oil were considered in this study. It was found that reproducibility of echo amplitude increased with decreasing couplant viscosity, surface tension, and density. Amplitude differences up to 20 dB were observed for liquid thickness variations on the order of 0.1 mm (0.004 in.). A resilient protective layer over the transducer face not only decreased transducer wear, but improved echo amplitude reproducibility. It was observed, however, that maximum transducer efficiency was obtained at a particular thickness of protective layer.

Kiskachi *et al.* (Ref. 118) have investigated a variety of coupling materials and have found a thin cotton cloth saturated with distilled water to be an effective coupling medium. Compared with direct water or glycerin coupling, use of a moistened cloth reduced round-trip system sensitivity approximately 30 percent. Advantages of this technique were greatly reduced transducer wear and greatly reduced clean-up effort after inspection.

Hsu and Sachse (Ref. 90) developed a rotatable shear-wave transducer for studying acoustical birefringence in elastically deformed solids. Normally, liquid couplants do not transmit shear waves; however, at high frequencies (on the order of 10 MHz) certain viscous fluids, such as Dow resin 276-V9, respond elastically and, therefore, will transmit shear waves. With a liquid couplant of this type, normal- or zero-incidence shear waves can be generated.

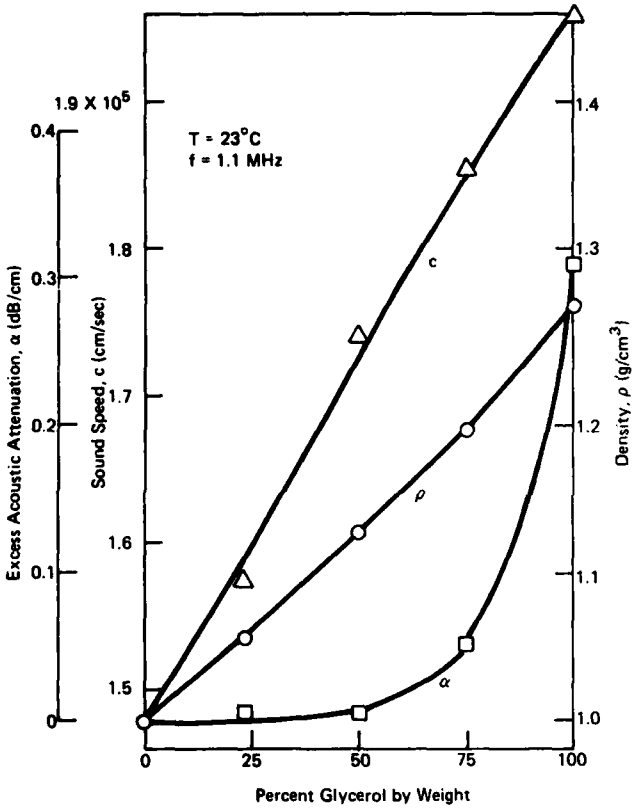

FIGURE 72. PROPERTIES OF WATER-GLYCEROL SOLUTIONS
(From Ref. 119, Reproduced by permission of the American Institute of Physics, New York, NY)

In immersion testing of various material shapes, surface curvature can have the effect of an acoustical lens which may distort test results. Additionally, reflections at the immersion fluid-material interface may substantially reduce actual energy which enters the test specimen. These effects may be minimized if the immersion fluid has the same velocity of propagation as the material being inspected. Knollman *et al.* (Ref. 119) have encountered this problem in imaging the interior of a tapered cylindrical billet. These authors investigated the coupling properties of solutions of glycerol and distilled water, and presented graphs (reproduced in Figure 72) of sound speed, excess acoustic attenuation (i.e., attenuation in excess of that in distilled water), and density of water-glycerol mixtures as functions of percent glycerol by weight. If the velocity of propagation in a particular material being inspected is known, the appropriate water-glycerol solution can be selected from the graph of Figure 72.

B. Scanners

1. General

Scanners are mechanical devices which move a transducer or a transducer array over an object to be inspected. A variety of scanning devices can be conceived. Erikson *et al.* (Ref. 18) mentioned in their review of ultrasound in medicine a number of scanning devices for medical applications and gave references to such applications in their extensive bibliography. Also, Knollman *et al.* (Ref. 119) described a variety of means of scanning by moving the object or the transducer.

2. Circular

Clement and Griffiths (Ref. 120) have studied ways in which scanning geometry affects resolution in the image reconstructed from an acoustical hologram. In general, under-sampling of the acoustical field degrades the reconstructed image. Analysis of the properties of the two-dimensional Fourier transformation showed that a 120-degree circular-arc scan can tolerate substantially coarser sampling than a rectilinear system for the same image resolution. To illustrate the technique, an acoustical hologram of a 250-mm (10-in.)-long part was recorded in 2.5 minutes using a circular-arc scan sampling every 3.3 wavelengths of the 2-MHz acoustical field.

The image produced by this system confirmed that a satisfactory hologram could be obtained with a sampling density less than that tolerable in a slower rectilinear scanning system.

3. Compound

As geometry of the part to be inspected becomes more complex, scanning a transducer over the part surface becomes more difficult. Elaborate computer-based systems have been developed to accomplish compound scanning.

Maxson (Ref. 121) has used a small general-purpose computer as the basis of a scanning system capable of inspecting free-form surfaces of revolution. The system automatically maintained the transducer axis perpendicular to the part surface and the face of the transducer at constant distance from the surface of the part. The front-surface echo was used in this system as the feedback-control parameter.

Yee *et al.* (Ref. 5 and 6) also have built a computer-controlled system for scanning compound-curved surfaces. Their device had capability for positioning the transducer by servo control for automatic contour following or by computer command for numerically controlled operation. This system was discussed in greater detail in Section II.B.

C. Transducer Exciters

A variety of systems have been developed for exciting transducers so that specific acoustical waveforms are produced. In general, these methods are intended to produce very short (and, hence, wideband) acoustical pulses. In some cases, special transducer configurations have been developed to achieve wideband operation, whereas in other cases, special excitation waveforms have been developed to take advantage of the inherent characteristics of relatively conventional transducers.

The need for short-duration acoustical pulses is forever present. Reduced pulse length increases range resolution in pulse-echo systems; new signal processing techniques, such as spectral analysis, require transmission of a broadband (i.e., short-duration) pulse. Unipolar pulses, because of their short durations, yield high resolution; additionally, the spectral content of a unipolar pulse is concentrated at lower frequencies, implying that such a pulse should propagate through materials having increasing attenuation with increasing frequency with less loss than a conventional damped-sinusoid pulse whose energy is concentrated at the (higher) carrier frequency.

Dixon and Davis (Ref. 122) have developed a system of exciting a conventional piezoelectric transducer so that the acoustical waveform produced is either a unipolar or bipolar triangular pulse. To produce a unipolar triangular acoustical pulse, electrical excitation was in the form of a simple ramp, the duration of which was carefully adjusted to equal the natural oscillation period of the transducer. A bipolar triangular acoustical pulse was generated by applying an equilateral triangular electrical pulse, the half-duration of which equaled the natural period of oscillation of the transducer.

Kazhis *et al.* (Ref. 123) and Korolev (Ref. 124) have developed similar methods of generating essentially unipolar pulses from a conventional resonant transducer. Both techniques employed excitation of the transducer by a multi-step staircase waveform, each step of which excited a damped ringing response in the transducer. Durations and amplitudes of the steps were adjusted so that damped oscillations produced by the second and subsequent excitation steps canceled all but the first half-cycle of the damped oscillation caused by the first excitation step. Kazhis *et al.* (Ref. 123) used a three-step waveform, whereas Korolev (Ref. 124) used a two-step waveform.

Lukoshevichus and Kazhis (Ref. 125) analyzed the pulse characteristics of a quartz transducer and derived the excitation waveshape required to produce a received pulse of specified characteristics. Part of the derivation included introduction of a four-pole network in the circuit to aid in compensating transient response. A transfer function for the correcting filter was derived.

Korolev (Ref. 115) described two generator circuits capable of producing pulses of arbitrary shapes. These generators were intended for use with the aperiodic transducer developed by the same author (Refs. 114 and 115).

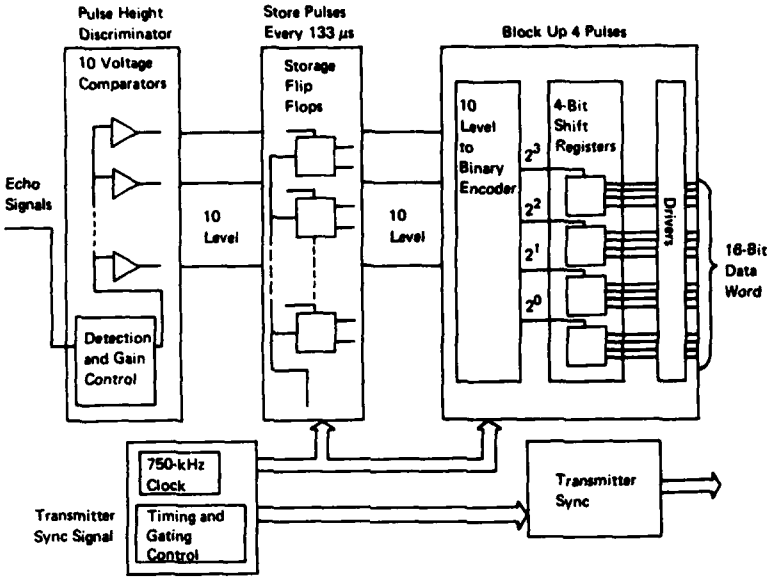

FIGURE 73. BLOCK DIAGRAM OF TEN-LEVEL DIGITIZER
(From Ref. 126, Reproduced by permission of IPC Science and Technology Press, Ltd., Guildford, England)

Generation of unipolar acoustical pulses of "bell" shape and rectangular form was reported. Other acoustical pulse shapes could be generated with an aperiodic transducer by simply driving that transducer electrically with the desired waveform.

D. Digitizers

In most cases in which signal digitization is used, conventional analog-to-digital converters are employed. However, Kay *et al.* (Ref. 126) described a limited-resolution, but relatively low-cost, digitizer which may be useful in many applications. A block diagram of this system is presented in Figure 73. The detected and filtered echo signal was applied in parallel to ten level detectors biased at sequentially increasing trip settings. A flip-flop register retained the highest level detected. The register output was converted to a 4-bit binary word, the individual bits of which were transferred to four 4-bit shift registers. Four successive 4-bit words were accumulated in the shift registers, following which they were read-out as a single 16-bit data word. The converter was clocked at a 750-kHz (1.33-μs) rate. Because of the method of quantization used, the converter was available and sensitive to input signal changes for over 90 percent of the operating time.

V. ACKNOWLEDGEMENTS

The author wishes to thank Dr. R. T. Smith, Director of the Nondestructive Testing Information Analysis Center (NTIAC) and Dr. C.G. Gardner, former Director of NTIAC, for their helpful comments and guidance during the preparation of this survey. Additional thanks go to R. R. King of NTIAC, who structured and conducted the computer literature search used as a basis for this survey. Thanks are also extended to G. A. Darcy, Jr., Chief of the NDT Applications Branch, and Dr. J. M. Smith, both of the Army Materials and Mechanics Research Center, Watertown, MA, for reviewing the draft of this document and making valuable suggestions. In addition, the author wishes to thank F. P. Hicks, D. J. Ivey, J. E. Wheeler, R. Johnson, D. Martin, R. M. Bryant, and N. Trevino for their invaluable help in typing the draft, locating documents and journals for review, preparing correspondence and organizing and handling illustration material received from authors around the world. Thanks are also extended to the many authors who provided original photographs required for illustration and who gave permission for reproducing the many line drawings used in this document. Finally, appreciation is expressed to the following publishers for granting permission to reproduce copyrighted material in this survey:

1. American Institute of Physics, New York, NY.
2. American Society for Testing and Materials, Philadelphia, PA.
3. Defense Advanced Research Projects Agency, Arlington, VA.
4. Institute of Electrical and Electronics Engineers, Inc., New York, NY.
5. IIT Research Institute, Chicago, IL.
6. IPC Science and Technology Press, Ltd., Guildford, England.
7. National Aeronautics and Space Administration, Marshall Space Flight Center, AL.
8. Noordhoff International Publishing, Leyden, The Netherlands.
9. Plenum Publishing Corp., New York, NY.
10. Society of Photo-optical Instrumentation Engineers, Palo Alto, CA.
11. The American Society for Nondestructive Testing, Inc., Columbus, OH.
12. The British Institute of Non-Destructive Testing, Southend-on-Sea, England.
13. The Institute of Physics, London, England.
14. The Institution of Electronic and Radio Engineers, London, England.
15. The Metallurgical Society of AIME, New York, NY.
16. U.S. Army Watervliet Arsenal, Watervliet, NY.

VI. REFERENCES

1. E.E. Weismantel, "Glossary of terms frequently used in nondestructive testing", *Materials Evaluation*, Vol. 33, No. 4, Apr. 1975, pp. 23A-46A.

2. J.A. Harlan, J.J. Connelly, C.J. Carter and R.A. Cellitti, "Automated computerized ultrasonic rating system provides new level of design confidence", Conference Proceedings, Automated Inspection and Product Control, IIT Research Institute, Chicago, Illinois, Oct. 15-17, 1974, pp. 165-202.

3. G. Kuenne, "Development of a large automatic ultrasonic plate testing installation with on-line computer data output", *Materials Evaluation*, Vol. 33, No. 4, Apr. 1975, pp. 73-80.

4. H.T. Ploegaert, "Die Prüfung von Blechen im Dickenbereich von 1,5 bis 6 mm mit einer automatischen Ultraschallanlage" [Testing of sheet within the thickness range of 1.5-6 mm with the aid of an automatic ultrasonic device], *Materialprüfung*, Vol. 16, No. 9, Sept. 1974, pp. 285-286. (In German).

5. B.G.W. Yee, E.E. Kerlin, A.H. Gardner, *et al.*, "Computer-Automated Ultrasonic Inspection System for Aircraft Forgings", Technical Report AFML-TR-73-194, Air Force Materials Laboratory, Wright-Patterson Air Force Base, Ohio, Oct. 1973.

6. B.G.W. Yee and J.E. Allison, "A computer automated ultrasonic inspection system for aircraft forgings", Conference Proceedings, Automated Inspection and Product Control, IIT Research Institute, Chicago, Illinois, Oct. 15-17, 1974, pp. 265-275.

7. G. Boulanger, J.P. Dufayet, A. Samoel, B. Spriet and A. Stossel, "Automatic nondestructive testing system for thin tubes", *Materials Evaluation*, Vol. 32, No. 1, Jan. 1974, pp. 18-24.

8. G.H. Kyte and K.R. Whittington, "A high-speed ultrasonic testing machine for tubes", *The Radio and Electronic Engineer*, Vol. 41, No. 5, May 1971, pp. 213-222.

9. R. Lewis and A.R. Cornforth, "Automatic rotary probe system for the ultrasonic inspection of steel tube", *Non-Destructive Testing*, Vol. 3, No. 2, Apr. 1970, pp. 128-131.

10. D.C. Winters, "Automated Crack Position and Depth Measurements on Cannon Tubes", Technical Report WVT-7248, Benét Weapons Laboratory, U.S. Army Watervliet Arsenal, Watervliet, New York, Sept. 1972, AD-756401.

11. J.J. Miller, R.R. Fujczak and D.C. Winters, "The measurement and analysis of fatigue crack growth in cylindrical shapes", *Fra. .res and Flaws*, Proceedings of the 13th Annual Symposium, Mar. 1-2, 1973, pp. 55-61.

12. J.J. Miller, D.C. Winters and R.R. Fujczak, "The Measurement and Analysis of Fatigue Crack Growth in Thick-Walled Cylinders", Technical Report WVT-TR-74040, Benét Weapons Laboratory, U.S. Army Watervliet Arsenal, Watervliet, New York, Sept. 1974.

13. D.C. Winters, "Automated Crack Measurement System", Technical Report WVT-TR-75018, Benét Weapons Laboratory, U.S. Army Watervliet Arsenal, Watervliet, New York, Apr. 1975.

14. D.C. Winters, "Automatic End-On Fatigue Crack Measurements on Thick-Walled Cylinders", Technical Report WVT-TR-75025, U.S. Army Watervliet Arsenal, Watervliet, New York, May 1975, AD-A012758.

15. T. Suzuchi and S. Kikuchi, "The application of mechanized ultrasonic testing in shipbuilding", *The British Journal of Non-Destructive Testing*, Vol. 17, No. 3, May 1975, pp. 65-70.

16. J.H. Gieske, "Some applications of computerized ultrasonic data acquisition and display system", Conference Proceedings, Automated Inspection and Product Control, IIT Research Institute, Chicago, Illinois, Oct 15-17, 1974, pp. 39-61.

17. B. Stiefeld, "A strategy for the use of a minicomputer-based test system as a general-purpose NDE laboratory tool", *Materials Evaluation*, Vol. 31, No. 6, June 1973, pp. 97-103.

18. K.R. Erikson, F.J. Fry and J.P. Jones, "Ultrasound in medicine–a review", *IEEE Transactions on Sonics and Ultrasonics*, Vol. SU-21, No. 3, July 1974, pp. 144-170.

19. J.C. Kennedy and W.E. Woodmansee, "Signal processing in nondestructive testing", *Journal of Testing and Evaluation*, Vol. 3, No. 1, Jan. 1975, pp. 26-45.

20. J.L. Rose and P.A. Meyer, "Signal processing concepts for flaw characterisation", *The British Journal of Non-Destructive Testing*, Vol. 16, No. 4, July 1974, pp. 97-106.

21. J.L. Rose and P.A. Meyer, "Ultrasonic signal-processing concepts for measuring the thickness of thin layers", *Materials Evaluation*, Vol. 32, No. 12, Dec. 1974, pp. 249-255, 258.

22. O.R. Gericke, "Determination of the geometry of hidden defects by ultrasonic pulse analysis testing", *Journal of the Acoustical Society of America*, Vol. 35, No. 3, Mar. 1963, pp. 364-368.

23. O.R. Gericke, "Ultrasonic spectroscopy of steel", *Materials Research and Standards*, Vol. 5, No. 1, Jan. 1965, pp. 23-30.

24. O.R. Gericke, "Defect determination by ultrasonic spectroscopy", *Journal of Metals*, Vol. 18, No. 8, Aug. 1966, pp. 932-937.

25. O.R. Gericke, "Ultrasonic pulse-echo spectroscopy", *Proceedings: 1968 Symposium on the NDT of Welds and Materials Joining*, Los Angeles, California, Mar. 11-13, 1968, pp. 267-287.

26. H.L. Whaley and K.V. Cook, "Ultrasonic frequency analysis", *Materials Evaluation*, Vol. 28, No. 3, Mar. 1970, pp. 61-66.

27. H.L. Whaley and L. Adler, "Flaw characterization by ultrasonic frequency analysis", *Materials Evaluation*, Vol. 29, No. 8, Aug. 1971, pp. 182-188, 192.

28. H.L. Whaley and L. Adler, "A new approach to the old problem of determining flaw size", *International Journal of Fracture Mechanics*, Vol. 8, No. 1, Mar. 1972, pp. 112-113.

29. L. Adler and H.L. Whaley, "Interference effect in a multifrequency ultrasonic pulse echo and its application to flaw characterization", *Journal of the Acoustical Society of America*, Vol. 51, No. 3, Mar. 1972, pp. 881-887.

30. H.L. Whaley, K.V. Cook, L. Adler and R.W. McClung, "Applications of frequency analysis in ultrasonic testing", *Materials Evaluation*, Vol. 33, No. 1, Jan. 1975, pp. 19-24.

31. J.A. Seydel and J.R. Frederick, "A computer-processed ultrasonic pulse-echo NDT system", *Materials Evaluation*, Vol. 31, No. 11, Nov. 1973, pp. 223-228.

32. E.P. Papadakis, "Ultrasonic spectroscopy applied to double refraction in worked metals", *Journal of the Acoustical Society of America*, Vol. 55, No. 4, Apr. 1974, pp. 783-784.

33. B.G.W. Yee, F.H. Chang and J.C. Couchman, "Applications of ultrasonic interference spectroscopy to materials and flaw detection", *Materials Evaluation*, Vol. 33, No. 8, Aug. 1975, pp. 193-199, 202.

34. S.E. Baryshev, "Spectral density of an echo-signal train", *The Soviet Journal of Nondestructive Testing*, Vol. 10, No. 2, Jan. 1975 (Russian original, Mar.-Apr. 1974), pp. 137-141.

35. D.H. McSherry, "Computer processing of diagnostic ultrasound data", *IEEE Transactions on Sonics and Ultrasonics*, Vol. SU-21, No. 2, Apr. 1974, pp. 91-97.

36. D.L. Waidelich, "Data correlation methods in NDE", Conference Proceedings, Automated Inspection and Product Control, IIT Research Institute, Chicago, Illinois, Oct. 15-17, 1974, pp. 63-71.

37. E.S. Furgason, V.L. Newhouse, N.M. Bilgutay and G.R. Cooper, "Application of random signal correlation techniques to ultrasonic flaw detection", *Ultrasonics*, Vol. 13, No. 1, Jan. 1975, pp. 11-17.

38. V.L. Newhouse, N.M. Bilgutay and E.S. Furgason, "Random noise signal processing", *Proceedings of the ARPA/AFML Review of Quantitative NDE*, Technical Report AFML-TR-75-212, Air Force Materials Laboratory, Wright-Patterson Air Force Base, Ohio, Jan. 1976, pp. 343-362.

39. V.S. Yamshchikov and V.N. Nosov, "Apparatus for correlative ultrasonic flaw detection in coarse-structured materials", *The Soviet Journal of Nondestructive Testing*, Vol. 11, No. 1, Nov. 1975 (Russian original, Jan.-Feb. 1975), pp. 62-68.

40. V.D. Koryachenko, "Statistical processing of flaw detector signals to enhance the signal-to-noise ratio associated with structural reverberation noise", *The Soviet Journal of Nondestructive Testing*, Vol. 11, No. 1, Nov. 1975 (Russian original, Jan.-Feb. 1975), pp. 69-75.

41. A.N. Mucciardi, R. Shankar, J. Cleveland, W.E. Lawrie and H.L. Reeves, "Adaptive Nonlinear Signal Processing for Characterization of Ultrasonic NDE Waveforms–Task 1: Inference of Flatbottom Hole Size", Interim Technical Report AFML-TR-75-24, Air Force Materials Laboratory, Wright-Patterson Air Force Base, Ohio, Feb. 1975.

42. M.G. Silk and B.H. Lidington, "Better ultrasonic resolution by data unfolding", *Non-Destructive Testing*, Vol. 8, No. 2, Apr. 1975, pp. 94-99.

43. H. Berger, "Ultrasonic imaging systems for nondestructive testing", *Journal of the Acoustical Society of America*, Vol. 45, No. 4, Apr. 1969, pp. 859-867.

44. H.W. Jones, "Some aspects of ultrasonic imaging at frequencies of 1 to 100 MHz", Ultrasonics International 1973 Conference Proceedings, London, Mar. 27-29, 1973, published by IPC Science and Technology Press, Ltd., Guildford, England, pp. 257-264.

45. R.C. Addison, "Recent advances in ultrasonic imaging", *Proceedings of the ARPA/AFML Review of Quantitative NDE*, Technical Report AFML-TR-75-212, Air Force Materials Laboratory, Wright-Patterson Air Force Base, Ohio, Jan. 1976, pp. 273-301.

46. N. Bom, C.T. Lancée, G. van Zwieten, F.E. Kloster and J. Roelandt, "Multiscan echocardiography", *Circulation*, Vol. 48, Nov. 1973, pp. 1066-1074.

47. S.O. Harrold, "Solid state ultrasonic camera", *Ultrasonics*, Vol. 7, No. 2, Apr. 1969, pp. 95-101.

48. M.G. Maginness and L. Kay, "Ultrasonic imaging in solids", *The Radio and Electronic Engineer*, Vol. 41, No. 2, Feb. 1971, pp. 91-93.

49. M.G. Maginness, J.D. Plummer and J.D. Meindl, "An acoustic image sensor using a transmit-receive array", *Acoustical Holography*, Vol. 5, Proceedings of the Fifth International Symposium on Acoustical Holography and Imaging, Palo Alto, California, July 18-20, 1973; P.S. Green, ed., Plenum Press, New York, 1974, pp. 619-631.

50. P.S. Green, L.F. Schaefer, E.D. Jones and J.R. Suarez, "A new, high-performance ultrasonic camera", *Acoustical Holography*, Vol. 5, Proceedings of the Fifth International Symposium on Acoustical Holography and Imaging, Palo Alto, California, July 18-20, 1973; P.S. Green, ed., Plenum Press, New York, 1974, pp. 493-503.

51. G.C. Knollman and A.E. Brown, "Hydroacoustic image transducer", *Review of Scientific Instruments*, Vol. 42, No. 8, Aug. 1971, pp. 1202-1214.

52. G.C. Knollman, J.L. Weaver and J.J. Hartog, "Linear receiving array for acoustic imaging and holography", *Acoustical Holography*, Vol. 5, Proceedings of the Fifth International Symposium on Acoustical Holography and Imaging, Palo Alto, California, July 18-20, 1973; P.S. Green, ed., Plenum Press, New York, 1974, pp. 647-658.

53. P. Alais, "Real-time acoustical imaging with a 256 X 256 matrix of electrostatic transducers", *Acoustical Holography*, Vol. 5, Proceedings of the Fifth International Symposium on Acoustical Holography and Imaging, Palo Alto, California, July 18-20, 1973; P.S. Green, ed., Plenum Press, New York, 1974, pp. 671-684.

54. P.D. Hanstead, "A new ultrasonic focusing system for materials inspection", *Journal of Physics D: Applied Physics*, Vol. 7, No. 2, 21 Jan. 1974, pp. 226-241 (plus 4 pages of plates in plate section).

55. R.S. Mezrich, K.F. Etzold and D.H.R. Vilkomerson, "System for visualizing and measuring ultrasonic wavefronts", *RCA Review*, Vol. 35, No. 4, Dec. 1974, pp. 483-519.

56. R. Mezrich, D. Vilkomerson, and K. Etzold, "Ultrasonic imaging exploits phase contrast", *IEEE Spectrum*, Vol. 12, No. 12, Dec. 1975, pp. 35-39.

57. O.R. Gericke and R.C. Grubinskas, "Utilization of the liquid surface levitation effect as a means of ultrasonic image conversion for materials inspection", *Journal of the Acoustical Society of America*, Vol. 45, No. 4, Apr. 1969, p. 872-880.

58. P.S. Green, "A new liquid-surface-relief method of acoustic image conversion", *Acoustical Holography*, Vol. 3, Proceedings of the Third International Symposium on Acoustical Holography, Newport Beach, California, July 29-31, 1970; A.F. Metherell, ed., Plenum Press, New York, 1971, pp. 173-187.

59. B.B. Brenden, "Recent developments in acoustical imaging", *Materials Research and Standards*, Vol. 11, No. 9, Sept. 1971, pp. 16-18, 52.

60. H.D. Collins and R.P. Gribble, "Acoustic holographic scanning techniques for imaging flaws in thick metal sections", *Imaging Techniques for Testing and Inspection*, Proceedings of the Society of Photo-optical Instrumentation Engineers, Vol. 29, Feb. 1972, pp. 67-82.

61. B.P. Hildebrand, "Current and potential applications of acoustical holography", *Proceedings of the Engineering Applications of Holography Symposium*, Los Angeles, California, Feb. 16-17, 1972, pp. 37-53.

62. M.J. Intlekofer, D.C. Auth and M.E. Fourney, "Display of HF acoustic holograms utilizing liquid crystals", *Imaging Techniques for Testing and Inspection*, Proceedings of the Society of Photo-optical Instrumentation Engineers, Vol. 29, Feb. 1972, pp. 83-88.

63. G.C. Knollman and J.L. Weaver, "Acoustical holography with a scanned linear array", *Journal of Applied Physics*, Vol. 43, No. 10, Oct 1972, pp. 3906-3913.

64. E. Marom, R.K. Mueller, R.F. Koppelmann and G. Zilinskas, "Design and preliminary test of an underwater viewing system using sound holography", *Acoustical Holography*, Vol. 3, Proceedings of the Third International Symposium on Acoustical Holography, Newport Beach, California, July 29-31, 1970; A.F. Metherell, ed., Plenum Press, New York, 1971, pp. 191-209.

65. S.P. Ying, R.A. Baker and A.S. Greer, "Scanned single transducer ultrasonic holography", *Proceedings of the 1974 Educational Seminar on Inservice Inspection and Quality Assurance*, National Fall Conference of the American Society for Nondestructive Testing, Oct. 1-5, 1973, Chicago, Illinois, published by Quality Assurance Systems and Engineering Division, Southwest Research Institute, San Antonio, Texas, pp. 32.1-32.14.

66. P. Pille and B.P. Hildebrand, "Rigorous analysis of the liquid-surface acoustical holography system", *Acoustical Holography*, Vol. 5, Proceedings of the Fifth International Symposium on Acoustical Holography and Imaging, Palo Alto, California, July 18-20, 1973; P.S. Green, ed., Plenum Press, New York, 1974, pp. 335-371.

67. C.B. Burckhardt, P.-A. Grandchamp and H. Hoffmann, "An experimental 2 MHz synthetic aperture sonar system intended for medical use", *IEEE Transactions on Sonics and Ultrasonics*, Vol. SU-21, No. 1, Jan. 1974, pp. 1-6.

68. C.B. Burckhardt, P.-A. Grandchamp and H. Hoffmann, "Methods for increasing the lateral resolution of B-scan", *Acoustical Holography*, Vol. 5, Proceedings of the Fifth International Symposium on Acoustical Holography and Imaging, Palo Alto, California, July 18-20, 1973; P.S. Green, ed., Plenum Press, New York, 1974, pp. 391-413.

69. D.W. Prine, "Synthetic aperture ultrasonic imaging", *Proceedings of the Engineering Applications of Holography Symposium*, Los Angeles, California, Feb. 16-17, 1972, pp. 287-294.

70. F.L. Becker and R.L. Trantow, "Ultrasonic isometric imaging", *Imaging Techniques for Testing and Inspection*, Proceedings of the Society of Photo-optical Instrumentation Engineers, Vol. 29, Feb. 1972, pp. 61-65.

71. C.-H. Lee, G.R. Heidbreder and A.C. Berggreen, "Digital image enhancement techniques applied to acoustical imaging", Ultrasonics Symposium Proceedings, 1973, Monterey, California, Nov. 5-7, 1973, pp. 31-36.

72. M. Takagi, N.B. Tse, G.R. Heidbreder, C.-H. Lee and G. Wade, "Computer enhancement of acoustical images", *Acoustical Holography*, Vol. 5, Proceedings of the Fifth International Symposium on Acoustical Holography and Imaging, Palo Alto, California, July 18-20, 1973; P.S. Green, ed., Plenum Press, New York, 1974, pp. 541-550.

73. L.W. Kessler, "Acoustic microscopy–a new dimension in ultrasonic visualization", Ultrasonics International 1973 Conference Proceedings, London, Mar. 27-29, 1973, published by IPC Science and Technology Press, Ltd., Guildford, England, pp. 173-176.

74. R.A. Lemons and C.F. Quate, "A scanning acoustic microscope", Ultrasonics Symposium Proceedings, 1973, Monterey, California, Nov. 5-7, 1973, pp. 18-21.

75. R.C. Addison, "A progress report on the Sokolov tube utilizing a metal fiber faceplate", *Acoustical Holography*, Vol. 5, Proceedings of the Fifth International Symposium on Acoustical Holography and Imaging, Palo Alto, California, July 18-20, 1973, P.S. Green, ed., Plenum Press, New York, 1974, pp. 659-670.

76. J.E. Jacobs and D.A. Peterson, "The use of discrete, shaped matching sections to increase the aperture of the Sokoloff tube", Ultrasonics International 1973 Conference Proceedings, London, Mar. 27-29, 1973, published by IPC Science and Technology Press, Ltd., Guildford, England, pp. 275-282.

77. J.E. Jacobs and D.A. Peterson, "Advances in the Sokolov tube", *Acoustical Holography*, Vol. 5, Proceedings of the Fifth International Symposium on Acoustical Holography and Imaging, Palo Alto, California, July 18-20, 1973; P.S. Green, ed., Plenum Press, New York, 1974, pp. 633-645.

78. S.A. Lund and P.R. Jensen, "The projection scan, a new method for recording and visualizing data from ultrasonic weld inspection", *Non-Destructive Testing*, Vol. 6, No. 6, Dec. 1973, pp. 307-313.

79. W.H. Sproat and S.E. Cohen, "AGIS–An acoustographic imaging system", *Materials Evaluation*, Vol. 28, No. 3, Mar. 1970, pp. 73-76.

80. R. Adler, A. Korpel and P. Desmares, "An instrument for making surface waves visible", *IEEE Transactions on Sonics and Ultrasonics*, Vol. SU-15, No. 3, July 1968, pp. 157-161.

81. G. Alers, M.A. Tennison, R.B. Thompson and B.R. Tittmann, "Visualization of surface elastic waves on structural materials", *Ultrasonics*, Vol. 11, No. 4, July 1973, pp. 174-177.

82. R. Aprahamian and P.G. Bhuta, "NDT by acousto-optical imaging", *Materials Evaluation*, Vol. 29, No. 5, May 1971, pp. 112-116.

83. H. Keyani, J. Landry and G. Wade, "Bragg-diffraction imaging: A potential technique for medical diagnosis and material inspection, Part II", *Acoustical Holography*, Vol. 5, Proceedings of the Fifth International Symposium on Acoustical Holography and Imaging, Palo Alto, California, July 18-20, 1973; P.S. Green, ed., Plenum Press, New York, 1974, pp. 25-39.

84. J.F. Greenleaf, S.A. Johnson, S.L. Lee, G.T. Herman and E.H. Wood, "Algebraic reconstruction of spatial distributions of acoustic absorption within tissue from their two-dimensional acoustic projections", *Acoustical Holography*, Vol. 5, Proceedings of the Fifth International Symposium on Acoustical Holography and Imaging, Palo Alto, California, July 18-20, 1973; P.S. Green, ed., Plenum Press, New York, 1974, pp. 591-603.

85. J.F. Greenleaf, S.A. Johnson, W.F. Samayoa and F.A. Duck, "Algebraic reconstruction of spatial distributions of acoustic velocities in tissue from their time-of-flight profiles", *Acoustical Holography*, Vol. 6, Proceedings of the Sixth International Symposium on Acoustical Holography, San Diego, California, Feb. 4-7, 1975; N. Booth, ed., Plenum Press, New York, 1975, pp. 71-90.

86. S. Lees, "Data reduction from critical angle reflection measurements", *Ultrasonics*, Vol. 13, No. 5, Sept. 1975, pp. 213-215.

87. G.A. Alers, "Measurement of hardness vs. depth contours by ultrasonic velocity", Conference Proceedings, Automated Inspection and Product Control, IIT Research Institute, Chicago, Illinois, Oct. 15-17, 1974, pp. 85-92.

88. T.J. Moran, R.L. Thomas, G.F. Hawkins and M.J. Lin, "Electromagnetic generation of bulk and surface sound waves at megahertz frequencies for NDE", Proceedings of the Tenth Symposium on Nondestructive Evaluation, San Antonio, Texas, Apr. 23-25, 1975, pp. 105-111.

89. P.J. Noronha, J.J. Wert and D.L. Kinser, "Characterization of material parameters and the measurement of residual stress using ultrasonic techniques", Ultrasonics Symposium Proceedings, 1973, Monterey, California, Nov. 5-7, 1973, pp. 230-233.

90. N.N. Hsu and W. Sachse, "Generation and detection of plane-polarized ultrasound with a rotatable transducer", *Review of Scientific Instruments*, Vol. 46, No. 7, July 1975, pp. 923-926.

91. R.E. Green, Jr., "Ultrasonic attenuation detection of fatigue damage", Ultrasonics International 1973 Conference Proceedings, London, Mar. 27-29, 1973, published by IPC Science and Technology Press, Ltd., Guildford, England, pp. 187-193.

92. J.P. Jones, "Impediography: a new ultrasonic technique for non-destructive testing and medical diagnosis", Ultrasonics International 1973 Conference Proceedings, London, Mar. 27-29, 1973, published by IPC Science and Technology Press, Ltd., Guildford, England, pp. 214-218.

93. B.R. Tittmann, "Strength prediction by ultrasonic defect characterization", Conference Proceedings, Automated Inspection and Product Control, IIT Research Institute, Chicago, Illinois, Oct. 15-17, 1974, pp. 73-84.

94. B.T. Cross, K.J. Hannah and W.M. Tooley, "The delta technique—a research tool, a quality assurance tool", *Proceedings: 1968 Symposium on the NDT of Welds and Materials Joining*, Los Angeles, California, Mar. 11-13, 1968, pp. 482-511.

95. K.J. Hannah, B.T. Cross and W.M. Tooley, "Development of the Ultrasonic Delta Technique for Aluminum Welds and Materials", Final Report, Contract NAS-8-18009, NASA—George C. Marshall Space Flight Center, Alabama, NASA CR-61952, May 15, 1968.

96. J.R. Barton and B.E. Leonard, "Evaluation of Compressor Blade Crack Detection by Dynamic Load Ultrasonic Inspection", Summary report, Contract No. F41608-67-A-6604, Kelly Air Force Base, Texas, June 1968.

97. W.W. Lake, J. Thorp, J.R. Barton and W.D. Perry, "Development of stress-enhanced ultrasonic compressor blade inspection equipment", Proceedings of the Tenth Symposium on Nondestructive Evaluation, San Antonio, Texas, Apr. 23-25, 1975, pp. 181-193.

98. J.F. Havlice, G.S. Kino and C.F. Quate, "A new acoustic imaging device", Ultrasonics Symposium Proceedings, 1973, Monterey, California, Nov. 5-7, 1973, pp. 13-17.

99. G.S. Kino, "Applications of electronically scanned acoustic imaging techniques to NDT", *Proceedings of the ARPA/AFML Review of Quantitative NDE*, Technical Report AFML-TR-75-212, Air Force Materials Laboratory, Wright-Patterson Air Force Base, Ohio, Jan. 1976, pp. 303-319.

100. F.L. Thurstone and O.T. von Ramm, "A new ultrasound imaging technique employing two-dimensional electronic beam steering", *Acoustical Holography*, Vol. 5, Proceedings of the Fifth International Symposium on Acoustical Holography and Imaging, Palo Alto, California, July 18-20, 1973; P.S. Green, ed., Plenum Press, New York, 1974, pp. 249-259.

101. M. Pappalardo, "Transducer line-arrays in the high-frequency range", *Ultrasonics*, Vol. 11, No. 2, Mar. 1973, pp. 77-82.

102. V.S. Yamshchikov, V.N. Nosov and V.L. Shkuratnik, "Formation and rotation of a correlation directivity diagram for ultrasonic flaw detection in coarse-structured materials", *The Soviet Journal of Nondestructive Testing*, Vol. 10, No. 5, July 1975 (Russian original, Sept.-Oct. 1974), pp. 537-542.

103. C.B. Burckhardt, H. Hoffmann and P.-A. Grandchamp, "Ultrasound axicon: a device for focusing over a large depth", *Journal of the Acoustical Society of America*, Vol. 54, No. 6, Dec. 1973, pp. 1628-1630.

104. M.J. Hurwitz, "Transducer for a High-Resolution Ultrasonic Scanning System", Technical Report, Contract No. N00140-70-C-0065, Defense Advanced Research Projects Agency, Nov. 1970.

105. D. Vilkomerson, "Acoustic imaging with thin annular apertures", *Acoustical Holography*, Vol. 5, Proceedings of the Fifth International Symposium on Acoustical Holography and Imaging, Palo Alto, California, July 18-20, 1973; P.S. Green, ed., Plenum Press, New York, 1974, pp. 283-316.

106. R.E. Beissner, "Electromagnetic-Acoustic Transducers–A Survey of the State of the Art", Nondestructive Testing Information Analysis Center, NTIAC-76-1, Jan. 1976.

107. E. Burstein, H. Talaat, J. Schoenwald, J.J. Quinn, and E.G.H. Lean, "Direct EM generation and detection of surface elastic waves on conducting solids. I. Theoretical considerations", Ultrasonics Symposium Proceedings, 1973, Monterey, California, Nov. 5-7, 1973, pp. 564-568.

108. H. Talaat and E. Burstein, "Direct electromagnetic generation and detection of surface elastic waves on conducting solids. II. Experiment", Ultrasonics Symposium Proceedings, 1973, Monterey, California, Nov. 5-7, 1973, pp. 569-571.

109. B.W. Maxfield and J.K. Hulbert, "Electromagnetic acoustic wave transducers (EMATS): Their operation and mode patterns", Proceedings of the Tenth Symposium on Nondestructive Evaluation, San Antonio, Texas, Apr. 23-25, 1975, pp. 44-62.

110. R.B. Thompson, "Electromagnetic, noncontact transducer", Ultrasonics Symposium Proceedings, 1973, Monterey, California, Nov. 5-7, 1973, pp. 385-392.

111. A.P. Edson and E.L. Huston, "High-performance magnetostrictive transducers", *Journal of the Acoustical Society of America*, Vol. 55, No. 5, May 1974, pp. 1076-1079.

112. D. Legros and J. Lewiner, "Electrostatic ultrasonic transducers and their utilization with foil electrets", *Journal of the Acoustical Society of America*, Vol. 53, No. 6, June 1973, pp. 1663-1672.

113. R.B. Thompson and G.A. Alers, "Ultrasonic transducers for inspecting porous materials", Proceedings of the Tenth Symposium on Nondestructive Evaluation, San Antonio, Texas, Apr. 23-25, 1975, pp. 98-104.

114. M.V. Korolev, "Aperiodic piezoelectric transducer for ultrasonic flaw detectors", *The Soviet Journal of Nondestructive Testing*, Vol. 9, No. 4, May 1974 (Russian original, July-Aug. 1973), pp. 389-394.

115. M.V. Korolev, "The transceiver section of a high-resolution ultrasonic echo flaw detector", *The Soviet Journal of Nondestructive Testing*, Vol. 10, No. 1, Nov. 1974 (Russian original, Jan.-Feb. 1974), pp. 73-77.

116. M.V. Korolev and O.G. Galkin, "Transmit-receive unit for a pulsed ultrasonic thickness gauge", *The Soviet Journal of Nondestructive Testing*, Vol. 10, No. 3, March 1975 (Russian original, May-June 1974), pp. 342-344.

117. G. Canella, "The effect of couplant thickness in ultrasonic contact testing", *The British Journal of Non-Destructive Testing*, Vol. 16, No. 6, Nov. 1974, pp. 179-182.

118. Yu. S. Kiskachi, V.I. Abramov, I.N. Babushkin, and B.M. Buranov, "Acoustic contact with the help of moistened cloth", *The Soviet Journal of Nondestructive Testing*, Vol. 11, No. 1, Nov. 1975 (Russian original, Jan.-Feb. 1975), pp. 113-114.

119. G.C. Knollman, J.L. Weaver, J.J. Hartog and J.L. Bellin, "Real-time ultrasonic imaging methodology in nondestructive testing", *Journal of the Acoustical Society of America*, Vol. 58, No. 2, Aug. 1975, pp. 455-470.

120. M.J.-M. Clement and J.W.R. Griffiths, "Some properties of circular scanning systems", Ultrasonics International 1973 Conference Proceedings, London, Mar. 27-29, 1973, published by IPC Science and Technology Press, Ltd., Guildford, England, pp. 270-274.

121. R.C. Maxson, "Automated ultrasonic nondestructive testing system", Document Y-1693, Contract No. W-7405-eng-26, U.S. Atomic Energy Commission, Oak Ridge, Tennessee, Nov. 1969.

122. N.E. Dixon and T.J. Davis, "A New Triangular Acoustic Pulse: Its Generation and Unique Properties for NDT Applications", Report BNWL-1526, Battelle-Northwest, Pacific Northwest Laboratory, Richland, Washington, Feb. 1971.

123. R.-I.Yu. Kazhis, A.I. Lukoshevichyus and S.I. Sayauskas, "Unipolar narrow ultrasonic pulse generator", *The Soviet Journal of Nondestructive Testing*, Vol. 9, No. 5, July 1974 (Russian original, Sept.-Oct. 1973), pp. 628-630.

124. M.V. Korolev, "Short-pulse generator for ultrasonic flaw detectors", *The Soviet Journal of Nondestructive Testing*, No. 1, Jan.-Feb. 1970, pp. 110-111.

125. A.I. Lukoshevichus and R.-I.Yu. Kazhis, "Possibility of using thick piezosensitive converters for generating and receiving short acoustic pulses", *The Soviet Journal of Nondestructive Testing*, Vol. 10, No. 5, July 1975 (Russian original, Sept.-Oct. 1974), pp. 543-550.

126. M. Kay, J. Shimmins, G. Manson and M.E. England, "A computer interface for digitizing ultrasonic information", *Ultrasonics*, Vol. 13, No. 1, Jan. 1975, pp. 18-20.

VII. AUTHOR INDEX

AUTHOR INDEX (Cont'd)

AUTHOR INDEX (Cont'd)

AUTHOR INDEX (Cont'd)

AUTHOR INDEX (Cont'd)